KRISTHIANO CHAGAS

MORPHO-PHYSIOLOGICAL EVALUATION OF *Pfaffia glomerata* (SPRENG.) PEDERSEN ACCESSIONS GROWN UNDER PHOTOAUTOTROPHY AND WATER DEFICIT CONDITIONS

Thesis presented to the Universidade Federal de Viçosa as part of the requirement of the Plant Physiology Graduate Program for obtention of the degree of *Doctor Scientiae*.

VIÇOSA
MINAS GERAIS-BRASIL
2019

KRISTHIANO CHAGAS

MORPHO-PHYSIOLOGICAL EVALUATION OF *Pfaffia glomerata* (SPRENG.) PEDERSEN ACCESSIONS GROWN UNDER PHOTOAUTOTROPHY AND WATER DEFICIT CONDITIONS

Thesis presented to the Universidade Federal de Viçosa as part of the requirement of the Plant Physiology Graduate Program for obtention of the degree of *Doctor Scientiae*.

APPROVED: February 28, 2019.

Lorena Melo Vieira

Camilo Elber Vital

Fábio Murilo DaMatta
(Co-advisor)

Diego Silva Batista
(Co-advisor)

Wagner Campos Otoni
(Advisor)

My Refuge and My Fortress

[1]He who dwells in the shelter of the Most High will abide in the shadow of the Almighty. [2]I will say to the Lord, “My refuge and my fortress, my God, in whom I trust.” [3]For he will deliver you from the snare of the fowler and from the deadly pestilence.[4]He will cover you with his pinions, and under his wings you will find refuge; his faithfulness is a shield and buckler.[5]You will not fear the terror of the night, nor the arrow that flies by day, [6]nor the pestilence that stalks in darkness, nor the destruction that wastes at noonday. [7]A thousand may fall at your side, ten thousand at your right hand, but it will not come near you. [8]You will only look with your eyes and see the recompense of the wicked. [9]Because you have made the Lord your dwelling place the Most High, who is my refuge [10]no evil shall be allowed to befall you, no plague come near your tent. [11]For he will command his angels concerning you to guard you in all your ways. [12]On their hands they will bear you up, lest you strike your foot against a stone. [13]You will tread on the lion and the adder; the young lion and the serpent you will trample underfoot. [14]“Because he holds fast to me in love, I will deliver him; I will protect him, because he knows my name. [15]When he calls to me, I will answer him; I will be with him in trouble; I will rescue him and honor him. [16]With long life I will satisfy him and show him my salvation.”

Psalm 91 (Holy Bible)

BIOGRAPHY

KRISTHIANO CHAGAS, son of Domingos Felix Chagas and Suely Vitorino de Oliveira, was born in the city of Linhares, ES, in April 01, 1988. In 2006, he joined the first class of Agronomy course of Universidade Federal do Espírito Santo in the Centro Universitário Norte do Espírito Santo, where he graduated in Agronomy in 2012. During the graduation period, he had experience in the area of soil and water management and conservation, tropical fruit, specifically with passion fruit and papaya, conducting research applied to propagation and production of these fruit species. Joined in 2012 the in Tropical Agriculture Graduate Program of the Universidade Federal do Espírito Santo, where obtained a master's degree in Tropical Agriculture, working with plant propagation by means of somatic embryogenesis, submitting to dissertation defense on February 20, 2014. On March 2014 joined the in Plant Physiology Graduate Program of the Universidade Federal de Viçosa, working with *in vitro* photoautotrophic propagation, developed a new light source apparatus to aid *in vitro* photosynthetic rate measurements, and elicitation of secondary metabolites by drought stress in *Pfaffia glomerata,* submitting to the defense of thesis on February 28, 2019

ACKNOWLEDGMENTS

To the almighty and everlasting GOD, the Alpha and the Omega, the beginning and the end. I am grateful to you, my God, because without you I am nothing and I can do nothing.

To the Universidade Federal de Viçosa, in particular, to the Plant Physiology Graduate Program, for the opportunity to carry out the course and Bioagro.

To the Conselho Nacional de Desenvolvimento Científico e Tecnológico (CNPq) and Fundação de Amparo à Pesquisa do Estado de Minas Gerais (FAPEMIG) by funding supporters, and CAPES for granting the scholarship.

To Professor Wagner Campos Otoni, for orientation and provide the opportunity to navigate the waves of knowledge before ever navigated by me. Co-advisers Fábio Murilo DaMatta and Diego Silva Batista for advice and support

To my father Domingos Felix Chagas and mother Suely Vitorino de Oliveira, for loving me, by prayers in my favor, by the support, for being directly related in the formation of my personality and for teaching me that without struggle there is no victory.

To my girlfriend, Camila Soares de Castro, even distant, has always been a source of love, affection, support in difficulties, joy in victories and the concern of always offering me the best.

To my brothers and the whole family for believing in me so much, for getting carried away with my achievements and they feel so proud.

The big family LCTII and all friends of Viçosa, who directly or indirectly contributed to the conclusion of this important stage of my life.

SUMMARY

ABSTRACT

CHAGAS, Kristhiano D.Sc., Universidade Federal de Viçosa, February, 2019. **Morpho-physiological evaluation of *Pfaffia glomerata* (Spreng.) Pedersen accessions grown under photoautotrophy and water stress conditions** Advisor: Wagner Campos Otoni. Co-Advisors: Fábio Murilo DaMatta and Diego Silva Batista.

This study aimed to evaluate the morpho-physiological aspects of *Pfaffia glomerata* (Spreng.) Pedersen accessions grown under photoautotrophy and water stress conditions. In order to address that three experiments were conducted. In the first experiment, diploid (Ac 04, 22 and 43) and synthetic polyploid (Poly 28, 60, 68 and 74) accessions of *P. glomerata* were grown *in vitro* under photoautotrophy on a sugar-free MS-based medium, using cellulose and vermiculite (1:2 ratio) as supporting material, and maintained in a growth room at 25 ± 2°C and 60 μmol m^{-2} s^{-1} irradiation, provided by red/blue led lamps for 30 days. In the second experiment, two *P. glomerata* accessions (Ac 22 and 43) propagated *in vitro* were acclimatized in a greenhouse and submitted to moderate and severe water deficit for 15 days, after 7 days were rehydrated and performed analysis in conditions stressed and recovery. In the third experiment, the effects water deficit elicited *in vitro* by supplementing a MS-based medium withof polyethyleneglycol (PEG 6000) at 0, 0.1, 0.2, 0.3%) evaluated by comparing plants grown for 20 days under stress and after 7 days rehydration. Here, a versatile light chamber formed by 8 high brightness white LEDs disposed on the inside wall of an expanded polystyrene (EPS) box and used with source photosynthetic photon flux (600 μmol m^{-2} s^{-1}) in measurements of photosynthesis *in vitro*. Under photoautotrophic conditions, the polyploids exhibited lower leaf number, and thicker and more expanded leaves, increased stomata size and reduced stomata density compared to the diploid counterparts. Even with the morphological differences, all assayed accessions showed average *in vitro* photosynthetic rate of 7.31 μmol m^{-2} s^{-1} and *Fv/Fm* 0.79. The Ac 04 presented and 20-hydroxyecdysone (20E) contents. The drought stress led to a marked decrease in biomass, height, leaf expansion, epidermis and mesophyll, and increased stomatal density, for both accessions (Ac 22 and Ac 43) raised *in vitro* and *ex vitro*. The photosynthetic rate and dark respiration increased in stressed plants in greenhouse, whereas the addition of PEG *in vitro* decreased photosynthesis. On topo of that, the water deficit led to increased contents of abscisic and salicylic acid, stimulated antioxidant enzyme activities, and osmoregulatory status, but to a decreased zeatin levels. The Ac 43 maintained under full irrigation exhibit higher content and field yield

of 20E than Ac 22, both accessions the water deficit in greenhouse and *in vitro* increased 20E levels and decrease in production total of metabolite. This work proposes an innovative, practical and efficient LED-based apparatus to efficiently evaluate the photosynthetic rates of vitroplants, thus providing foundations to expand the understanding of the acquisition of photosynthetic competence during plant development under photoautotrophic *in vitro* environment. These findings also provide a better understanding of the different morpho-physiological responses of synthetic polyploids *P. glomerata* under photoautotrophy, and acclimation strategies adopted by the species that enable drought tolerance and pave the way for further studies that can lead to improved 20E production, a bioactive compound with high economic value and biochemical interest.

Keywords: Light source; gas exchange; synthetic polyploidy; Brazilian ginseng; 20-hydroxyecdysone; endogenous hormone levels; water stress

RESUMO

CHAGAS, Kristhiano D.Sc., Universidade Federal de Viçosa, Fevereiro, 2019. **Avaliação morfo-fisiológica de acessos de *Pfaffia glomerata* (Spreng.) Pedersen cultivados sob condições de fotoautotrofia e estresse hídrico** Orientador: Wagner Campos Otoni. Co-Oreientadores: Fábio Murilo DaMatta and Diego Silva Batista.

Este estudo teve como objetivo avaliar os aspectos morfo-fisiológicos dos acessos de *Pfaffia glomerata* (Spreng.) Pedersen crescidos sob condições de fotoautotrofia e estresse hídrico. A fim de abordar foram realizados três experimentos. No primeiro experimento, os acessos diplóides (Ac 04, 22 e 43) e poliploides sintéticos (Poli 28, 60, 68 e 74) de *P. glomerata* foram cultivados *in vitro* sob fotoautotrofia em meio à base de MS sem açúcar, usando celulose e vermiculita (proporção 1: 2) como material de suporte, mantidos em sala de crescimento a 25 ± 2 ° C e irradiação a 60 μmol m^{-2} s^{-1}, fornecidos por lâmpadas led vermelho/azul por 30 dias. No segundo experimento, dois acessos de *P. glomerata* (Ac 22 e 43) propagados *in vitro* foram aclimatados em casa de vegetação e submetidos a déficit hídrico moderado e grave por 15 dias, após 7 dias foram reidratados e realizaram análises em condições de estresse e recuperação. No terceiro experimento, os efeitos do déficit hídrico foram indizidos *in vitro* em um meio à base de MS suplementando com polietilenoglicol (PEG 6000) a 0, 0,1, 0,2, 0,3%) avaliado comparando plantas cultivadas por 20 dias sob estresse e após 7 dias de reidratação. Aqui, uma câmara de luz versátil formada por 8 LEDs brancos de alto brilho dispostos na parede interna de uma caixa de poliestireno expandido (EPS) e usada com o fluxo fotossintético de fonte (600 μmol m^{-2} s^{-1}) nas medições da fotossíntese *in vitro*. Sob condições fotoautotróficas, os poliploides exibiram menor número de folhas e folhas mais espessas e expandidas, aumento do tamanho dos estômatos e densidade estomáticas reduzida em comparação com os homólogos diplóides. Mesmo com as diferenças morfológicas, todos os acessos avaliados apresentaram taxa fotossintética média *in vitro* de 7,31 μmol m^{-2} s^{-1} e *Fv/Fm* 0,79. O Ac 04 apresentou e o conteúdo de 20-hidroxiecdisona (20E). O estresse hídrico levou a uma diminuição acentuada da biomassa, altura, expansão foliar, epiderme e mesofilo e aumento da densidade estomática, para os dois acessos (Ac 22 e Ac 43) desenvolvidos *in vitro* e *ex vitro*. A taxa fotossintética e a respiração noturna aumentaram nas plantas

estressadas em casa de vegetação, enquanto a adição de PEG *in vitro* diminuiu a fotossíntese. Além disso, o déficit hídrico levou ao aumento do conteúdo de ácido abscísico e salicílico, estimulou as atividades das enzimas antioxidantes e o estado osmorregulador, mas diminuiu os níveis de zeatina. O Ac 43 mantido sob irrigação total apresenta maior conteúdo e rendimento de campo de 20E que o Ac 22, tanto o déficit hídrico em casa de vegetação quanto *in vitro* aumentaram os níveis de 20E e diminuíram a produção total de metabólitos. Este trabalho propõe um aparelho inovador, prático e eficiente à base de LED para avaliar com eficiência as taxas fotossintéticas de vitroplantas, fornecendo bases para expandir o entendimento da aquisição de competência fotossintética durante o desenvolvimento da planta em ambiente fotoautotrófico *in vitro*. Os resultados também fornecem uma melhor compreensão das diferentes respostas morfo-fisiológicas dos poliploides sintéticos *P. glomerata* sob fotoautotrofia e estratégias de aclimatação adotadas pelas espécies que permitem tolerância à seca e abrem caminho para novos estudos que podem levar a uma melhor produção de 20E, composto bioativo com alto valor econômico e interesse bioquímico.

Palavras chave: Fonte de luz; trocas de gasosas; poliploidia sintética; Ginseng brasileiro; 20-hidroxiecdisona; hormonios endógenos; estresse hídrico.

INTRODUCTION

Plants are a rich source of several biochemical compounds, which are exploited as food additives, pharmaceuticals, pesticides, fragrances, colors and cosmetic ingredients (Altemimi et al., 2017). However, many of these secondary metabolites are often very complex and their chemical synthesis can be difficult and expensive, making it unfeasible to artificial production (Hidalgo et al., 2018; Guerriero et al., 2018). Thus, the studies development with medicinal plants and their respective metabolites of biotechnological and pharmacological interest directly contributes to the domestication of these species and development of the pharmaceutical industry.

Secondary plant metabolites are compounds that play a crucial role in the adaptation of plants to the environment (Yang et al., 2018). Among the metabolites with high biotechnological interest, there are ecdysteroids (ECDs), which comprise a class of 5β-androstane steroid hormones found in invertebrate species (e.g., insects; zooecdysteroids - ZEs), but which can also be found in different organisms such as plants (phytoecdysteroids - PEs) and fungi (mycoecdysteroids - Mes) (Festucci-Buselli et al., 2008). In arthropods, ECDs are potent development regulators, with direct action on ecdysis, reproduction, and response to stress (Avilés-Pagán & Orr-Weaver, 2018), while in plants there is a report of the PEs action on cell growth and proliferation (Machackova et al., 1995), synthesize from mevalonic acid in the mevalonate pathway in cell using acetyl-CoA as a precursor (Tarkowská & Strnad, 2016). However, there is strong evidence that may play a role in the defense of plants against non-adapted phytophagous insects (Chaubey, 2018).

The 20-hydroxydecysone (20E) molecule is the main active ecdysteroid hormone of insects and it is acted at different development stages, being required specific 20E pulses in order that larval development is completed (Liu et al., 2018). And supplementation with 20E doses in feeding unadapted insects can lead to their death, thereby exemplifying the agrochemical potential of the 20E (see; Rharrabe et al., 2009; Rharrabe et al., 2010; Kayani et al., 2016; Jurenka et al., 2017).

Overall, 20E has agrochemical, biotechnological, pharmacological and medicinal potential and may interfere with physiological and morphological processes in plants (Festucci-Buselli et al., 2008). Currently, in ECDYBASE - which presents data on different ecdysteroids in plants, fungi, and nematodes - information on different species of the plant kingdom is contained, with approximately 23 families inserted in

the database and 114 species contained in these families (Lafont et al., 2019). In this context, among the 20E-producing plants with high potential for use in the pharmacological and biotechnological industry, we highlight *Pfaffia glomerata* (Spreng.) Pedersen (Amaranthaceae), which can accumulate to concentrations as high as ranging from 2.4 to 5.9 mg g^{-1}, highlighting the value of this plant as a source for phytoecdysteroids (Corrêa et al., 2015)

P. glomerata is marketed and used in folk medicine for the treatment of various diseases because its various biological properties as gastro-protective (Freitas et al., 2004; Mazzeo et al., 2013), anti-inflammatory and analgesic (Neto et al., 2005), antioxidant activity (Leal et al., 2010), leishmanicidal (Neto et al., 2004), antimicrobial action as adjuvant in control of dental caries (Moura et al., 2011), and to combat memory problems (Oliveira et al., 2016).

We highlight that although *P. glomerata* is an important medicinal plant, few studies have explored the physiological aspects in order to contribute with a better understanding of the factors that can modulate the biosynthetic pathway of its most interesting metabolite (i.e., 20E). The propagation of *P. glomerata* has been traditionally conducted through the proliferation of axillary buds of nodal segments, usually by in vitro culture techniques (Nicoloso et al., 2001; Flores et al., 2010). On this outlook, our research group has carried out different studies with *P. glomerata* in order to provide information for a better understanding of the morphophysiological aspects and 20E production in *in vitro* and *ex vitro* conditions. Among the approaches performed, three stand out: photoautotrophic potential evaluation (Iarema et al., 2012; Saldanha et al., 2012; 2013; 2014; Corrêa et al., 2015); induction of polyploidy; and the application of different biotic (e.g., insects and nematodes) and abiotic mechanisms (e.g., physical damages) for the induction of 20E (Cruz, 2011; Maldaner, 2011).

The application of artificial polyploidy in *P. glomerata* provided basic and essential information for the conservation and reproduction of this species (Gomes et al., 2014). Besides, in these polyploid accessions, the analysis of photoautotrophic potential was performed *in vitro* and *ex vitro*, evidencing that greater accumulations of biomass and 20E production (Corrêa et al., 2016). In context, the morphological, cytological and metabolic changes vary depending on the plant species studied (Cohen et al., 2013) and often show new phenotypes that are not present in all their progenitors (Iannicelli et al, 2016). However, a deeper characterization of the morphophysiological

aspects of these polyploid accesses is still necessary for a better understanding of the mechanisms involved that can lead to a higher production of 20E.

The water deficit is one of the main environmental constraints that contribute to the reduction of agricultural productivity worldwide (Lamaoui et al., 2018). On the other hand, some species have phenotypic plasticity in which secondary metabolism can be altered positively by osmotic stress (Ashraf et al., 2018). Hydric deficit has been demonstrated to cause accumulation of various secondary metabolites in plants (Zandalinas et al., 2017; Jia et al., 2015; Jaafar et al. 2012; Adnan et al. 2014). Thus, the evaluation of the water deficit in *P. glomerata* may reveal important morphophysiological traits for use in breeding programs of this species, contributing directly to agriculture development.

In this work, morphological, physiological and molecular aspects were studied during *in vitro* photoautotrophic grown and under *in vitro* and *ex vitro* conditions of water deficit in *P. glomerata* polyploid and diploid accessions, in order to generate information that can be used in biotechnology strategies and to enable a better understanding of 20E regulation.

REFERENCES

Adnan Z, Bilal HA, Muhammad A, Sumaira A, Muhammad Z, Ihsanul-haq (2014) Synergistic effects of drought stress and photoperiods on phenology and secondary metabolism of *Silybum marianum*. **Applied Biochemistry and Biotechnology** 174: 693-707. doi.org/10.1007/s12010-014-1098-5

Altemimi A, Lakhssassi N, Baharlouei A, Watson D, Lightfoot D. (2017). Phytochemicals: Extraction, isolation, and identification of bioactive compounds from plant extracts. **Plants**, 6: 42. doi.org/10.3390/plants6040042

Ashraf AM, Iqbal M, Rasheed R, Hussain I, Riaz M and Arif MS. (2018). Environmental stress and secondary metabolites in plants: an overview. In *Plant Metabolites and Regulation Under Environmental Stress*, Ahmad P. (ed). Academic Press, New York, NY, pp. 153-167.

Avilés-Pagán EE, Orr-Weaver TL. (2018). Activating embryonic development in Drosophila. **Seminars in Cell & Developmental Biology**. 84: 100-110. https://doi.org/10.1016/j.semcdb.2018.02.019

Chaubey MK. (2018). Role of phytoecdysteroids in insect pest management: A review. **Journal of Agronomy**, 17: 1-10. doi: 10.3923/ja.2018.1.10

Cohen H, Fait A, Tel-Zur N. (2013). Morphological, cytological and metabolic consequences of autopolyploidization in *Hylocereus* (Cactaceae) species. **BMC Plant Biology**, 13:173. doi.org/10.1186/1471-2229-13-173

Corrêa JPO, Vital CE, Pinheiro MVM, Batista DS, Azevedo JFL, Saldanha CW, Cruz ACF, Damatta FM, Otoni WC. (2015). *In vitro* photoautotrophic potential and ex vitro photosynthetic competence of *Pfaffia glomerata* (Spreng.) Pedersen accessions. **Plant Cell, Tissue and Organ Culture**, 121: 289-300. doi.org/10.1007/s11240-014-0700-4

Corrêa JPO, Vital CE, Pinheiro MVM, Batista DS, Saldanha CW, Cruz ACF, Notini MM, Freitas DMS, Damatta FM, Otoni WC. (2016). Induced polyploidization increases 20-hydroxyecdysone content, *in vitro* photoautotrophic growth, and *ex vitro* biomass accumulation in *Pfaffia glomerata* (Spreng.) Pedersen. **In Vitro Cellular and Developmental Biology - Plant**, 52: 45-55. doi.org/10.1007/s1162

CRUZ ACF. **Interações entre acessos de fáfia [*Pfaffia glomerata* (Spreng.) Pedersen] com nematoides (*Meloidogyne incognita* e *M. javanica*): aspectos fitoquímicos e estruturais**. 2011. 86 f. Tese (Doutorado em Botânica) - Departamento de Biologia Geral, Universidade Federal de Viçosa, Viçosa. 2011.

Festucci-Buselli RA, Contim LAS, Barbosa LCA, Stuart JJ, Otoni WC. (2008). Biosynthesis and potential functions of the ecdysteroid 20-hydroxyecdysone - A review. **Botany**, 86: 978-98. doi.org/10.1139/B08-049

Flores R, Brondani D, Cezarotto V, Giacomelli SR, Nicoloso FT. (2010). Micropropagation and β-ecdysone content of the Brazilian ginsengs *Pfaffia glomerata* and *Pfaffia tuberosa*. **In Vitro Cellular & Developmental Biology-Plant**, 46: 210-217. doi.org/10.1007/s11627-010-9286-7

Freitas CS, Baggio CH, Silva-Santos JE, Rieck L, Santos CAM, Júnior CC, Ming LC, Cortez DAG, Marques MCA. (2004). Involvement of nitric oxide in the gastroprotective effects of an aqueous extract of *Pfaffia glomerata* (Spreng) Pedersen, Amaranthaceae, in rats. **Life Sciences**, 74 1167-1179. doi.org/10.1016/j.lfs.2003.08.003

Gomes SSL, Saldanha CW, Neves CS, Trevizani M, Raposo NRB, Notini MM, Santos MO, Campos JMS, Otoni WC, Viccini LF. (2014) Karyotype, genome size, and *in vitro* chromosome doubling of *Pfaffia glomerata* (Spreng.) Pedersen. **Plant Cell, Tissue and Organ Culture**, 118: 45-56. doi.org/10.1007/s11240-014-0460-1

Guerriero G, Berni R, Muñoz-Sanchez JA, Apone F, Abdel-Salam EM, Qahtan, AA, Alatar AA, Cantini C, Cai G, Hausman JF, Siddiqui KS, Hernández-Sotomayor SMT, Faisal M. (2018). Production of plant secondary metabolites: Examples, tips and suggestions for biotechnologists. **Genes**. 9: 309. doi.org/10.3390/genes9060309

Hidalgo D, Sanchez R, Lalaleo L, Bonfill M, Corchete P, Palazon J. (2018). Biotechnological production of pharmaceuticals and biopharmaceuticals in plant cell and organ cultures. **Current Medicinal Chemistry**. 25: 3577-3596. doi.org/10.2174/0929867325666180309124317

Iannicelli J, Elechosa MA, Juárez MA, Martínez A, Bugallo V, Bandoni AL, Escandón AS, Baren CM. (2016). Effect of polyploidization in the production of essential oils in *Lippia integrifolia*. **Industrial Crops and Products**, 81: 20-29. doi.org/10.1016/j.indcrop.2015.11.053

Iarema L, Cruz ACF, Saldanha CW, Dias LLC, Vieira RF, Oliveira EJ, Otoni WC. (2012). Photoautotrophic propagation of Brazilian ginseng [*Pfaffia glomerata* (Spreng.) Pedersen]. **Plant Cell, Tissue and Organ Culture**, 110: 227-238. doi.org/10.1007/s11240-012-0145-6

Jaafar HZE, Ibrahim MH, Fakri NFM (2012) Impact of soil field water capacity on secondary metabolites, phenylalanine ammonialyase (PAL), malondialdehyde (MDA) and photosynthetic responses of Malaysian kacip fatimah (*Labisia pumila* Benth). **Molecules**, 17: 7305-7322. doi.org/10.3390/molecules17067305

Jia X, Sun C, Li G, Li G, Chen G. (2015). Effects of progressive drought stress on the physiology, antioxidative enzymes and secondary metabolites of *Radix Astragali*. **Acta Physiologiae Plantarum**, 37: 262. doi.org/10.1007/s11738-015-2015-4

Jurenka R, Russell K, O'Neal M. (2017). Phytoecdysteroids as antifeedants towards several beetles that include polyphagous and monophagous feeding guilds. **Pest Management Science**, 73: 1633-1637. doi:10.1002/ps.4500.

Kayani WK, Palazòn J, Cusidò RM, Mirza B. (2016). The effect of rol genes on phytoecdysteroid biosynthesis in *Ajuga bracteosa* differs between transgenic plants and hairy roots. **RSC Advances**, 6: 22700-22708. doi:10.1039/c6ra00250a

Lafont R, Harmatha, J, Marion-Polli F, Dinan, L, Wilson D. (2019) The Ecdysone Handbook, 3rd edition, on-line. http://ecdybase.org/. Access in: February 14, 2019.

Lamaoui M, Jemo M, Datla R, Bekkaoui F. (2018). Heat and drought stresses in crops and approaches for their mitigation. **Frontiers in Chemistry**, 6, 26. doi.org/10.3389/fchem.2018.00026

Leal PF, Kfouri MB, Alexandre FC, Fagundes FH, Prado JM, Toyama MH, Meireles MAA. (2010). Brazilian Ginseng extraction via LPSE and SFE: Global yields, extraction kinetics, chemical composition and antioxidant activity. **The Journal of Supercritical Fluids**, 54, 38-45. doi.org/10.1016/j.supflu.2010.03.007

Liu S, Li K, Gao Y, Liu X, Chen W, Ge W, Feng Q, Palli SR, Li S. (2018). Antagonistic actions of juvenile hormone and 20-hydroxyecdysone within the ring gland determine developmental transitions in *Drosophila*. **Proceedings of the National Academy of Sciences**, 2018 115 (1) 139-144. doi.org/10.1073/pnas.1716897115

Machackova I, Vagner M, Slama K. (1995) Comparison between the effects of 20-hydroxyecdysone and phytohormones on growth and development in plants. European Journal of Entomology, v.92, p.309-316, 1995.

Maldaner J. **Preliminary analyses of 20-hidroxyecdysone elicitation under stress conditions, morphogenesis *in vitro*, and *Agrobacterium rhizogenes* transformation in *Pfaffia glomerata*.** 2011. 97 f. Tese (Doutorado em Fisiologia Vegetal) - Departamento de Biologia Geral, Universidade Federal de Viçosa, Viçosa. 2011.

Mazzeo GCCS, Cortez FS, Pusceddu FH, Santos AR, Guimarães LL, Amaral FP, Silva MPO, Toma W. (2013). Avaliação da atividade antiulcerogênica e ecotoxicológica do extrato hidroalcoólico 70% obtido a partir das folhas de *Pfaffia glomerata* (Spreng) Pedersen (Amaranthaceae). **Unisanta BioScience**, 2:75-80.

Moura CL, Casemiro LA, Martins CHG, Cunha WR, Silva MLA, Cury AHV. (2011). Evaluation of the antimicrobial activity of the plant species *Pfaffia glomerata* against oral pathogens. **Revista Investigação**, 11: 24-28. doi.org/10.26843/investigacao.v11i2.500

Neto AG, Costa JMLC, Belati C, Vinholis AHC, Possebom LS, Silva Filho AA, Cunha WR, Carvalho JCT, Bastos JK, Silva MLA. (2005) Analgesic and anti-inflammatory activity of a crude root extract of *Pfaffia glomerata* (Spreng.) Pedersen. **Journal of Ethnopharmacology** 96: 87-91. doi.org/10.1016/j.jep.2004.08.035

Neto AG, Silva Filho AA, Costa JMLC, Vinholis AHC, Souza HB, Cunha WR, Silva MLAE, Albuquerque S, Bastos JK. (2004). Evaluation of the trypanocidal and leishmanicidal *in vitro* activity of the crude hydroalcoholic extract of *Pfaffia glomerata* (Amarathanceae) roots. **Phytomedicine**, 11: 662-665. doi.org/10.1016/j.phymed.2003.06.005

Nicoloso FT, Erig AC, Martins CF, Russowski, D. (2001). Micropropagação do ginseng brasileiro [*Pfaffia glomerata* (Spreng.) Pedersen]. **Revista Brasileira de Plantas Medicinais**, 3: 11-18.

Oliveira DR, Oliveira ACD, Marques LC. (2016). O estado regulatório dos fitoterápicos no Brasil: Um paralelo entre a legislação e o mercado farmacêutico (1995-2015). **Revista Vigilância Sanitária em Debate: Sociedade, Ciência & Tecnologia**, 4: 139-148. doi: 10.22239/2317-269X.00806

Rharrabe K, Bouayad N, Sayah F (2009) Effects of ingested 20-hydroxyecdysone on development and midgut epithelial cells of *Plodia interpunctella* (Lepidoptera, Pyralidae). **Pesticide Biochemistry and Physiology**, 93:112-119. doi.org/10.1016/j.pestbp.2008.12.002

Rharrabe K, Sayan F, Lafont R (2010) Dietary effects of four phytoecdysteroids on growth and development of the Indian meal moth, *Plodia interpunctella*. **Journal of Insect Science** 10: 13. doi.org/10.1673/031.010.1301

Saldanha CW, Otoni CG, de Azevedo JLF, Dias LLC, do Rêgo MM, Otoni WC. (2012). A low-cost alternative membrane system that promotes growth in nodal cultures of Brazilian ginseng [*Pfaffia glomerata* (Spreng.) Pedersen]. **Plant Cell, Tissue and Organ Culture**. 110: 413-422. doi.org/10.1007/s11240-012-0162-5.

Saldanha CW, Otoni CG, Notini MM, Kuki KN, Cruz ACF, Neto AR, Dias LLC, Otoni WC. (2013) A CO_2-enriched atmosphere improves *in vitro* growth of Brazilian ginseng [*Pfaffia glomerata* (Spreng.) Pedersen]. **In Vitro Cellular & Developmental Biology - Plant**, 49: 433-444. doi.org/10.1007/s11627-013-9529-5

Saldanha CW, Otoni CG, Rocha DI, Cavatte PC, Detmann KDSC, Tanaka FAO, Dias LLC, DaMatta FM, Otoni WC. (2014). CO_2-enriched atmosphere and supporting material impact the growth, morphophysiology and ultrastructure of in vitro Brazilian-ginseng [*Pfaffia glomerata* (Spreng.) Pedersen] plantlets**. Plant Cell, Tissue and Organ Culture**. 118: 87-99. doi.org/10.1007/s11240-014-0464-x.

Tarkowská D, Strnad M. (2016). Plant ecdysteroids: plant sterols with intriguing distributions, biological effects and relations to plant hormones. **Planta**, 244: 545-555. doi.org/10.1007/s00425-016-2561-z

Yang L, Wen KS, Ruan X, Zhao YX, Wei F, Wang Q. (2018). Response of plant secondary metabolites to environmental factors. **Molecules**, 23: 762. doi: 10.3390/molecules23040762.

Zandalinas SI, Sales C, Beltrán J, Gómez-Cadenas A, Arbona V. (2017). Activation of secondary metabolism in citrus plants is associated to sensitivity to combined drought and high temperatures. **Frontiers in Plant science**, 7, 1954. doi.org/10.3389/fpls.2016.01954

CHAPTER I

Photosynthetic competence of diploid and synthetic polyploid accessions of Brazilian-ginseng [*Pfaffia glomerata* (Spreng.) Pedersen] in a novel and rapid tool to evaluate photosynthesis in *in vitro* plants

Kristhiano Chagas[1], Márcio Rosa[2], Alan Carlos Costa[3], Tatiane Dulcineia Silva[1], Sérgio Heitor Felipe[1], Diego Silva Batista[4], Rodrigo Sobreira Alexandre[5], Cleber Witt Saldanha[6], Fábio Murilo DaMatta[7], Wagner Campos Otoni[1,*]

[1]Laboratório de Cultura de Tecidos Vegetais (LCTII), Departamento de Biologia Vegetal/BIOAGRO, Universidade Federal de Viçosa, Av. P. H. Rolfs, 36570-900 Viçosa, MG, Brasil

[2]Universidade de Rio Verde - UniRV, Campus Rio Verde, Fazenda Fontes do Saber. C. P. 104, 75901-970 Rio Verde, GO, Brasil

[3]Instituto Federal de Educação, Ciência e Tecnologia Goiano, Campus Rio Verde, Rodovia Sul Goiana, km 01, Zona Rural, C.P. 66, 75901-970 Rio Verde, GO, Brasil

[4] Universidade Estadual do Maranhão, Av. Lourenço Vieira da Silva, s/nº, Cidade Universitária Paulo VI, 65055-310 São Luís, MA, Brasil (ORCID 0000-0002-5798-7761)

[5]Departamento de Ciências Florestais e da Madeira, Centro de Ciências Agrárias e Engenharias, Universidade Federal do Espírito Santo, Avenida Governador Lindemberg, 316, Centro, 29550-000 Jerônimo Monteiro, ES, Brasil

[6]Centro de Pesquisa em Florestas/DDPA/SEAPI, 97050-800 Santa Maria, RS, Brasil

[7]Departamento de Biologia Vegetal, Ed. CCBII, Av. P. H. Rolfs s/n, Universidade Federal de Viçosa, Campus Universitário, 36570-900 Viçosa, MG, Brasil

*Corresponding author: (email: wcotoni@gmail.com) Departamento de Biologia Vegetal, Laboratório de Cultura de Tecidos/BIOAGRO, Campus Universitário, Avenida Peter Henry Rolfs s/n, Universidade Federal de Viçosa, 36570-900 Viçosa, MG, Brasil (Fax:+55 31 3899 2580) (ORCID 0000-0002-9614-9373)

Abstract

The photosynthetic performance of plants grown under *in vitro* conditions is strongly influenced by the closed environmental characteristics that photosynthetic tissues experience. Notably, a wide variations of gases concentrated in the headspace of growing containers affect the rate and integrity of components of photosynthetic reactions. The measurements of the photosynthetic parameters are essential in the studies of photoautotrophic growth *in vitro*, however there are no reliable equipments fully adapted to such measurements. In this study, we aimed to evaluate the photosynthetic rate, chlorophyll fluorescence, morphoanatomy and 20-hydroxyecdysone (20E) of diploid (Ac 04, 22 and 43) and synthetic polyploid accessions (Poly 28, 60, 68 and 74) of *Pfaffia glomerata* plants grown under photoautotrophic *in vitro* conditions. The polyploids had thicker and more expanded leaves compared to the diploids, but in lower number. The greater leaf expansion in the polyploids provided increased stomata size and reduced stomata density. Even with all the morphological differences of the leaves of the assessed vitroplants, the average photosynthetic rate was 7.31 μmol m^{-2} s^{-1} and *Fv/Fm* 0.79, indicating that plants were not stressed. The Ac 04 showed greater content of photosynthetic pigments, retained highest electron transport rate (ETR), sucrose, and 20E contents. The results also suggest that photosystem II (PSII) activity in Ac 04 was more efficient, as indicated by fluorescence measurements. These findings reveal that increased carbon availability from rising sucrose of photosynthesis allowed for greater investment in the 20E content. Further, this work proposes a practical and efficient apparatus to efficiently evaluate the photosynthetic rate of plants *in vitro*.

Keywords: Light source; gas exchange; instrumentation; chlorophyll fluorescence; synthetic polyploidy.

Introduction

In vitro cultured plants are kept under specific physical and chemical conditions which promote rapid growth, high multiplication rates and which often result in the formation of morphoanatomical and physiologically abnormal plants (Hazarika, 2006). As a consequence of these abnormalities, cultures require an exogenous source of carbohydrates, most commonly sucrose. However, high sucrose concentrations affect the assimilation of carbon through photosynthesis by inhibition or reduction of the ribulose-1,5-bisphosphate carboxylase-oxygenase (RuBisCO) enzyme activity (Hdider & Desjardins, 1995; Roh and Choi, 2004; Dias et al., 2013; Nunes et al., 2016), through the blockage of active carboxylation sites of RuBisCO by phosphorylated sugars (Mayak et al., 1998). This process is referred to as feedback inhibition of photosynthesis (Martins et al., 2013; McCarthy et al, 2016). Additionally, the low or negative net photosynthetic rates of plants *in vitro* are not due to poor photosynthetic ability, but to the low CO_2 concentration in the air-tight culture vessel during the photoperiod (Park et al., 2011; Xiao et al., 2011).

The use of flasks that allow higher gas exchange allows a continuous supply of CO_2 during the light period and lower relative humidity (Martins et al., 2015), enhance characteristics like rusticity and maturity, which leads to positive effects on biomass gains and acclimatization (Batista et al., 2017).

The photosynthesis and the photochemical efficiency of plants *in vitro* must be measured in order to accurately evaluate phenotypes. Photosynthetic measurements can be made *in vitro* by assessing O_2 evolution rate (Kadlecek et al., 2003; Chen, 2006; Hopfner et al., 2014; Kitzing et al., 2014), quantifying the $C^{14}O_2$ fixation rate (Hanson and Edelman, 1971; Kennedy, 1977) or quantifying CO_2 by gas chromatography (Fujiwara et al., 1987; Supaibulwattana et al., 2011; Wu an Lin, 2013). Measuring CO_2 assimilation rate using infrared gas analyzers (IRGAs) is an efficient alternative for to these methods, with a many commercial systems providing real-time measurements of intact plant photosynthetic traits (e.g LI-6800, Li-Cor Inc., Lincoln, Nebraska, USA; CIRAS-3, PP Systems, Hitchin, UK; LCi T, ADC-Biosciences, Hoddesdon, UK; CI-340, CID Bio-Science, Inc., Camas, Washington, USA; GFS-3000, Heinz Walz GmbH, Effeltrich, Germany). While these systems continue to be improved, customized chambers, specific for conifer needles (Reinhardt and Smith, 2016), *Arabidopsis* and other herbaceous species (Kölling et al., 2015) are necessary for many applications.

This customized approach for *in vitro* grown plants is also required. Photochemical efficiency, expressed by chlorophyll *a* fluorescence, can be used to evaluate plant stress or injuries during *in vitro* cultivation, since kinetics changes in the chlorophyll emissions the result of frequent modifications in the photosynthetic activity due to the quantum efficiency of the electron transport chain in the photosystem II in the leaves (Baker and Rosenqvist, 2004; Yusuf et al., 2010; Roach & Krieger-Liszkay, 2014). By measuring chlorophyll *a* fluorescence, the maximum quantum yield of photosystem II (PSII) (*Fv*/*Fm*) can be determined and used to compare healthy and damaged tissues due biotic and abiotic factors (Baker, 2008; Rousseau et al., 2013); effective quantum yield of PSII (Δ*F/Fm'*); the relative rate of electron transport (ETR) and extinction coefficients for photochemical and non-photochemical quenching (Maxwell & Johnson, 2000; Goltsev et al., 2016). The integration of leaf cuvette and as a light source/pulse-amplitude modulated fluorometer for simultaneous measurement of gas exchange and fluorescence (Ireland et al., 1989). However, there is a need for techniques that combine these strategies to measure photosynthesis in a practical and rapid manner in *in vitro* cultured plants.

Pfaffia glomerata (Spreng.) Pedersen roots shows a large potential among Brazilian folk medicine treating gastric problems (Freitas et al., 2004; Mazzeo et al., 2013); as anti-inflammatory and analgesic (Neto et al., 2005); as anti-oxidant (Souza Daniel et al., 2005) and as antimicrobial and adjuvant in the control of dental cavities (Moura et al., 2011). These applications are due the production of the secondary metabolite 20-hydroxyecdysone (20E) in the species, which has high commercial and medicinal value because to its biological activities. Furthermore, 20E shows a remarkable antifeedant activity against adult striped leaf beetles (Xu et al., 2009) and also interferes in the *Bombyx mori* larvae hormonal balance, causing death (Wang et al., 2012).

The *in vitro* propagation of *P glomerata* has traditionally been made using agar under heterotrophic conditions, matched by axillary bud proliferation (Flores et al., 2010). Previous studies with *P. glomerata* in the *in vitro* environment demonstrated high photosynthetic competence in photoautotrophic system (Iarema et al., 2012; Saldanha et al., 2012, 2013, 2014; Corrêa et al., 2015, 2016). Therefore, the development of new methodologies for the evaluation of plants in a photoautotrophic environment is necessary.

Polyploidy induction in *P. glomerata* showed to be a promising alternative to increase in growth and 20E content (Corrêa et al., 2016; Gomes et al., 2014). However,

the characterization of plant genotypes producing commercial interest metabolites depends intrinsically on the environmental conditions in which these species are found. Thus, the *in vitro* cultivation with the control of the biotic and abiotic conditions may play an important role in the evaluation of the different genotypes regarding the production of secondary metabolites. In this sense, photosynthetic performance can directly impact plant growth and development.

Although *P. glomerata* has been widely used in the pharmacological industry, few studies explore the physiological aspects to contribute to a better understanding of the factors that modulate the 20E biosynthetic production. Furthermore, the investigation of *P. glomerata* diploid and synthetic polyploid accessions under photoautotrophic propagation will help to better understand the morphological and physiological changes occurring in these plants. Thus, this work aimed to study the photosynthetic performance, characterization of the leaf anatomy and 20E levels in *in vitro* photoautotrophic propagation of diploid and synthetic polyploid accessions of *P. glomerata*. Also, a rapid and integrated system for evaluation of *in vitro* photosynthesis was developed for these evaluations.

Materials and methods

Plant material and culture conditions

The plant material used in this study was obtained from the *P. glomerata in vitro* Germplasm Bank maintained at the Tissue Culture Laboratory II (LCTII-Bioagro, Federal University of Viçosa), which has 71 diploids accessions and 5 synthetic polyploids derived from accession 22 (Gomes et al., 2014) kept in culture medium MS (Murashige & Skoog, 1962).

Under laminar flow chamber, apical buds of diploid (Ac 04, 22 and 43) and synthetic polyploid accessions (Poly 28, 60, 68 and 74) were excised from plants with 30 days of *in vitro* culture and transferred one explant per flask (350 mL). Each flask contained 35 mL of MS, vitamins MS (0.05 g L^{-1} nicotinic acid, 0.05 g L^{-1} pyridoxine.HCl, 0.01 g L^{-1} thiamine.HCl and 0.2 g L^{-1} glycine), 100 mg L^{-1} myo-inositol, pH adjusted to 5.7 and using a 4 g substrate composed of unbleached cellulose plus vermiculite (ratio 1:2, respectively) as support material (Corrêa et al., 2015). The flasks containing culture medium were previously sterilized by autoclaving at 121ºC and 1.5 atm for 20 min.

Two 10 mm-diameter holes were made in the lid of each flask and covered with 0.5 µm-pore Fluoropore hydrophobic membranes (PFTE, MilliSeal® Air Vent, Tokyo, Japan), which allow a CO_2 exchange rate of 25 µL L^{-1} s^{-1} (Batista et al., 2017). Cultures were maintained in a growth room at 25 ± 2°C and 60 µmol m^{-2} s^{-1} photonic irradiation provided by two red and blue led lamps (LabPAR LL-HR/DB-480, 11.6 W) under 16-h photoperiod for 30 days. The spectral distribution of the light source is shown in Figure 1. Absorption spectra were recorded at wavelengths ranging from 400 to 750 nm on a spectroradiometer using the Ocean Optics Spectra-Suite data acquisition software (Ocean Optics®, Dunedin, FL).

Leaf area and dry mass

For the leaf area analysis, the leaves were fixed on laminated graph paper and photographed with the Nikon® digital camera. The images were processed in the ImageJ software (Schneider et al., 2012), available on https://imagej.nih.gov/ij/. Plants were dried in a forced air circulation oven at 50 °C until reaching a constant mass to determine the dry weight.

Photosynthetic pigments (chlorophylls a, b *and carotenoids)*

The concentrations of photosynthetic pigments were determined as described by Santos et al. (2008): three leaf disks (5 mm diameter) were incubated in 5 mL $CaCO_3$ saturated with dimethylsulfoxide (DMSO) in closed flasks covered with laminated paper. The absorbance readings were performed after 48 h of incubation at 480, 649 and 665 nm using the spectrophotometer (UV-Vis ThermoScientific^{TM}Genesys 10S). The determination of carotenoids and chlorophylls *a* and *b* followed Welburn (1994).

Glucose, fructose and sucrose content

Leaf samples, collected at the end of the experiment, were flash frozen in liquid nitrogen. The metabolites were extracted with ethanol and the glucose, fructose, and sucrose contents were determined in the soluble fraction according to Fernie et al. (2001). 160 µL of the reaction medium (100 mM HEPES/KOH, 3 mM $MgCl_2$, 118 mM ATP, 48.4 mM $NADP^+$, 56 IU G6PDH 5 mg mL^{-1} at pH 7) were added to the spots plus 30 µL of the ethanolic extract and 20 µL of ethanol 80%. The readings were performed in a microplate reader (OptiMax Tunable Microplate Reader) at 340 nm with 1-min intervals between readings.

Once the optical density (OD) was stabilized, 5 µL of the following enzymes were added successively: hexokinase (1.5 U per reaction), phosphorylose isomerase (0.7 U per reaction) and invertase (5 U per reaction), after approximately 25 min between each application. To estimate the sugar concentration (results expressed in µmol g^{-1}), an equation was used based on the Lambert-Beer law:

$$\mu mol\ NADPH = \Delta OD / (2{,}85 * 6{,}22)$$

Leaf Anatomy

For structural analysis under light microscopy, three samples to the central region of the first pair of fully expanded leaves were fixed in Karnovsky's solution (2.5% glutaraldehyde and 2.5% paraformaldehyde in 0.05 M cacodylate buffer, at pH 7,2) (Karnovsky, 1965). The samples were dehydrated in ethanolic series and included in methacrylate (Historesin, Leica Instruments, Heidelberg, Germany). Cross sections (5 µM) were obtained on a self-advanced rotary microtome (RM2155, Leica Microsystems Inc., Deerfield, U.S.A.) and colored with Toluidine Blue at pH 4.0 (O'Brien and McCully, 1981). The blades were mounted on Permount. Of each cross section made 3

photos of the leaf lamina, near the margin, center and near the midrib. The thickness of the mesophilic layer (µm) adaxial epidermis (µm), abaxial epidermis (µm), palisade parenchyma (µm) in three points within each photo.

The paradermal sections of three samples to the central region of the first pair of fully expanded leaves were processed by diaphanization conducted with an aqueous 2.5% sodium hydroxide and a 20% (v/v) commercial sodium hypochlorite solution. The diaphanized material was dehydrated in an ethanolic series and colored with alcoholic fuchsin, mounted with gelatin glycerin between blade and cover and sealed with colorless enamel.

Three photos were documented for each slide in the margin, center and near the midrib. The thickness of mesophilic layer (µm) adaxial epidermis (µm), abaxial epidermis (µm), palisade parenchyma (µm) in three points within each photo the cross sections and stomatal density and guard cells measurement in pardermal sections. Observations and photographic records were performed in a photomicroscope (AX70TRF, Olympus Optical, Tokyo, Japan) equipped with an U-Photo camera system (Spot Insight Color 3.2.0, Diagnostic Instruments Inc., USA). The digital images were manually processed with ImageJ software (Schneider et al., 2012).

Photosynthetic activity and chlorophyll a *fluorescence*

The *in vitro* photosynthetic activity was determined with a segmented infrared gas analyzer system (IRGA) (Figure 2) adapted from Costa et al. (2014). The light energy source is composed of eight white LEDs (Figure 3) disposed within the side of a polystyrene vessel (Figure 2F). The LEDs were connected in a direct continuous 12 volts current system, formed by two parallel sets of four series-connected LEDs (Figure 2E).

The chlorophyll *a* fluorescence parameters were determined by the MINI-PAM modulated fluorometer (Heinz Walz, Effeltrich, GmbH), the maximum quantum efficiency of PSII (*Fv/Fm*) was evaluated in leaves adapted to the dark for 30 min in order to completely open the reaction centers (oxidized primary acceptors). Initial fluorescence (F_0) and maximum fluorescence (*Fm*) were measured in order to determine the maximum quantum efficiency of photosystem II (*Fv/Fm*, in which $Fv = Fm-F_0$). The plants were subsequently exposed to light for a period of approximately 30 min under 65 µmol m^{-2} s^{-1} of irradiance, and then the measurements of the fluorescence parameters of the light-adapted plants were performed.

The photosynthetic performance in relation to photon flow density (PFD) was determined by programming the fluorometer with increasing light levels (0-1500 µmol m^{-2} s^{-1}) over 4 min divided into eight levels of 30 s each. The minimum fluorescence of the leaf in the illuminated region was calculated according to the formula: $F_0' = F_0/[(Fm-F_0/Fm)+F_0/Fm')]$ (Oxborough & Baker, 1997). The quantum yield effect of PSII ($\Delta F/Fm'$) on leaf lit according to Genty et al. (1989), using the formula $\Delta F/Fm' = (Fm'-F/Fm')$. The apparent rate of electron transport (ETR), was calculated by means of the formula: ETR= $\Delta F/Fm'$*PAR*0.84*0.5, in which: PAR is the photons flux (µmol $m^{-2}s^{-1}$) incident on the leaves; 0.5 is the value corresponding to the fraction of excitation energy distributed to the PSII; 0.84 corresponds to the fraction of incident light absorbed by the leaves (Bilger et al., 1995).

Determination of β-ecdysone levels

The β-ecdysone (20E) levels were determined in the shoot of the plants by high-performance liquid chromatography (HPLC), after a methanolic extraction, according to Kamada et al. (2009). The methanolic 20E extracts were obtained with 100 mg of *P. glomerata* dry material mixed with 10 mL of methanol, after extraction, the samples were stored in the dark at room temperature (25 ± 2 ºC) for seven days, under daily stirring of the extract. Subsequently, the extracts were centrifuged (15 min/5000 rpm) and the supernatant collected and centrifuged again (15 min/5000 rpm). The methanolic extracts were analyzed by HPLC using the following conditions: Shimadzu model LC-10AI equipment, equipped with SPD-10AI detector, CBM-10A; Bomdesil C 18 column (5.0 µm x 4.6 mm x 250 mm). The mobile phase was composed of 1:1 (v/v) methanol-water, with a flow of 1 mL min^{-1}, injected sample volume of 10 µL; reading at λ = 246 nm and sample run time of 15 min. The data was integrated through the Shimadzu LC10 software. The results were compared to a standard curve in the range of 0 to 120 mg L^{-1}

Statistical analysis

A completely randomized design was used. Each treatment had six replicates, composed by one flask with one explant, totalizing 6 explants per treatment. The data were subjected to analysis of variance. When necessary, the means were compared by the Tukey's test at 5% probability, using the GENES software (Cruz, 2016) and the regression models were adjusted using the SigmaPlot software.

Results

After 30 days of *in vitro* cultivation, the plants showed significant differences in the growth parameters evaluated (Figure 4). The Ac 04, Poly 28, and Poly 60 had higher leaf area, whereas the Ac 43 showed the lowest, becoming Ac 22, Poly 68 and Poly 74 with intermediate leaf area. The Ac 22 and Ac 43 presented greater leaf number and Poly 68 presented the lower average: 8.6 leaves per plant. However, both Poly 68 and Poly 60 presented more expanded leaves. The higher accumulation of biomass occurred in Ac 04 and Poly 28 with a mean of 88 mg, approximately 34% higher than the lower: Ac 43 (Table 1).

The morphoanatomic development of *P. glomerata* plants under *in vitro* photoautotrophic system varied significantly among the diploid and polyploid accessions. In general, polyploidy plants had greater epidermal abaxial and adaxial thickness (Figure 5 J, K). The mesophyll (Meso) was larger in Poly 60, 68 and 74 and smaller in Ac 04, whereas the Poly 28, Ac 22 and Ac 43 showed intermediate values (Figure 5H). Palisade parenchyma (PP) was larger in Poly 74, with Ac 04 presenting smaller thickness (PP) (Figure 5I). However, spongy parenchyma (SP) width did not differ, with an averange of 158.54 µm.

Regarding the area of the tissue that forms the internal parts of a leaf, the differences between the polyploid and diploid plants were more evident. The polyploids present more voluminous cells (Table 2). The Ac 04 presented the lower ratio PP/Meso and PP/SP, although higher SP/Meso.

Diploid plants (Ac 04, 22 and 43) showed 42% more stomata on the abaxial surface compared to the tetraploids (83.54 stomata mm^{-2} on diploids and 47.65 stomata mm^{-2} on tetraploids) (Figure 6-R). The adaxial surface of Ac 22 displayed the highest average (20.88 STD mm^{-2}) and Poly 74 the lower (9.14 STD mm^{-2}). The others plants (Ac 04, Ac 43, Poly 28, Poly 60 and Poly 68) showed intermediate results (Figure 6-O). The length and width of the stomata presented small variations among the diploids and polyploids, however a pattern of larger stomata for polyploid (Figure 6 A-C, E-Q, and S-T).

The highest content of photosynthetic pigments was observed in the diploid Ac 04. The Poly 28 and Poly 68 showed the lower averages for chlorophyll (Chl) *a*, *b* and total chlorophylls, whereas the Poly 68 displayed the lower mean for carotenoids. The Ac22, Ac43, Poly 60 and Poly 74 showed no statistically different averages, with intermediate

means (Table 3). The ratio of Chl *a/b* was higher in Ac 04, Ac 22, Ac 43, and Poly 68, and the lowest in Poly 74.

The photosynthetic rate did not show a significant difference for the evaluated accessions, with an average of 7.31 μmol m^{-2} s^{-1}. For the photochemical efficiency parameters, the *Fv/Fm* of 0.79 mean value indicates that plants were not stressed (Murchie & Lawson, 2013) under the experimental conditions. The fluorescence curves show the gain of ETR with the increase of photon flow density (PFD) (Figure 7). In all accessions the saturation irradiance was approximately 580 μmol m^{-2} s^{-1}, however, the *ΔF/Fm*' decreased with increasing PFD.

Regarding sugar contents, sucrose was the only sugar to present differences among assessed plants (Figure 8). Glucose and fructose presented mean values of 0.0008 and 0.0010 μmol mg^{-1}, respectively. The Ac4 and Ac43 showed the greater sucrose accumulation whilst Poly60 and Poly 68 had the lower averages. The other accessions (Ac 22, Poly 28 and Poly 74) presented intermediate values (Figure 8).

The HPLC analysis of the methanolic extracts showed significant differences for the 20-E contents, with Ac 04 showing the highest average, followed by the Ac 43. The Ac 22, Poly 28 and Poly 60 displayed intermediate values, in particular for the Poly 68 and Poly 74 with lower mean values (Figure 9).

Discussion

The use of portable infrared gas analysis for measurement of leaf photosynthesis has been described and the instrumentation of this method has been improved in the last decades. The main determining requirement of the chamber design is that the environment within the camera is as homogeneous as possible, since a chamber projected for a leaf or leaves of one species may be inadequate for many others (Long et al., 1996). Over time, different adaptations and designers of chambers were developed to meet specific demands, for example: sphere leaf chamber (Idle & Proctor, 1983); light-integrating spherical leaf chamber for simultaneous measurement of leaf absorbency, leaf gas exchange and modulated fluorescence emission (Ireland et al., 1989); the substitution of xenon are lamp by LED as a light source for photosynthesis research (Tennessen et al., 1994). The commercially available systems for measuring gas exchange are based on an infrared gas analyzer connected to a chamber clamped over a single leaf and the gas exchange of a small area of the leaf blade is measured (Kölling et al., 2015). More recently Fortineau & Bancal (2018) developed an innovative light chamber for measuring photosynthesis by three-dimensional plant organs, allowing obtaining more accurate estimates of photosynthesis by large 3-D organs. In this study, we developed a light chamber composed of high brightness white LEDs that surrounded a 15 cm long sealed transparent glass flask used to measure plant photosynthesis *in vitro* (Figure 2A). The set of LEDs connected at 12 volts DC provided photosynthetic photon flux density of 600 μmol m^{-2} s^{-1}. The temperature sensor introduced inside the flask (Figure 2B) provides a higher accuracy of the data collected for the estimation of the photosynthetic rate.

The adaptation of the lighting system using LEDs, it proved to be efficient for *in vitro* photosynthetic rate analysis, since the technology used in the development of LEDs allows a greater conversion of electric energy into light energy and low heat dissipation. Another advantage of the system developed is the arrangement of the LEDs in the walls of the box, that on the bottle around with the plant to be evaluated, ensuring that the plant receives light from all directions, with no shading leaves overlap when the light source is positioned in only one direction. However, there are still changes that can further improve the system, such as the use of red and blue LEDs, allowing the evaluation of the in vitro photosynthetic rate in the same conditions that our research group has been conducting in the development of studies related to quality of light.

Morpho-physiological characterization of different accessions may reveal important traits for the selection of plants with favourable characteristics for the better growth, development (biomass accumulation) and production of secondary metabolites (e.g., phytoecdysteroid 20E). In the present study, we report for the first time a comprehensive comparison of morphological and physiological differences of *P. glomerata* polyploid plants (Poly 28, 60, 68, and 74) and three other diploid accessions (Ac 04, 22, and 43). The accessions displayed strong differences in morpho-physiological traits (e.g., leaf expansion, number of leaves, stomata and ETR); in addition, also displayed differences in the 20E contents.

The anatomical characterization evidenced an increase of mesophyll cells from palisade parenchyma and spongy parenchyma in *P. glomerata* polyploids, but without causing differential impacts on photosynthetic performance. These results may be related to the fact that these polyploids developed smaller stomatal density, although the increased stomata size. The stomata play a role in establishing communication of the internal leaf environment with the atmosphere, directly affecting the internal CO_2 concentration. Overall, a greater diffusive resistance of the stomata reduces the photosynthesis by restricting the gas conduction throughout the leaf.

Since the polyploids had lower stomatal density, it was expected that the photosynthetic rate would be lower. However, maybe due the effect of the greater cellular expansion from DNA duplication, polyploids have larger ostioles (Figure 6), promising a greater stomatal conductance, and somehow compensating the lower stomatal density. Increase in leaf tissue cells in the polyploids was also observed in the stomata cells, in accordance with the results reported elsewhere (Gomes et al., 2014; Corrêa et al., 2016). In the same way, in *Populus temuloides* triploid plants had similar transpiration rates to diploid ones, due to the larger leaf size and the lower conductance of the boundary layers despite the higher stomatal conductance (Greer et al., 2017).

The main environmental factors that affect the photosynthetic rate are the availability of light, CO_2, temperature, water and nutrients. The plants of the present study were cultivated under *in vitro* photoautotrophic conditions, with light and controlled temperature, water and nutrients supply throughout the culture period. The PTFE membranes guaranteed the supply of CO_2 through the gas exchanges between the *in vitro* and *ex vitro* environment (Saldanha et al., 2012). This way, the only source of variation related to the photosynthetic rates would be related to the genotypic characteristics of each particular accession.

Field photosynthesis analyzers are designed to be used with leaf blades, by employing unidirectional light sources (Hogewoning et al., 2010), they are not adapted to plant evaluations in the *in vitro* environment. Since for the use of such equipment the plants are removed from the environment *in vitro* and only the pinched leaf area is evaluated. However, there is a need to study photosynthetic competence to improve our understanding of plant physiology, promote resistance and tolerance in the acclimation period. The use of LEDs as a light source and a cooler made it possible to obtain precise measurements of liquid photosynthesis thanks to its design, the system evenly illuminated every plant inside the bottle while preventing them from overheating.

The effective quantum yield of PSII (*ΔF/Fm'*), measuring the proportion of light absorbed by the chlorophyll associated with PSII that is used to reduce Q_A. Thus, this parameter provides an estimate of electron transport and an indicative of photosynthesis in general (Oxborough & Baker, 1997). This same pattern of decrease in *ΔF/Fm'* with increasing PFD was observed by Costa et al. (2014). It is an indication that not all electrons involved in photochemistry are used for the CO_2 fixation, can be influenced by the rate of photorespiration, cyclic electron transport in the PSII and by the water-water cycle. Since this parameter is the effective quantum yield of PSII, it is used to calculate the linear electron transport rate and, in this way, to infer *in vivo* photosynthetic competence.

Our data also showed that the ETR and sucrose levels can directly affect secondary metabolism (e.g., 20E) in *P. glomerata* plants, since the polyploid accesses showed lower ETR, sucrose levels and, as a consequence, there was a low investment in 20E when contrasted to the diploid accessions. This can also be confirmed by significant correlations between sucrose x ETR and sucrose x 20-E (Supplementary Figure 1). Indeed, secondary metabolic performance is directly linked to primary metabolism, which in turn, depends on the genetic characteristics that allow plants to set higher carbon rates to invest in growth and secondary metabolism.

Sucrose plays an important role in plant growth and provides C skeletons for the synthesis of secondary metabolism (Jing et al., 2018). Here, Ac04 showed a higher sucrose and 20E contents (Figure 8-9). In other studies, it was also shown that primary metabolites (glucose, fructose, sucrose and sorbitol) had a positive effect on secondary metabolites (Lu *et al*., 2017), corroborating our findings. We suppose that sucrose, as source of carbon (or carbon availability), may be directed to secondary metabolism and consequently contribute to increased 20E content in the whole-plant. Consequently, that

energetic pool related to the availability of carbohydrates (e.g., sucrose) have been also related to the synthesis of secondary metabolites (Huang et al., 2017a, b), including 20E biosynthesis (Figure 9).

Furthermore, in spite of the effects of polyploidization on morphological characteristics, the fluorescence and the 20E content were dependent on the genetic background, considering that the differences between polyploid plants and Ac 22 are not evidenced. Therefore, we can infer the existence of great biochemical plasticity among the accessions for the use of the CO_2 fixed by the photosynthetic process. Given this assumption, we can infer that the differences in the accumulation of biomass are related to other intrinsic factors of each plant, such as mitochondrial respiration, which is extremely important in the supply of ATP at night, energy is necessary for the accomplishment of other biochemical processes. Another important aim is to produce numerous intermediate molecules that can be used in other metabolic pathways, including for secondary metabolites, as seems to be the case in *P. glomerata*, with remarked phytoecdysteroids biosynthetic pathways, in Batista et al. (2018), affirmed that photoautotrophy produces 20E, and this regulation liked at the that genes *Phantom* and *Spook* of the P450 family.

Here, we showed for the first time the morphogenetic changes resulting from the *in vitro* induced polyploidization in *P. glomerata*, which did not affected the *in vitro* photosynthetic capacity of the evaluated accessions. However, among the observed differences the highest impact variable was observed for photosynthetic pigments (chlorophyll *a*, *b* and carotenoids), in which Ac04 presented the highest total chlorophyll, affecting the light absorption rate of the leaf and also the energy cycle between the reaction center, raising the relative ETR curve. With the greater absorption of light energy, Ac04 was also the plant with the highest content of sucrose. The increase of the content of non-structural carbohydrates is linked with 20E biosynthesis pathways. In addition, we constructed an innovative auxiliary light source for the measurement of photosynthetic competence of plants *in vitro*, which will be fundamental for studies aiming to evaluate the photosynthetic potential of plants grown in closed systems.

Conflict of Interest

The authors declare no conflict of interest.

Acknowledgements

The authors are grateful to the Universidade Federal de Viçosa, the Instituto de Biotecnologia Aplicada à Agropecuária – BIOAGRO and especially Laboratory of Plant Anatomy/DBV for supporting anatomical analysis.

Funding

This work was supported by the Conselho Nacional de Desenvolvimento Científico e Tecnológico (CNPq) (Brasília, DF, Brazil), Fundação de Amparo à Pesquisa do Estado de Minas Gerais (FAPEMIG) (Belo Horizonte, MG, Brazil) and Fundação Arthur Bernardes (Funarbe - UFV). KC was recipient of a scholarship from Coordenação de Aperfeiçoamento de Pessoal de Nível Superior (CAPES) (Brasília, DF, Brazil).

Author Contributions

KC, MR, ACC and WCO designed the experiment. KC, MR, ACC, TDS and SHSF performed analyses. KC, MR, ACC, SHSF and WCO contributed to the data interpretation and to the writing of the paper with contributions of all the authors. DSB, RSA CWS, and FMDM also collaborated effectively in drafting the final version of the paper. All authors read and approved the final paper.

References

Baker N R. (2008). Chlorophyll fluorescence: a probe of photosynthesis in vivo. **Annual Review of Plant Biology**, 59: 89-113. doi.org/10.1146/annurev.arplant.5-9.032607.092759

Baker NR, Rosenqvist E. (2004). Applications of chlorophyll fluorescence can improve crop production strategies: An examination of future possibilities. **Journal of Experimental Botany**, 55: 1607-1621. doi.org/10.1093/jxb/erh196

Batista DS, Dias LLC, Rêgo MM, Saldanha CW, Otoni WC. (2017). Flask sealing on in vitro seed germination and morphogenesis of two types of ornamental pepper explants. **Ciência Rural**, 47: 1-6. doi.org/10.1590/0103-8478cr20150245

Batista DS, Koehler AD, Romanel E, de Souza VC, Silva TD, Almeida MC, Maciel TEF, Ferreira PRB, Felipe SHS, Saldanha CW, Maldaner J, Dias LLC, Festucci-Buselli RA, Otoni WC. (2018). De novo assembly and transcriptome of *Pfaffia glomerata* uncovers the role of photoautotrophy and the P450 family genes in 20-hydroxyecdysone production. **Protoplasma**, 1-14. doi.org/10.1007/s00709-018-1322-1

Bilger W, Schreiber U, Bock M. (1995). Determination of the quantum efficiency of photosystem II and nonphotochemical quenching of chlorophyll fluorescence in the field. **Oecologia**, 102: 425-432. doi.org/10.1007/BF00341354

Chen C. (2006). In situ measurement of microclimate for the plantlets cultured *in vitro*. **Biosystems Engineering**, 95:413-423. doi.org/10.1016/j.biosystemseng.2006.08.001

Cohen H, Fait A, Tel-Zur N. (2013). Morphological, cytological and metabolic consequences of autopolyploidization in *Hylocereus* (Cactaceae) species. **BMC Plant Biology**, 13: 173. doi.org/10.1186/1471-2229-13-173

Corrêa JPO, Vital CE, Pinheiro MVM, Batista DS, Azevedo JFL, Saldanha CW, Cruz ACF, Damatta FM, Otoni WC. (2015). *In vitro* photoautotrophic potential and ex vitro photosynthetic competence of *Pfaffia glomerata* (Spreng.) Pedersen accessions. **Plant Cell, Tissue and Organ Culture**, 121: 289-300. doi.org/10.1007/s11240-014-0700-4

Corrêa JPO, Vital CE, Pinheiro MVM, Batista DS, Saldanha CW, Cruz ACF, Notini MM, Freitas DMS, Damatta FM, Otoni WC. (2016). Induced polyploidization increases 20-hydroxyecdysone content, *in vitro* photoautotrophic growth, and *ex*

vitro biomass accumulation in *Pfaffia glomerata* (Spreng.) Pedersen. **In Vitro Cellular and Developmental Biology - Plant**, 52: 45-55. doi.org/10.1007/s1162

Costa AC, Rosa M, Megguer CA, Silva FG, Pereira, FD, Otoni, WC. (2014). A reliable methodology for assessing the in vitro photosynthetic competence of two Brazilian savanna species: *Hyptismarrubioides* and *Hancorniaspeciosa*. **Plant Cell, Tissue and Organ Culture**, 117: 443-454. doi.org/10.1007/s11240-014-0455-y

Cruz CD. (2016). Genes Software - extended and integrated with the R, Matlab and Selegen. **Acta Scientiarum. Agronomy**, 38: 547-552. doi.org/10.4025/actasciagron.v38i4.32629

Dias MC, Pinto G, Correia CM, Moutinho-Pereira J, Silva S, Santos C. (2013). Photosynthetic parameters of *Ulmus minor* plantlets affected by irradiance during acclimatization. **Biologia Plantarum**, 57: 33-40. doi.org/10.1007/s10535-012-0234-8

Fernie AR, Roscher A, Ratcliffe RG, Kruger NJ. (2001). Fructose 2,6-bisphosphate activates pyrophosphate: fructose-6-phosphate 1-phosphotransferase and increases triose phosphate to hexose phosphate cycling in heterotrophic cells. **Planta**, 212: 250-263. doi.org/10.1007/s004250000386

Flores R, Brondani Jr D, Cezarotto Jr V, Giacomelli SR, Nicoloso FT (2010) Micropropagation and ecdysone content of the Brazilian ginsengs *Pfaffia glomerata* and *Pfaffia tuberosa*. **In Vitro Cellular and Developmental Biology - Plant** 46: 210-217. doi: 10.1007/s11627-010-9286-7

Fortineau A, Bancal P. (2018). An innovative light chamber for measuring photosynthesis by three-dimensional plant organs. **Plant Methods** 14: 21. doi.org/10.1186/s13007-018-0288-5

Freitas CS, Baggio CH, Da Silva-Santos JE, Rieck L, De Moraes Santos CA, Correa JRC, Ming LC, Cortez DAG, Marques MCA. (2004). Involvement of nitric oxide in the gastroprotective effects of an aqueous extract of *Pfaffia glomerata* (Spreng) Pedersen, Amaranthaceae, in rats. **Life Sciences**, 74: 1167-1179. doi.org/10.1016/j.lfs.2003.08.003

Fuentes G, Talavera C, Desjardins Y, Santamaria JM. (2005). High irradiance can minimize the negative effect of exogenous sucrose on the photosynthetic capacity of *in vitro* grown coconut plantlets. **Biologia Plantarum**, 49: 7-15. doi.org/10.1007/s10535-005-7015-6

Fujiwara K, Kozai T, Watanabe I. (1987). Measurements of carbon dioxide gas concentration in closed vessels containing tissue cultured plantlets and estimates of net photosynthetic rates of the plantlets. **Journal of Agricultural Meteorology**, 43: 21-30.

Gallone A, Hunter A, Douglas GC. (2014). Polyploid induction *in vitro* using colchicine and oryzalin on Hebe 'Oratia Beauty': Production and characterization of the vegetative traits. **Scientia Horticulturae**, 179: 59-66. doi.org/10.1016/j.scienta.-2014.09.014

Genty B, Briantais JM, Baker NR (1989) The relationship between the quantum yield of photosynthetic electron transport and quenching of chlorophyll fluorescence. **Biochimica et Biophysica Acta**, 990: 87-92. doi.org/10.1016/S0304-4165(89)80016-9

Goltsev VN, Kalaji HM, Paunov M, Bąba W, Horaczek T, Mojski J, Kociel H, Allakhverdiev SI. (2016). Variable chlorophyll fluorescence and its use for assessing physiological condition of plant photosynthetic apparatus. **Russian Journal of Plant Physiology**, 63: 869-893. doi.org/10.1134/S1021

Gomes SSL, Saldanha CW, Neves CS, Trevizani M, Raposo NRB, Notini MM, Santos MO, Campos JMS, Otoni WC, Viccini LF. (2014) Karyotype, genome size, and *in vitro* chromosome doubling of *Pfaffia glomerata* (Spreng.) Pedersen. **Plant Cell, Tissue and Organ Culture**, 118: 45-56. doi.org/10.1007/s11240-014-0460-1

Greer BT, Still C, Cullinan GL, Brooks JR, Meinzer FC. (2017). Polyploidy influences plant–environment interactions in quaking aspen (*Populustremuloides*Michx.). **Tree Physiology**, 1-11. doi.org/10.1093/treephys/tpx120

Hanson AD. Edelman J. (1971) Photosynthesis by carrot tissue cultures. **Planta**, 102: 11-25. doi.org/10.1007/BF00391446

Hazarika BN (2006). Morpho-physiological disorders in *in vitro* culture of plants. **Scientia Horticulturae**, 108: 105-120. doi.org/10.1016/j.scienta.2006.01.038

Hdider C, Desjardins Y. (1995). Reduction of ribulose-1,5-bisphosphate carboxylase/oxygenase efficiency by the presence of sucrose during the tissue culture of strawberry plantlets. **In Vitro Cellular & Developmental Biology - Plant**, 31: 165-170. doi.org/10.1007/BF02632014

Hogewoning SW, Trouwborst G, Harbinson J, Van Ieperen W. (2010). Light distribution in leaf chambers and its consequences for photosynthesis measurements. **Photosynthetica**, 48: 219-226. doi.org/10.1007/s11099-010-0027-2

Hopfner U, Schenck TL, Chávez MN, Machens HG, Bohne AV, Nickelsen J, Giunta RE, Egaña JT. (2014). Development of photosynthetic biomaterials for *in vitro* tissue engineering. **Acta Biomaterialia**, 10: 2712-2717. doi.org/10.1016/j.actbio.20-13.12.055

Huang J, Hammerbacher A, Forkelova L, Hartmann H. (2017a). Release of resource constraints allows greater carbon allocation to secondary metabolites and storage in winter wheat. **Plant Cell & Environment**, 40: 672-685. doi.org/10.1111/pce.12885

Huang JB, Reichelt M, Chowdhury S, Hammerbacher A, Hartmann H. (2017b). Increasing carbon availability stimulates growth and secondary metabolites via modulation of phytohormones in winter wheat. **Journal of Experimental Botany**, 68: 1251-1263. doi.org/10.1093/jxb/erx008

Iannicelli J, Elechosa MA, Juárez MA, Martínez A, Bugallo V, Bandoni AL, Escandón AS, Baren CM. (2016). Effect of polyploidization in the production of essential oils in *Lippia integrifolia*. **Industrial Crops and Products**, 81: 20-29. doi.org/10.1016/j.indcrop.2015.11.053

Iarema L, Cruz ACF, Saldanha CW, Dias LLC, Vieira RF, Oliveira EJ, Otoni WC. (2012). Photoautotrophic propagation of Brazilian ginseng [*Pfaffia glomerata* (Spreng.) Pedersen]. **Plant Cell, Tissue and Organ Culture**, 110: 227-238. doi.org/10.1007/s11240-012-0145-6

Idle DB, Proctor CW. (1983). An integrating sphere leaf chamber. **Plant, Cell & Environment**, 6: 437-439. doi.org/10.1111/j.1365-3040.1983.tb01279.x

Ireland CR, Long SP, Baker NR. (1989). An integrated portable apparatus for the simultaneous field measurement of photosynthetic CO_2 and water vapour exchange, light absorption and chlorophyll fluorescence emission of attached leaves. **Plant, Cell & Environment** 12: 947-958. doi.org/10.1111/j.1365-3040.1989.tb01975.x

Jing X, Wang H, Gong B, Liu S, Wei M, Ai X, Li Y, Shi Q. (2018) Secondary and sucrose metabolism regulated by different light quality combinations involved in melon tolerance to powdery mildew. **Plant Physiology and Biochemistry**, 124: 77-87.

Kadleček P, Rank B, Tichá, I. (2003). Photosynthesis and photoprotection in *Nicotiana tabacum* L. *in vitro*-grown plantlets. **Journal of Plant Physiology**, 160: 1017-1024. doi.org/10.1078/0176-1617-00980

Kamada T, Picoli EAT, Vieira RF, Barbosa LCA, Cruz CD, Otoni WC (2009) Variação de caracteres morfológicos e fisiológicos de populações naturais de *Pfaffia*

glomerata (Spreng.) Pedersen e correlação com a produção de β-ecdisona. **Revista Brasileira Plantas Medicinais**, 11: 247-256.

Karnovsky MJ. (1965). A formaldehyde-glutaraldehyde fixative of high osmolarity for use in electron microscopy. **Journal of Cell Biology**, 27: 37-138.

Kennedy RA, Barnes JE, Laetsch WM. (1977). Photosynthesis in C4 plant tissue cultures significance of Kranz anatomy to C4 acid metabolism in C4 plants. **Plant Physiology**, 59: 600-603. doi.org/10.1104/pp.59.4.600

Kitzing C, Pröschold T, Karsten U. (2014). UV-induced effects on growth, photosynthetic performance and sunscreen contents in different populations of the green alga *Klebsormidium fluitans* (Streptophyta) from alpine soil crusts. **Microbial Ecology**, 67: 327-340. doi.org/10.1007/s00248-013-0317-x

Kölling K, George GM, Künzli R, Flütsch P, Zeeman SC. (2015). A whole-plant chamber system for parallel gas exchange measurements of Arabidopsis and other herbaceous species. **Plant Methods** 11: 48. doi.org/10.1186/s13007-015-0089-z

Long SP, Farage PK, Garcia RL. (1996). Measurement of leaf and canopy photosynthetic CO_2 exchange in the field. **Journal of Experimental Botany** 47: 1629-1642. doi.org/10.1093/jxb/47.11.1629

Lu Y, Chen Q, Bu Y, Luo R, Hao S, Zhang J, Tian J, Yao Y. (2017). Flavonoid accumulation plays an important role in the rust resistance of *Malus* plant leaves. **Frontiers in Plant Science**, 1286. doi.org/10.3389/fpls.2017.01286

Martins JPR, Verdoodt V, Pasqual M, De Proft, M. (2015). Impacts of photoautotrophic and photomixotrophic conditions on *in vitro* propagated *Billbergia zebrina* (Bromeliaceae). **Plant Cell, Tissue and Organ Culture**, 123: 121-132. doi.org/10.1007/s11240-015-0820-5

Martins MCM, Hejazi M, Fettke J, Steup M, Feil R, Krause U, Arrivault S, Vosloh D, Figueroa CM, Ivakov A, Yadav UP, Piques M, Metzner D, Stitt M, Lunn JE. (2013). Feedback inhibition of starch degradation in *Arabidopsis* leaves mediated by trehalose 6-phosphate. **Plant Physiology**, 163: 1142-1163. doi.org/10.1-104/pp.113.226787

Maxwell K, Johnson GN. (2000). Chlorophyll fluorescence: a practical guide. **Journal of Experimental Botany**, 51: 659-668. doi.org/10.1093/jexbot/51.345.659

Mayak S, Tirosh T, Ilan A, Duvdevani A, Khayat E. (1998) Growth and development of pineapple (*Ananas comosus* L.) plantlets cultured *in vitro* at enriched and ambient

CO_2 environments. **Acta Horticulturae**, 461: 225-229. doi: 10.17660/ActaHortic.1998.461.23

Mazzeo GCCS, Cortez FS, Pusceddu FH, Santos AR, Guimarães LL, Amaral FP, Silva MPO, Toma W. (2013) Evaluation of antiulcerogenic and ecotoxicological activities of 70% hydroalcoholic extract obtained from *Pfaffia glomerata* (Spreng) Pedersen (Amaranthaceae) leaves. **Unisanta BioScience**, 2: 75-80.

Mccarthy A, Chung M, Ivanov AG, Krol M, Inman M, Maxwell DP, Hüner NPA. (2016) An established *Arabidopsis thaliana* var. Landsberg erecta cell suspension culture accumulates chlorophyll and exhibits a stay-green phenotype in response to high external sucrose concentrations. **Journal of Plant Physiology**, 199: 40-51. doi.org/10.1016/j.jplph.2016.05.008

Moura CL, Casemiro LA, Martins CHG, Cunha WR, Silva MLA, Cury, AHV. (2011). Evaluation of the antimicrobial activity of the plant species *Pfaffia glomerata* against oral pathogens. **Revista Investigação**, 11: 24-28.

Murchie EH, Lawson T. (2013). Chlorophyll fluorescence analysis: a guide to good practice and understanding some new applications, **Journal of Experimental Botany**, 64: 3983-3998. doi.org/10.1093/jxb/ert208

Neto AG, Costa JMLC, Belati C, Vinholis AHC, Possebom LS, Da Silva Filho AA, Cunha R Carvalho JCT, Bastos JK, Silva MLA. (2005). Analgesic and anti-inflammatory activity of a crude root extract of *Pfaffia glomerata* (Spreng.) Pedersen. **Journal of Ethnopharmacology**, 96: 87-91. doi.org/10.1016/j.jep.2004.08.035

Nunes S, Santos C, Moutinho-Pereira J, Correia C., Oliveira H, De Oliveira JMF, Pereira VT Almeida T, Marum L, Dias MC. (2016). Physiological characterization and true-to-typeness evaluation of *in vitro* and *ex vitro* seedlings of *Pinus elliottii*: A contribution to breeding programs. **Plant Physiology and Biochemistry**, 107: 222-227. doi.org/10.1016/j.plaphy.2016.05.039

O'Brien TP, McCully ME. (1981). The study of plant structure: principles and selected methods. Melbourne: Termarcarphy Pty

Oxborough K, Baker NR. (1997). Resolving chlorophyll*a* fluorescence images of photosynthetic efficiency into photochemical and non-photochemical components – calculation of *qP* and *Fv'/Fm'* without measuring *Fo'*.**Photosynthesis Research**, 54: 135-142. doi.org/10.1023/A:1005936823310

Park SY, Moon HK, Murthy HN, Kim YW. (2011) Improved growth and acclimatization of somatic embryo-derived *Oplopanaxelatus* plantlets by ventilated photoautotrophic culture. **Biologia Plantarum**, 55: 559-562. doi.org/10.1007/s10535-011-0125-4

Reinhardt K, Smith WK. (2016). Chlorophyll fluorescence and photosynthetic gas exchange under direct versus diffuse light in evergreen conifer (*Picea pungens*) shoots and broadleaf shrub (*Rhododendron ponticum*) leaves. **Plant Ecology** 217: 443-450. doi.org/10.1007/s11258-016-0586-9

Roach T, Krieger-Liszkay A. (2014). Regulation of photosynthetic electron transport and photoinhibition. **Current Protein and Peptide Science**, 15: 351-362.

Roh KS, Choi BY. (2004). Sucrose regulates growth and activation of rubisco in tobacco leaves *in vitro*. **Biotechnology and Bioprocess Engineering**, 9: 229-235. doi.org/10.1007/BF02942298

Rousseau C, Belin E, Bove E, Rousseau D, Fabre F, Berruyer R, Guillaumés J, Manceau C, Jacques MA, Boureau T. (2013). High throughput quantitative phenotyping of plant resistance using chlorophyll fluorescence image analysis. **Plant Methods**, 9: 17. doi.org/10.1186/1746-4811-9-17

Sáez PL, Bravo LA, Cavieres LA, Vallejos V, Sanhueza C, Font-Carrascosa M, Gil-Pelegrín E, Peguero-Pina JJ, Galmés J. (2017). Photosynthetic limitations in two Antarctic vascular plants: importance of leaf anatomical traits and Rubisco kinetic parameters. **Journal of Experimental Botany,** 68: 2871-2883. doi.org/10.1093/jxb/erx148

Saldanha CW, Otoni CG, Azevedo JLF, Dias LLC, Rêgo MM, Otoni WC. (2012). A low-cost alternative membrane system that promotes growth in nodal cultures of Brazilian ginseng [*Pfaffia glomerata* (Spreng.) Pedersen]. **Plant Cell, Tissue and Organ Culture** 110: 413-422. doi.org/10.1007/s11240-012-0162-5

Saldanha CW, Otoni CG, Azevedo JLF, Dias LLC, Rêgo MM, Otoni WC. (2012) A low-cost alternative membrane system that promotes growth in nodal cultures of Brazilian ginseng [*Pfaffia glomerata* (Spreng.) Pedersen]. **Plant Cell, Tissue and Organ Culture**, 110: 413-422. doi.org/10.1007/s11240-012-0162-5

Saldanha CW, Otoni CG, Notini MM, Kuki KN, Cruz ACF, Neto AR, Dias LLC, Otoni WC. (2013). A CO_2-enriched atmosphere improves *in vitro* growth of Brazilian ginseng [*Pfaffia glomerata* (Spreng.) Pedersen]. **In Vitro Cellular and Developmental Biology - Plant**, 49: 433-444. doi.org/10.1007/s11627-013-9529-5

Saldanha CW, Otoni CG, Rocha DI, Cavatte PC, Detmann KSC, Tanaka FAO, Dias LLC, DaMatta FM, Otoni WC. (2014). CO_2-enriched atmosphere and supporting material impact the growth, morphophysiology and ultrastructure of *in vitro* Brazilian-ginseng [*Pfaffia glomerata* (Spreng.) Pedersen] plantlets. **Plant Cell, Tissue and Organ Culture**, 118:87–99. doi.org/10.1007/s11240-014-0464-x

Schneider CA, Rasband WS, Eliceiri KW. (2012). NIH Image to ImageJ: 25 years of image analysis. **Nature Methods**, 9:671. dx.doi.org/10.1038/nmeth.2089.

Souza Daniel JF, Alves KZ, Silva Jacques D, Silva E, Souza PV, Carvalho MG, Freire RB, Ferreira DT, Freire MFI. (2005). Free radical scavenging activity of *Pfaffia glomerata* (Spreng.) Pederson (Amaranthaceae). **Indian Journal of Pharmacology**, 37:174–178. doi: 10.4103/0253-7613.16215

Supaibulwattana K, Kuntawunginn W, Cha-Um S, Kirdmanee C. (2011). Artemisinin accumulation and enhanced net photosynthetic rate in Qinghao (*Artemisia annua* L.) hardened *in vitro* in enriched-CO_2 photoautotrophic conditions. **Plant Omics**, 4: 75-81.

Tennessen DJ, Singsaas EL, Sharkey TD. (1994). Light-emitting diodes as a light source for photosynthesis research. **Photosynthesis Research**, 39: 85-92. doi.org/10.1007/BF00027146

Wang H-B, Md. Ali S, Moriyama M, Iwanaga M, Kawasaki H, (2012) 20-hydroxyecdysone and juvenile hormone analog prevent precocious metamorphosis in recessive trimolter mutants of *Bombyx mori*. **Insect Biochemistry and Molecular Biology**, 42: 102-108.

Welburn AR. (1994). The spectral determination of chlorophylls *a* and *b*, as well as total carotenoids, using various solvents with spectrophotometers of different resolution. **Journal of Plant Physiology**, 144: 307-313. doi.org/10.1016/S0176-1617(11)81192-2

Wu HC, Lin CC. (2013). Carbon dioxide enrichment during photoautotrophic micropropagation of *Protea cynaroides* L. plantlets improves *in vitro* growth, net photosynthetic rate, and acclimatization. **HortScience**, 48: 1293-1297.

Xiao Y, Niu G, Kozai T (2011) Development and application of photoautotrophic micropropagation plant system. **Plant Cell, Tissue and Organ Culture,** 105: 149-158. doi: 10.1007/s11240-010-9863-9

Xu D, Huanget Z, Cen Y-J, Chen Y, Freed S, Hu X-G. (2009). Antifeedant activities of secondary metabolites from *Ajuga nipponensis* against adult of striped flea beetles, *Phyllotreta striolata*. **Journal of Pest Science,** 82: 195-202.

Yusuf MA, Kumar D, Rajwanshi R, Strasser RJ, Tsimilli-Michael M, Govindjee, Sarin NB. (2010). Overexpression of γ-totopherol methyl transferase gene in transgenic *Brassica juncea* plants alleviates abiotic stress: Physiological and chlorophyll a fluorescence measurements. **Biochimica et Biophysica Acta,** 1797: 1428-1438. doi.org/10.1016/j.bbabio.2010.02.002

Table 1. Means values of leaf area (LA), leaf number (LN), leaf area ratio (LAR) and dry weight (DW) in *P. glomerata* plants grown in *in vitro* photoautotrophic after 30 days of *in vitro* culture.

Accession	**LA** (cm^{-2})	**LN**	**LAR**	**DW** (g)
Ac 04	27.80 a*	12.2 ab	2.322 abc	0.088 a
Ac 22	24.07 ab	12.6 a	1.895 bc	0.079 ab
Ac 43	15.56 b	12.4 a	1.274 c	0.054 b
Poly 28	28.64 a	9.4 ab	3.057 ab	0.088 a
Poly 60	31.20 a	9.4 ab	3.333 a	0.083 ab
Poly 68	25.03 ab	8.6 b	3.098 ab	0.081 ab
Poly 74	22.92 ab	10.8 ab	2.131 abc	0.074 ab
CV** (%)	21.45	17.50	25.79	18.82
lsd***	10.77	3.78	1.264	0.029

*Means followed by the same letter in columns do not differ significantly at the level of $p \leq 0.05$, by the Tukey test. **CV: Coefficient of variation ***lsd: least significant difference.

Table 2. Average area occupied by each tissue found in the inner layers of leaves *P. glomerata* plants grown under photoautotrophic*in vitro* culture after 30 days.

Accession	**Mesophyll** (μm^2)	**PP** (μm^{-2})	**SP** (μm^{-2})	**PP/Meso**	**SP/Meso**	**PP/ SP**
Ac 04	79815.67 b*	31184.79 c	48630.89 c	0.390 b	0.609 a	0.649 b
Ac 22	101328.84 b	44901.97b	56426.87 bc	0.443 ab	0.557 ab	0.799 ab
Ac 43	99386.32 b	43217.80 b	56168.52 bc	0.436 ab	0.563 ab	0.783 ab
Poly 28	131438.16 a	59236.44 a	72201.73 ab	0.452 ab	0.548 ab	0.827 ab
Poly 60	135845.32 a	62428.54 a	73416.78 a	0.461 a	0.539 b	0.867 a
Poly 68	138293.17 a	62295.84 a	75997.32 a	0.450 ab	0.549 ab	0.835 ab
Poly 74	139205.99 a	63391.10 a	75814.89 a	0.457 a	0.542 b	0.849 ab
CV** (%)	11.69	12.64	15.12	8.91	7.05	16.23
lsd***	22678.97	10892.38	16289.93	0.064	0.064	0.213

*Means followed by the same letter in columns do not differ significantly at the level of $p \leq 0.05$, by the Tukey test. *Abbreviations*: Meso: mesophyll, palisade parenchyma (PP), spongy parenchyma (SP), and PP/Meso, SP/Meso and PP/SP ratio; ** CV: Coefficient of variation ***lsd: least significant difference.

Table 3. The content of chlorophyll *a* (Chl*a*) and *b* (Chl*b*), carotenoids, total chlorophylls (Total Chl) and Chl*a/b* ratio in *P. glomerata* plants grown under *in vitro* photoautotrophic conditions, after 30 days of culture.

Accession	**Chl*a*** ($\mu g\ cm^{-2}$)	**Chl*b*** ($\mu g\ cm^{-2}$)	**Carotenoids** ($\mu g\ cm^{-2}$)	**Total Chl** ($\mu g\ cm^{-2}$)	**Chl*a/b***
Ac 04	39.85 a*	12.17 a	8.02 a	52.02 a	3.28 a
Ac 22	33.58 ab	10.07 ab	6.91 ab	43.65ab	3.33 a
Ac 43	34.17 ab	10.27 ab	7.12 ab	44.43ab	3.33 a
Poly 28	31.79 b	9.81 b	7.20 ab	41.60b	3.24 ab
Poly 60	33.23 ab	10.33 ab	7.14 ab	43.56ab	3.22 ab
Poly 68	30.15 b	9.20 b	6.39 b	39.35b	3.28 a
Poly 74	33.40 ab	10.92 ab	7.34 ab	44.31ab	3.06 b
CV** (%)	10.42	10.79	10.61	10.41	3.26
lsd***	7.05	2.25	1.52	9.22	0.21

*Means followed by the same letter in columns do not differ significantly at the level of $p \leq 0.05$, by the Tukey test. ** CV: Coefficient of variation ***lsd: least significant difference.

Figure Captions

Figure 1. Visible light spectrum distribution of red and blue led lamps.

Figure 2. IRGA system scheme targeted to evaluate the photosynthetic rate of plants in conditions *in vitro* (A): Computer (1); Interface Lab Pro (2); CO_2 analyzer S151 (3); desiccant agent (4); LEDs lightbox where the bottle containing the plant to be analyzed is inserted (5); Thermo-hygrometer (6); Tube adapted to humidify the air (7); Flowmeter (8); and flow pump (9). B – Detail of the culture bottle with an adapted lid with air inlet and outlet and temperature and humidity sensor inside. C – Detail of the tube containing distilled water, responsible for air humidification. D – Flowmeter and airflow pump. E – Circuit diagram responsible for lighting the LEDs. F – Light box: *left* - top view of the interior of the culture vial during analysis; *right* - front view of lightbox, pointed arrows highlight the direction of cooling air. The Black arrows indicate the airflow.

Figure 3. Visible light spectrum distribution of white LEDs used as light source.

Figure 4. Growth of diploid and polyploid *P. glomerata* plants under *in vitro* photoautotrophic conditions, after 30 days of culture. Left to right: diploid accessions 04, 22, and 43 (Ac 04, Ac 22, and Ac43), and synthetic polyploids 28, 60, 68, and 74 (Poly 28, Poly 60, Poly 68, and Poly 74). Bar = 2 cm.

Figure 5. Photomicrographs (A-G) and micromorphometry (H-K) of cross-section regions of the leaf blade of *P. glomerata* plants grown *in vitro* under photoautotrophic conditions, after 30 days of culture. Adaxial epidermis (Ad ep), abaxial epidermis (Ab ep), palisade parenchyma (PP), stomata (St). Bars: 100 µm. Vertical bars represent standard errors of the means. Same letters do not differ at 5% level by Tukey's test.

Figure 6. Stomata characteristics of the leaf *P. glomerata* plants grown under photoautotrophic *in vitro* culture after 30 days. Electron photomicrographs of the adaxialepidermis and abaxial epidermis (A-N), top right, highlight for stomata in each electron photomicrographs. Graphics of means stomatal density (STD) and stomatal

measurements (O-T). Bars: 50 µm. In graphics, the bars represent standard errors of the means. Same letters do not differ at 5% level by Tukey's test.

Figure 7. Relative ETR (*A*) and effective quantum yield of PSII (*ΔF/Fm'*) (B) in *P. glomerata* plants grown after 30 days of under photoautotrophic*in vitro* culture increasing photon flow density. The performance of both species is explained by the exponential decay single of 3 parameter model. Bars represent standard errors of the means.

Equations:

ETR	***ΔF/Fm'***
Ac 04: $\mathbf{f_{(x)}}$= 62.5065-62.4466*$e^{(-0.0051*x)}$ r^2: 0.9991	**Ac 04:** $\mathbf{f_{(x)}}$= 0.0975+ 0.6605*$e^{(-0.0027*x)}$ r^2: 0.9979
Ac 22: $\mathbf{f_{(x)}}$= 52.3393-52.3123*$e^{(-0.0065*x)}$ r^2: 0.9988	**Ac 22:** $\mathbf{f_{(x)}}$= 0.0808+0.6896*$e^{(-0.0029*x)}$ r^2: 0.9987
Ac 43: $\mathbf{f_{(x)}}$= 58.6647-59.0106*$e^{(-0.0058*x)}$ r^2: 0.9977	**Ac 43:** $\mathbf{f_{(x)}}$= 0.0845+0.6754*$e^{(-0.0026*x)}$ r^2: 0.9990
Poli 28: $\mathbf{f_{(x)}}$= 50.4752-50.3465*$e^{(-0.0070*x)}$ r^2: 0.9985	**Poli 28:** $\mathbf{f_{(x)}}$= 0.0817+0.7061*$e^{(-0.0031*x)}$ r^2: 0.9964
Poli 60: $\mathbf{f_{(x)}}$= 45.8200-45.9868*$e^{(-0.0079*x)}$ r^2: 0.9994	**Poli 60:** $\mathbf{f_{(x)}}$= 0.0727+0.7036*$e^{(-0.0032*x)}$ r^2: 0.9976
Poli 68: $\mathbf{f_{(x)}}$= 50.9001-51.1592*$e^{(-0.0072*x)}$ r^2: 0.9994	**Poli 68:** $\mathbf{f_{(x)}}$= 0.0744+0.7054*$e^{(-0.0029*x)}$ r^2: 0.9979
Poli 74: $\mathbf{f_{(x)}}$= 54.6846-54.4237*$e^{(-0.0063*x)}$ r^2: 0.9987	**Poli 74:** $\mathbf{f_{(x)}}$= 0.0824+0.7041*$e^{(-0.0029*x)}$ r^2: 0.9969

Figure 8. Sucrose content in *P. glomerata* plants grown under *in vitro* photoautotrophic conditions, after 30 days of culture. Bars represent standard errors of the means. Same letters do not differ at 5% level by Tukey's test.

Figure 9. Content of 20-Hydroxyecdysone (20-E) in *P. glomerata* plants grown under *in vitro* photoautotrophic conditions, after 30 days of culture. The bars represent standard errors of the means. Same letters do not differ at 5% level by Tukey's test.

Figure 1.

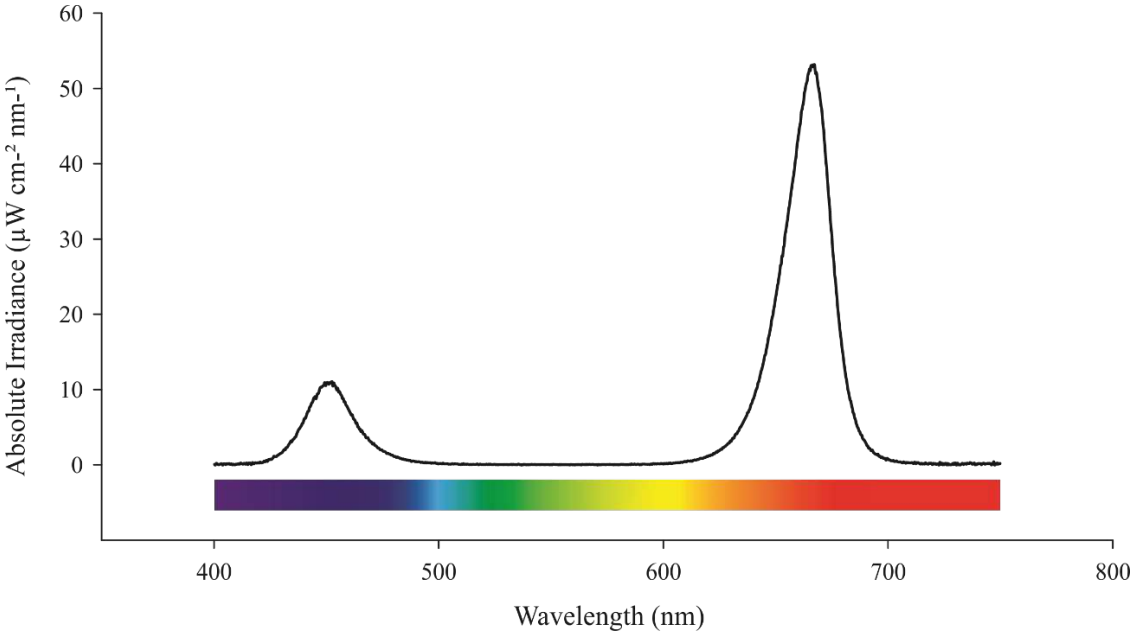
Absolute Irradiance (µW cm-2 nm-1)
60
50
40
30
20
10
0
400
500
600
700
800
Wavelength (nm)

Figure 2.

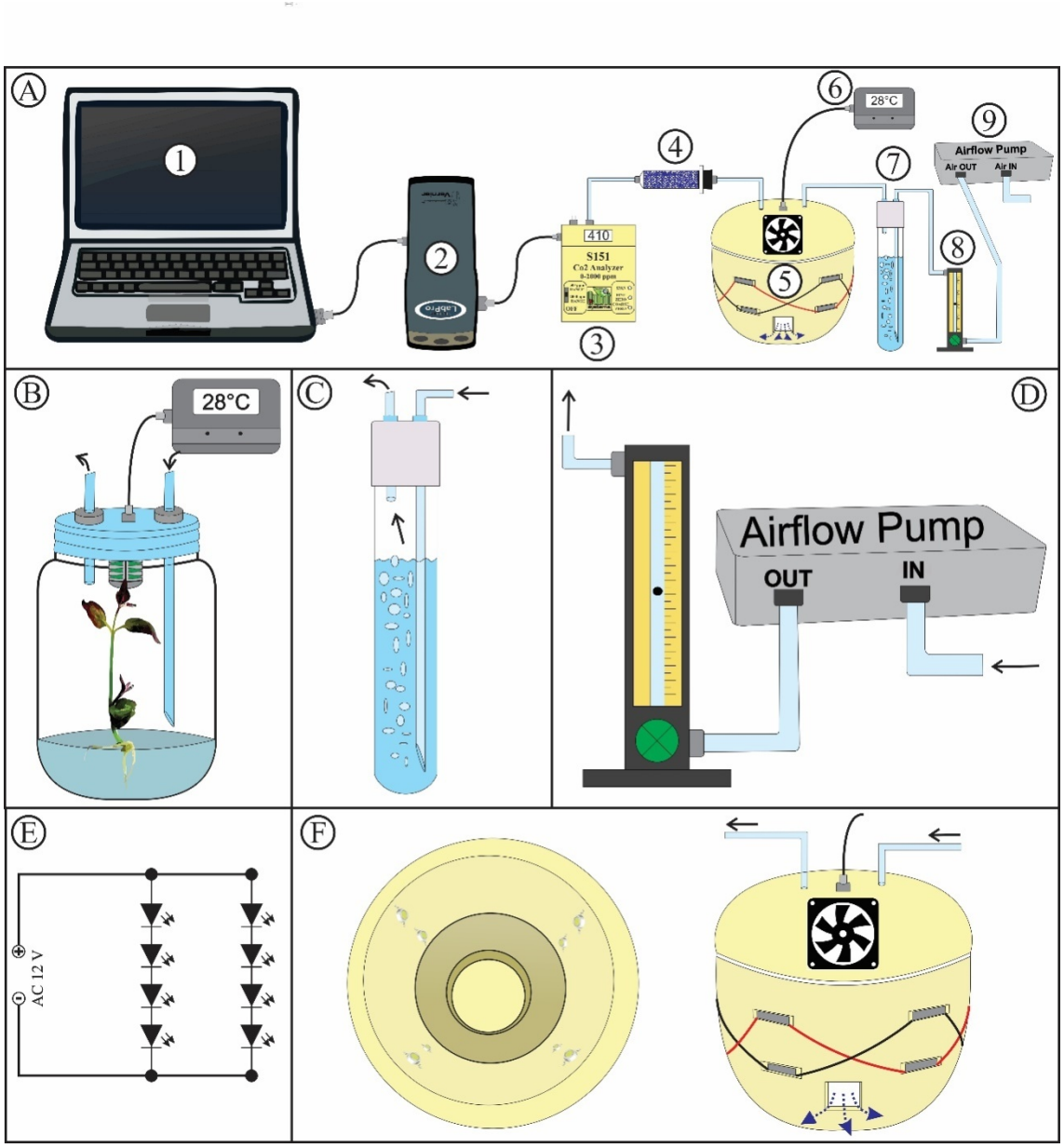
A
1
2
3
4
5
6
28°C
7
8
9
Airflow Pump
Air OUT
Air IN
410
S151
Co2 Analyzer
B
28°C
C
D
Airflow Pump
OUT
IN
E
AC 12 V
F

Figure 3.

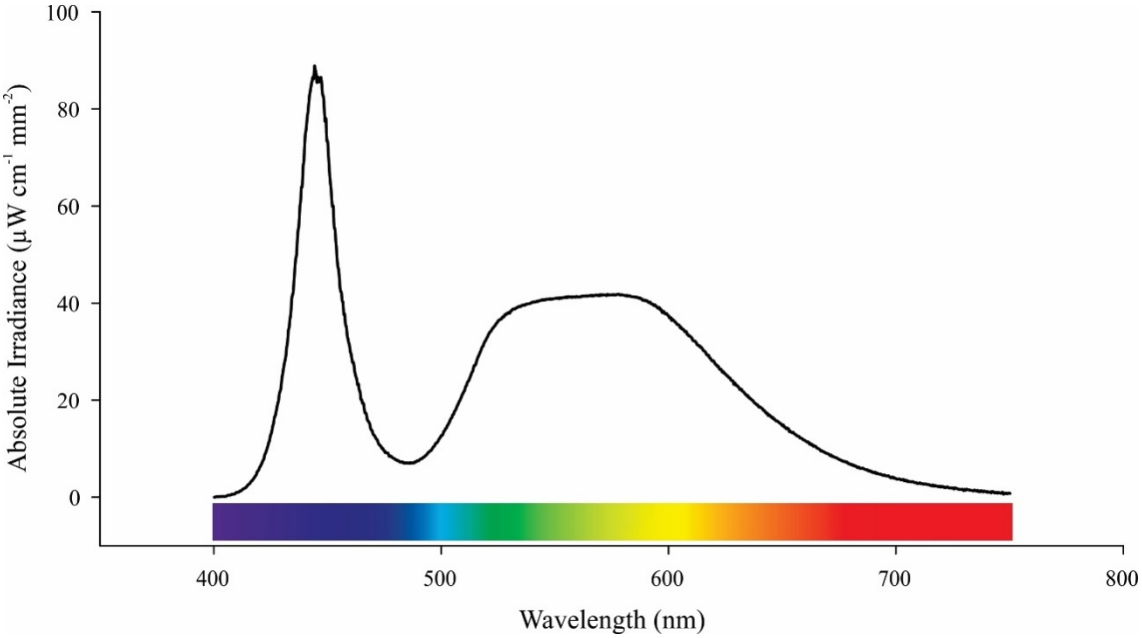
100
80
60
40
20
0
Absolute Irradiance (μW cm-1 mm-2)
400
500
600
700
800
Wavelength (nm)

Figure 4.

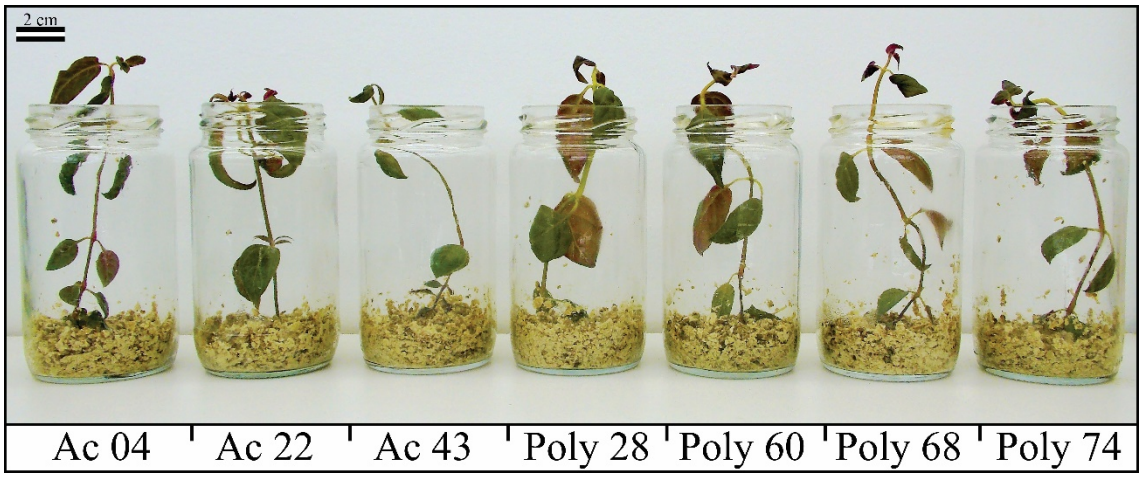

Figure 5.

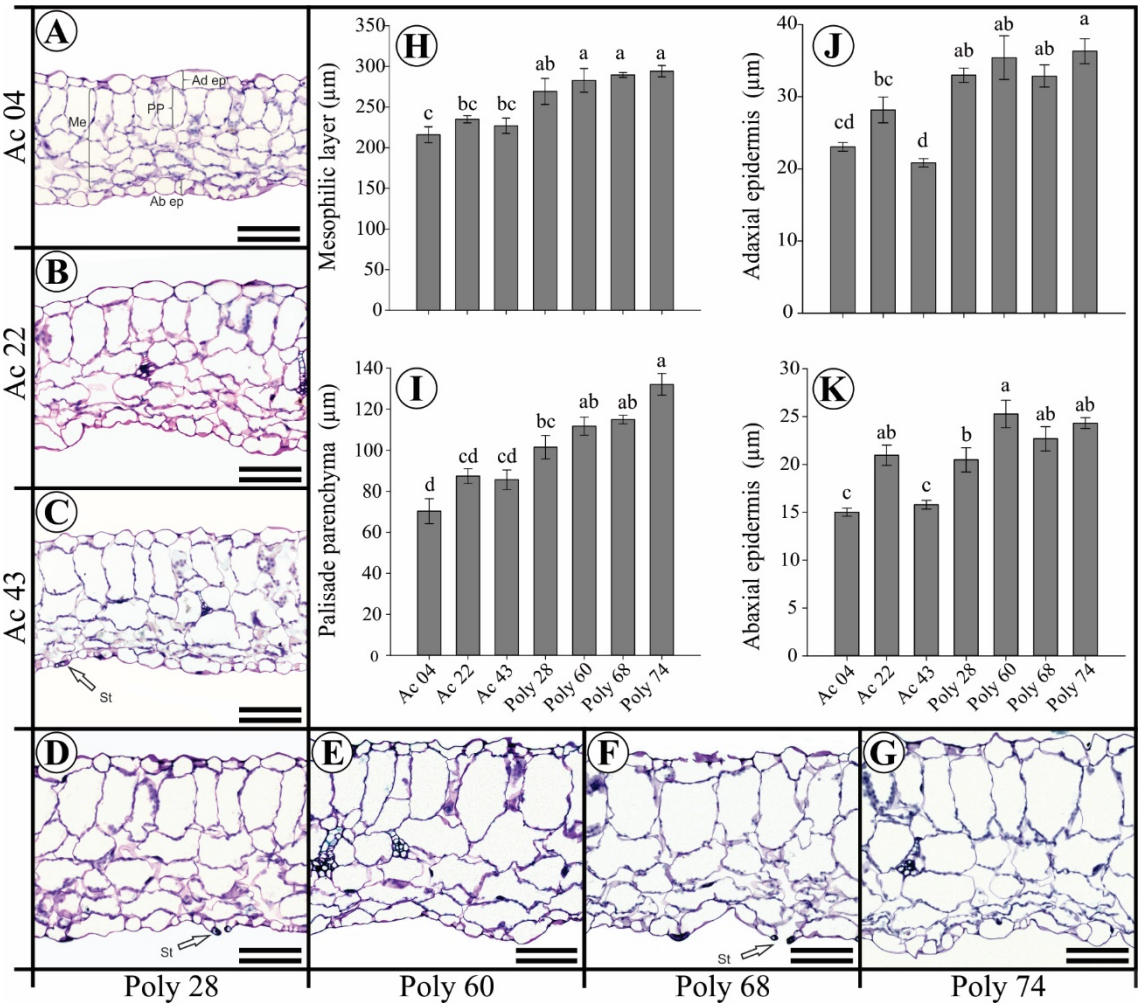
A
Ac 04
Ad ep
Me
PP
Ab ep
B
Ac 22
C
Ac 43
St
H
Mesophilic layer (µm)
I
Palisade parenchyma (µm)
J
Adaxial epidermis (µm)
K
Abaxial epidermis (µm)
Ac 04
Ac 22
Ac 43
Poly 28
Poly 60
Poly 68
Poly 74
D
E
F
G
Poly 28
Poly 60
Poly 68
Poly 74

Figure 6.

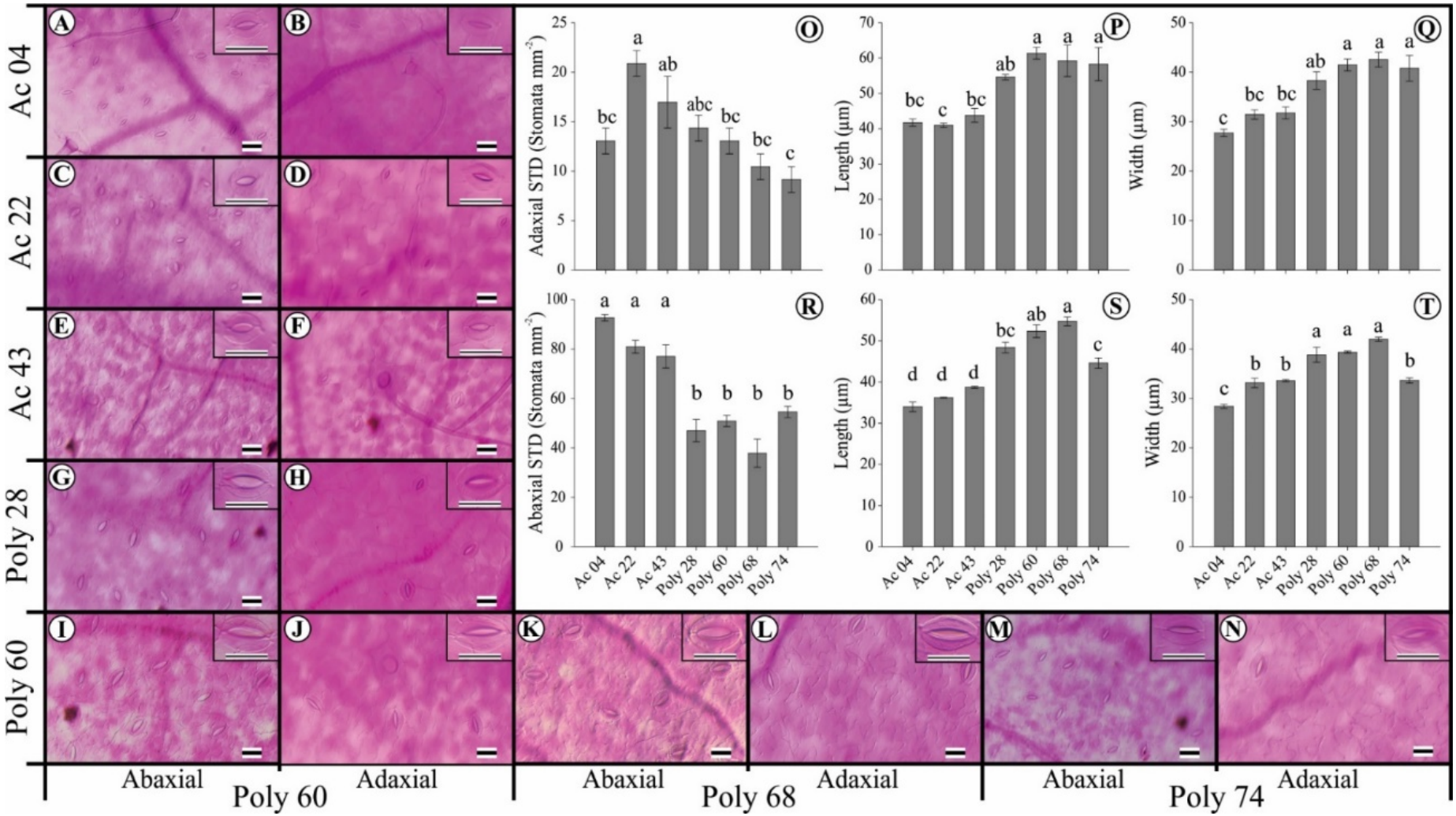
A
B
C
D
E
F
G
H
I
J
K
L
M
N
Ac 04
Ac 22
Ac 43
Poly 28
Poly 60
Abaxial
Adaxial
Poly 60
Abaxial
Adaxial
Poly 68
Abaxial
Adaxial
Poly 74
O
P
Q
R
S
T
Adaxial STD (Stomata mm-2)
Abaxial STD (Stomata mm-2)
Length (µm)
Width (µm)
Ac 04
Ac 22
Ac 43
Poly 28
Poly 60
Poly 68
Poly 74

Figure 7.

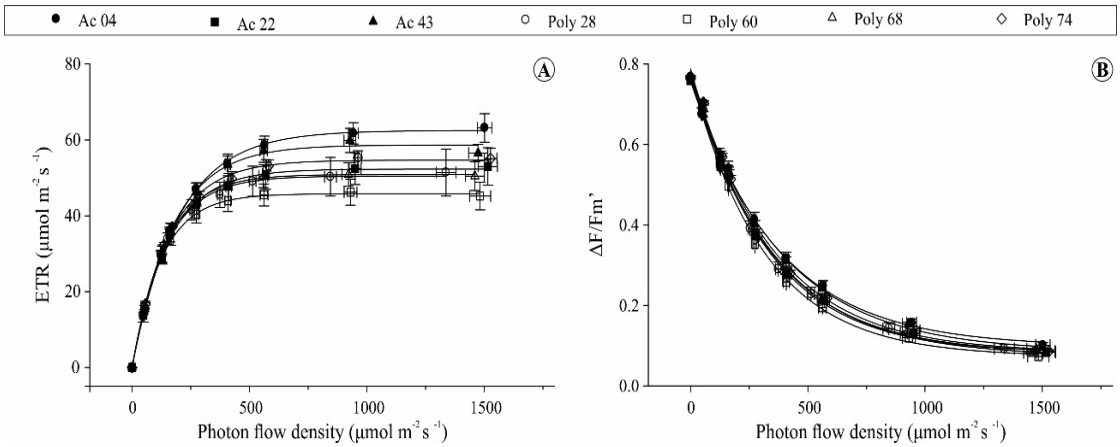
Ac 04
Ac 22
Ac 43
Poly 28
Poly 60
Poly 68
Poly 74
A
B
ETR (µmol m-2 s-1)
ΔF/Fm'
Photon flow density (µmol m-2 s-1)
Photon flow density (µmol m-2 s-1)

Figure 8.

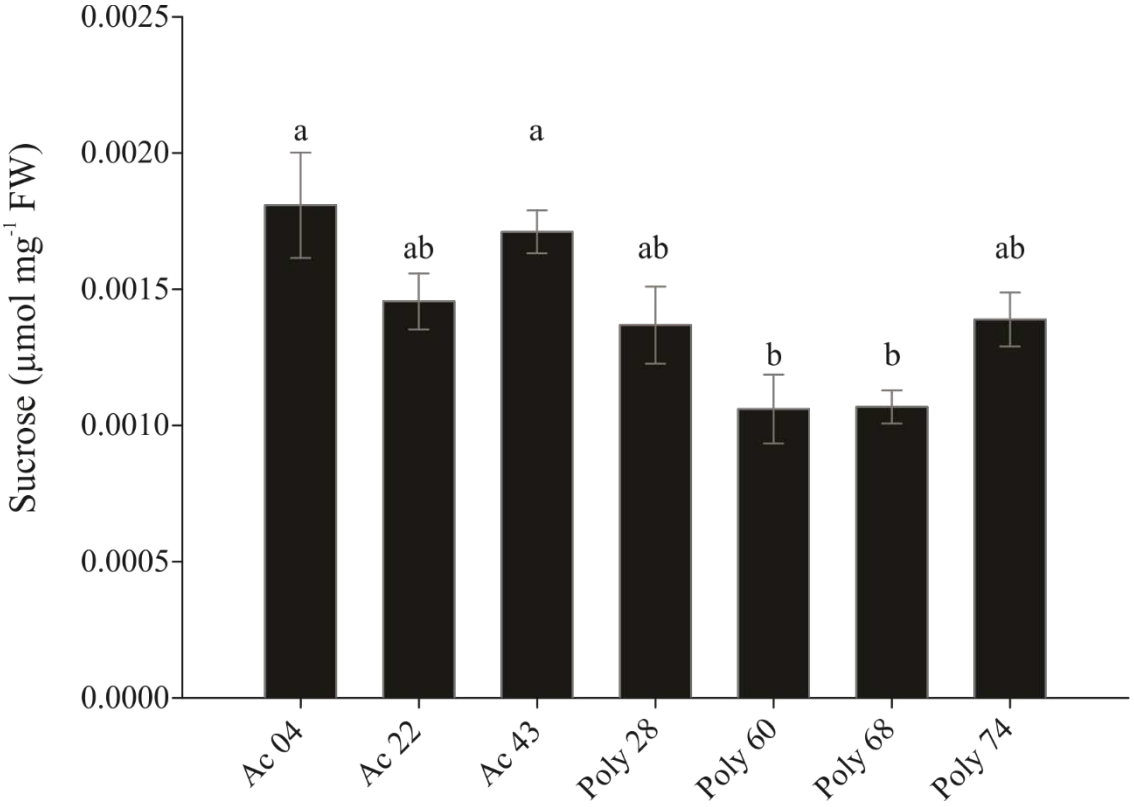
0.0025
0.0020
0.0015
0.0010
0.0005
0.0000
Sucrose (µmol mg-1 FW)
a
ab
a
ab
b
b
ab
Ac 04
Ac 22
Ac 43
Poly 28
Poly 60
Poly 68
Poly 74

Figure 9.

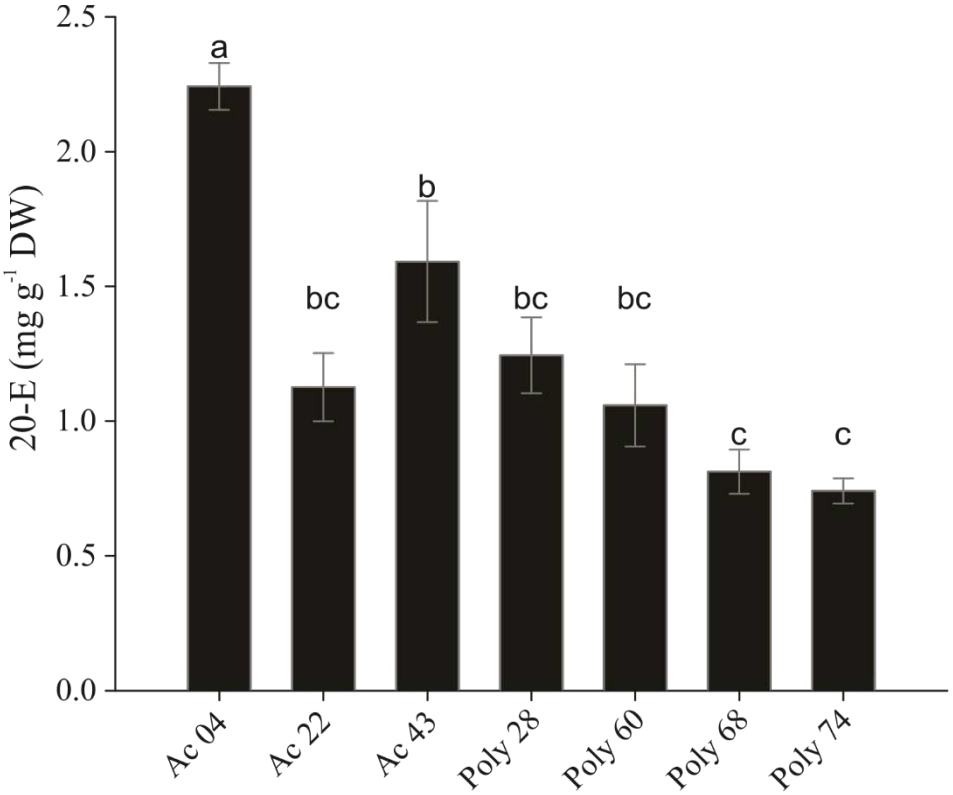
20-E (mg g-1 DW)
2.5
2.0
1.5
1.0
0.5
0.0
a
b
bc
bc
bc
c
c
Ac 04
Ac 22
Ac 43
Poly 28
Poly 60
Poly 68
Poly 74

Supplementary Figure 1: Correlations of Sucrose x ETR (A) and Sucrose x 20-E (B)

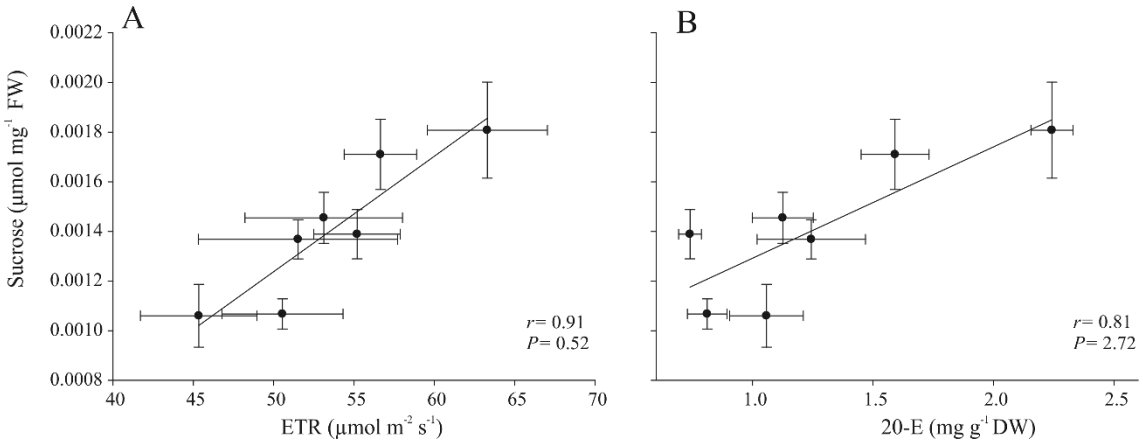

CHAPTER II

Physiological and morpho-anatomical effects of the induction and recovery of water deficit in *in vitro* and greenhouse grown *Pfaffia glomerata* (Spreng.) Pedersen plants

Kristhiano Chagas[1], Sérgio Heitor Sousa Felipe[1], Tatiane Dulcineia Silva[1], Diego Silva Batista[2], Camilo Elber Vital[3], Leticia Monteiro Farias[4], Joseila Maldaner[5], Cleber Witt Saldanha[5], Fábio Murilo DaMatta[6], Wagner Campos Otoni[1,*]

[1]Laboratório de Cultura de Tecidos Vegetais (LCTII), Departamento de Biologia Vegetal/BIOAGRO, Universidade Federal de Viçosa, Av. P. H. Rolfs, 36570-900, Viçosa, MG, Brasil.

[2]Universidade Estadual do Maranhão, Av. Lourenço Vieira da Silva, s/nº, Cidade Universitária Paulo VI, 65055-310, São Luís, MA, Brasil (ORCID 0000-0002-5798-7761).

[3]Departamento de Biologia Vegetal/BIOAGRO, Universidade Federal de Viçosa, Viçosa, Minas Gerais, Brazil.

[4]Faculdade Dinâmica do Vale do Piranga, 35430-324, Ponte Nova, MG, Brasil.

[5]Centro de Pesquisa em Florestas/DDPA/SEAPI, 97050-800 Santa Maria, RS, Brasil.

[6]Departamento de Biologia Vegetal, Ed. CCBII, Av. P. H. Rolfs s/n, Universidade Federal de Viçosa, Campus Universitário, 36570-900 Viçosa, MG, Brasil.

*Corresponding author: (email: wcotoni@gmail.com) Departamento de Biologia Vegetal, Laboratório de Cultura de Tecidos/BIOAGRO, Campus Universitário, Avenida Peter Henry Rolfs s/n, Universidade Federal de Viçosa, 36570-900 Viçosa, MG, Brasil (Fax:+55 31 3899 2580) (ORCID 0000-0002-9614-9373)

Abstract

Drought is the major abiotic stress factor that threatens the sustainability of global agricultural production due to its negative impact on plant growth and metabolism. To mitigate the damages caused by the water stress, plants undergo modifications in their metabolism and gene expression, in the sense of acclimatizing and tolerating stress. The present study aimed at evaluating physiological and morpho-anatomical aspects in *Pfaffia glomerata* plants challenged with water stress under greenhouse (*ex vitro*) and *in vitro* conditions, during induction and stress recovery periods. Our results showed that *in vitro* and *ex vitro* grown *P. glomerata* accessions (Ac 22 and Ac 43) displayed decreased biomass and height values in stressed plants. Water stress led to a marked reduction of the photosynthetic rates in plants rasised *in vitro*, while e*x vitro*, even with increased photosynthetic rates, dark respiration was as high as 74% in stressed plants. The drought stress in greenhouse and *in vitro* led to a reduced in epidermis, mesophyll and parenchyma of leaf and increased in stomatal density for both accessions. The water deficit stress led to a change in the endogenous content of phytohormone, with increased acid abscisic (ABA) and salicylic acid levels and decrease in zeatin. After rehydration, greenhouse-grown plants presented reduction in the phytohormone contents with similar means to control or intermediates with moderate stress. However, *in vitro* plants maintained high average for ABA. High levels of water deficit also strongly stimulated antioxidant enzyme activities, and osmoregulatory status. The Ac 43 in unrestricted hydric conditions present higher content and productive potential of 20-hydroxyecdysone (20E) than Ac 22. In conditions stressed both accessions had the highest levels of 20E in the *ex vitro* leaves and in the whole plants *in vitro* as well, but the total production of 20E was negatively affected. Our findings show that *P. glomerata* adopts various acclimatization strategies that provide tolerance to the water deficit. Thus, confirming the hypothesis that water stress enhances 20E levels in *P. glomerata*, despite the negative physiological effects caused by stress cause a fall in the productivity of this compound in accessions superiors.

Keywords: Brazilian ginseng; 20-hydroxyecdysone; chlorophyll *a* fluorescence; endogenous hormone levels; oxidative stress; photosynthetic gas exchange; water stress.

Introduction

The water deficit is one of the main environmental constraints that contributes to the reduction of world agricultural productivity (Boyer, 1982) and plays an important role in the distribution of plant species in different environments (Ashraf, 2010) and it is considered one of the most impacting abiotic stresses that affect plant growth and development (Oliveira et al., 2013), being the mechanisms that allow the plant to acclimate to drought generally negatively related to productivity, since the allocation of resources must be destined for overcome the stress (Griffiths & Paul, 2017).

In response to the water deficit, plants normally exhibit a greater accumulation of abscisic acid (ABA) promoting the reduction of the stomatal opening, which is a vantage in prevent dehydration of plant tissues and contribute to a greater resistance to drought (Egea et al., 2011; Lim et al., 2015; Kowitcharoen et al., 2015). The phytohormones have a rapid response to abiotic stress and play crucial roles in the physiological processes during the adaptation to adverse environments (Gururani et al., 2015). Other endogenous phytohormones such as cytokinins, jasmonate, salicylic acid and ethylene contribute in changes in plant metabolism during drought, however, these responses are often inconsistent due to the existence of a complex network with an extensive cross-talk among different hormone signaling pathways (Peleg & Blumwald, 2011; Daszkowska-Golec & Szarejko, 2013; Li et al., 2018; Munné-Bosch, 2018).

With the stomatal closure, there is a limitation in the diffusion of gases, reducing the availability of CO_2 for RubisCO, the low CO_2/O_2 conditions reduces the RuBisCO efficiency to fix CO_2 due to high oxygenase activity, and the consequence of this is the production of ROS (Turkan et al., 2018), which production is increased under high irradiance, when plastoquinone pool is over-reduced (Dietz et al., 2016).

In general, the abiotic stresses in plants are associated to the ROS production, being, in low concentrations, a necessary signaling of the acclimatization process (Ren et al., 2016), but when there is an imbalance between production and elimination they cause damage to proteins and nucleic acids, as well as the peroxidation of membrane lipids (Miller et al., 2010; Tenhaken, 2015; Foyer, 2018; Kanojia, 2018). Moreover, ROS elicits oxidative injuries to components of the photosynthetic machinery, leading to the photoinhibition of photosystem II (PSII) (Nishiyama & Murata, 2014; Gururani et al., 2015). The evaluation of chlorophyll fluorescence is an efficient way to verify the physiological status of the photosynthetic apparatus in plants exposed to environmental

stresses (Zivcak et al., 2013) and is a useful and appropriate tool to estimate inhibition and/or damage in the PSII (Choudhury et al., 2017, Guan et al., 2015, Su et al., 2015). Plants have developed a variety of enzymatic and nonenzymatic components for ROS scavenging (Pandy et al., 2016; Choudhury et al., 2017), such as superoxide dismutase (SOD), catalase (CAT), ascorbate peroxidase (APX), and total peroxidases (POXs) (Turkan et al., 2018; Silva et al., 2012). The maintenance of a high antioxidant capacity for the elimination of ROS has been associated to the increase of the tolerance of plants to abiotic stresses (Mishra et al., 2012; Caverzan et al., 2016).

The osmotic adjustment is another important mechanism of tolerance in plants under water deficit, inducing the accumulation of osmotically active substances in the cell, such as carbohydrates, amino acids and nitrogen compounds (Fang & Xiang, 2015; Blum, 2017; Turner, 2017) and ensuring the maintenance of water absorption and cell turgescence, which are considered key mechanisms that allow plants to maintain a higher photosynthetic rate, stomatal opening, and cell expansion under water deficient conditions (Cattivelli et al., 2008; Sanders & Arndt, 2016; Turner, 2018).

In vitro culture techniques allow rapid tracing of the required number of genotypes, since *in vitro* cultured plant, even at different stages of development, may exhibit their ability to withstand stress. The water deficit is elicited by the addition of osmorregulatory agents, such as mannitol, sorbitol or polyethyleneglycol (Verslues et al., 2006; Gupta et al., 2016; Ebad et al., 2017; Rezende et al., 2018), which increase the osmotic potential of the medium and can modulate the plant secondary metabolism. Nevertheless, the variety and intensity of stress is underestimated in studies of stress physiology, often seen as a binary condition, comparing a stressful treatment with a control (Claeys et al., 2014), contradicting the reality of field conditions, in which plants are imposed to a wide variety of stress levels, which requires a series of different response mechanisms.

In addition to changes in osmotic adjustment, reprogramming plant metabolism under dry conditions results in multiple other changes in their secondary metabolism (Niinemets, 2016). Different abiotic (e.g. physical, chemical, and hormonal) and biotic (e.g. polysaccharides, fungi, bacteria and yeast extract) elicitors can be used in plants to induce the production of secondary metabolites *in vitro* and *ex vitro* (Naik & Al-Khayri, 2016; Park et al., 2017), and directly contribute to develop model studies for the analysis of differential biosynthetic pathways (non-elicited plant x elicited plant).

Secondary metabolites are often referred as compounds that play no key role in maintaining vital processes but are important for the plant to interact and to defense with its ambient (Ramakrishna & Ravishankar, 2011). They also have a wide range of industrial and commercial applications.

The study of *P. glomerata* in exposure to different abiotic stress conditions has great relevance (e.g. aluminum, cadmium, lead, mercury, zinc and salt stress) (Skrebsky et al., 2008; Calgaroto et al., 2010; Calgaroto et al., 2011; Gupta et al., 2011; Maldaner et al., 2015 Felipe, 2019). The screening for genotypes that accumulate heavy metals and chemical interest must be prioritized since it is a species marketed and used in folk medicine due to the pharmacological properties of its secondary metabolite (e.g. 20-hydroxyecdysone or 20E), which biosynthesis occurs in shoots and the accumulation in the roots throughout the plant development (Festucci-Buselli et al., 2008). The 20E is a phytoecdysteroid that exhibits potential therapeutic applications (Jhon et. al., 2018), such as antioxidant activity, antibiofilm and anti-microbial (Rosa et al., 2015; Rosa et al., 2016). Although 20E biosynthetic pathway and function in plants is not fully elucidated, its production is modulated by different biotic and abiotic stimuli (Wang et al., 2013; Jhon et al., 2018). The increased content of 20E in *P. glomerata* grown *in vitro* under photoautotrophic conditions was associated with differentiated expression of the *Phantom* gene, which belongs to the P450 family and is possible a member of the phytosteroids synthesis pathway (Batista et al., 2018). However, there is a lack in studies of the effects of the water deficit on the morpho-physiological processes and the production of 20E during the growth and development of *P. glomerata.*

In this sense, understanding the physiological and biochemical mechanisms involved in differential tolerance to water deficit in *P. glomerata* may lead to mechanisms to enhance the 20E levels and can contribute to the develop strategies to its cultivation under drought stress.

Materials and methods

Plant material

The plants came from the *in vitro* Germplasm Bank of *P. glomerata* of the Tissue Culture Laboratory II (LCTII), which contains 71 accessions subcultured on a bimonthly basis onto a basal MS (Murashige & Skoog, 1962) medium. Leafless nodal segments of accessions 22 (Ac 22) and 43 (Ac43) were grown in test tubes containing 10 mL of MS medium and vitamins, 100 mg L^{-1} myo-inositol and pH adjusted to 5.7, solidified with 5.5 g L^{-1} agar (Phytotechnology Laboratories, LLC, Shawnee Mission, KS, USA) and sterilized by autoclaving at 121°C and 1.5 atm for 20 min. The plants were cultivated for 40 days under 25 ± 2°C, with 60 μmol m^{-2} s^{-1} of irradiance in a 16-h photoperiod.

Water deficit in greenhouse

After *in vitro* cultivation, the cloned plants were acclimatized for a period of 15 days in 200 mL disposable polypropylene cups and then transplanted to polypropylene pots (24 x 21 x 15 cm; EME-A-EME Ind. Com. Ltda., Petrópolis - RJ, Brazil) 2.2 kg capacity, containing commercial substrate Tropstrato HT ® (Vida Verde Ind. Com. de Insumos Orgânicos Ltda., Mogi Mirim - SP, Brazil), fertilized with 5g osmocote (NPK: respectively 9%, 14%, 19% and trace elements) and kept in greenhouse conditions.

The plants were kept in a greenhouse with full irrigation for 30 days, when they were divided into 3 groups of 20 plants of each accession: Control, maintained full irrigation throughout the experimental period; and Moderate; and Severe deficit, suspended the irrigation until a potential water leaf in the early hours the morning (Ψ_{wam}) smaller than -0.35 e -0.85 Mpa, respectively, after this, plants were cultured for more 15 days (Figure 1). The water status of plants was monitored daily through measurements of leaf water potential of the youngest fully expanded leaf, using a pressure pump type-Schölander (model 1000, PMS Instruments, Albany, NY, USA). The vessels were weighed daily for the determination of water loss and adjust the irrigation required for each water deficit condition. After 15 days of the imposed conditions, in 10 plants of each group (control, moderate and severe) all the collections and evaluations in the stressed condition were performed and for the other 10, the irrigation was restored daily for more 7 days, after this the evaluations and collections were made. The experimental design was completely randomized, in a factorial scheme

with 2 accessions (Ac 22 and Ac 43), 3 levels of water deficit (control, moderate and severe) and 2 conditions (stress and rehydration), each treatment with 10 replicates, being the experimental unit composed of a vessel with one plant.

Gas exchanges and fluorescence of chlorophyll a *in greenhouse*

The net CO_2 assimilation rate (A), dark respiration (R_d) stomatal conductance to water vapor (g_s), transpiration rate (E) and internal CO_2 concentration (C_i) were performed in the third fully expanded leaf from the top of plants using the open gas exchange system LI-6400xt (LI-COR Biosciences Inc., Lincon, Nebraska, USA) equipped with integrated fluorescence chamber heads (LI-6400-40; LI-COR Inc.). The dark respiration was evaluated between 22h and 0h, all other measurements were performed between 8:30h and 12h in the greenhouse under an external CO_2 concentration, ambient temperature and humidity, using photosynthetically active radiation (PAR) of 1000 μmol fotons m^{-2} s^{-1} that was provided by a light-emitting diode with 10% blue light in order to maximize stomata opening. The instantaneous water use efficiency (WUE) was calculated by the A/E ratio.

The chlorophyll fluorescence variables were obtained on the same leaf used to measure gas exchange, with the fluorometer coupled to IRGA. Along with dark respiration was obtained initial fluorescence (F_0) and ensure maximum fluorescence emissions (Fm), calculated the potential quantum yield of photosystem II (Fv/Fm). With the plants adapted to the light were obtained and calculated the following parameters: the coefficient for photochemical quenching (qP) was calculated as qP = $(F_m'-F_s)/(F_m'-F_0')$ and that for non-photochemical quenching (NQP) =$(F_m/F_m')- F_m'$. The actual quantum yield of PS II electron transport ($\Phi_{PSII}=F_m'–F)/F_m'$). The apparent electron transport rate (ETR) was estimated as ETR= Φ_{PSII} *PAR*f*α where PAR is the photons flux (μmol m^{-2} s^{-1}) incident on the leaves, f is a factor that accounts for the partitioning of energy between PS II and PSI and is assumed to be 0.5, which indicates that excitation energy is distributed equally between the two photosystems, and α is the leaf absorptance by photosynthetic tissues and is assumed to be 0.84 (Bilger et al., 1995).

Water deficit in vitro

Leafless nodal segments from Ac 22 and Ac 43 were initially inoculated in liquid stationary MS-based medium, 100 mg L^{-1} myo-inositol, pH adjusted to 5.7 and devoid

sucrose. Explants were in contact with medium and supported by home-made bridges from a bottom of a 200 ml plastic cup cut approximately 2.5 cm high and a paper disc (Figure 2). The bridges were placed within two inverted Magenta® boxes assembled with a coupler (Sigma Chemical Company, EUA), containing 100 ml of the abovementioned medium. After 10 days culture, the induction of water stress was imposed *to* simulate the water loss, Polyethyleneglycol (PEG 6000) was progressively added to the culture media. 3 times the culture medium was replaced with another containing 1/3, 2/3 and 1/1 of the final concentrations of PEG 6000, 0, 0.1, 0.2 and 0.3%, each exchange performed with an interval of 3 days. After 20 days of stress elicitation, the cultures were divided into two groups, for the first were performed all the collections and evaluations in the stressed condition and to the second the medium was replaced by another one without PEG, for stress recovery for 7 days, after this were made the collections and measurements. All the cultures were maintained at 25 ± 2° C under irradiation of 60 μmol m^{-2} s^{-1} with 16 h photoperiod provided by fluorescent lamp (110 W, HO Sylvania T12). Two 10 mm-diameter holes that were covered with 0.5 μm-pore Fluoropore hydrophobic membranes (PFTE, MilliSeal® Air Vent, Tokyo, Japan) at the top Magenta box allowed gas exchange rate of 25 μL L^{-1} s^{-1} (Batista et al., 2017) between the headspace inside the culture flasks and the ambient. The experimental design was completely randomized in a factorial scheme, with 2 accessions (Ac 22 and Ac 43), 4 concentrations of PEG 6000 (0, 0.1, 0.2 and 0.3%) and 2 conditions (stressed and rehydration), each treatment with six replicates, being the experimental unit composed by a flask with 3 explants.

Evaluation of the gas exchanges in vitro

The *in vitro* photosynthetic activity was determined with a segmented infrared gas analyzer system (IRGA) adapted from Costa et al. (2014). The light energy source was composed of eight white LEDs disposed within the side of a polystyrene vessel as described in the previous chapter, using constant photosynthetically active radiation (PAR) of 600 μmol photons m^{-2} s^{-1}, atmospheric concentration of CO_2 and ambient temperature and humidity.

Growth and biometric analyzes

With the exception of plants *in vitro*, greenhouse plants were collected and separated into roots, stem and leaves, after which they were oven dried at 50 °C for 72 h to obtain dry weight (DW). Growth analyzes were performed only at the end of the water deficit period. For accessing the leaf area, leaves were detached and fixed individually on laminated graph paper and photographed with the Nikon® digital camera. The images were processed in the ImageJ software (Schneider et al., 2012).

Morpho-anatomical structural characterization

Samples of fully expanded leaves were collected at each treatment and fixed in Karnovsky solution (glutaraldehyde 2.5% + paraformaldehyde 2.5% in 0.05 M cacodylate buffer, pH 7.2) (Karnovsky, 1965). For light microscopy, three samples of each treatment were dehydrated in ethanolic series and included in methacrylate (Historesin, Leica Instruments, Heidelberg, Germany). Cross sections of the 5 μm thickness were obtained on an automatic feed rotary microtome (Reichert-Jung 820 II, Cambridge Instruments, Nussloch, Germany), and colored with Toluidine Blue at pH 4.0 (O'Brien and McCully, 1981). The slides-containing sections were mounted in Permount. The micromorphometric characterization, each cross section made 3 photos of the leaf lamina, near the margin, center and near the midrib. The thickness of the mesophilic layer (μm), adaxial epidermis (μm), abaxial epidermis (μm), palisade parenchyma (μm) in three points within each photo.

The observation of the stomatal density in light microscopy was performed from paradermic sections of three samples to the central region of the first pair of fully expanded leaves were processed by diaphanization conducted with an aqueous 2.5% sodium hydroxide and a 20% (v/v) commercial sodium hypochlorite solution. To make the permanent slides, the diaphanized material was dehydrated in an ethanolic series and colored with alcoholic fuchsin, mounted with gelatin glycerin between slide and the cover and sealed with colorless enamel. Were made 3 photos of each paradermal section of the leaf lamina, near the margin, center and near the midrib in 3 replicates of each treatment. Observations and photographic records were performed in a photomicroscope (MCX51LED, Micros Austria, Wien, Áustria) equipped with an Moticam 580 camera

system (Image Pro Insight 9.1, Media Cybernetics, Inc., USA). The digital images were manually processed with ImageJ software (Schneider et al., 2012).

Quantification of pigments

Leaf samples were collected at each stage of the experiments in liquid nitrogen, pulverized, extracted in acetone and determination of photosynthetic pigments and total carotenoids, as described by Wellburn (1994).

Quantification of phytohormones

The hormones were extracted from leaves follow the methodology described by Napoleão *et al*. (2017) with modifications. Approximately 150 mg of fresh tissue was powdered in liquid nitrogen and 400 µL of extraction solvents has been added (methanol: isopropyl alcohol: acetic acid 20:79:1). The samples were mixed in vortex (4 times for 20 s), sonicated (5 min) and keep in ice (30 min). After centrifuged (13000g, 10 min in 4°C), 350 µL of supernatant was removed and put in a new tube. The process was repeated with the resulting pellet and then the supernatants were pooled. A last centrifugation (20000g, 10 min in 4 °C) was done to remove the rest of tissue in suspension. Then, the supernatant was filtered (Econofltr PVDF 13 mm and 0.2 µm; Agilent Technologies, Santa Clara, CA, USA) and used for liquid chromatography-mass spectrometry (LC-MS) analysis.

The samples were automatically injected (5 µL) in the system LC - MS/MS using an Agilent 1200 Infinity Series coupled to a Mass Spectrometry type triple Quadrupole (QqQ), model 6430 Agilent Technologies. Chromatographic separation was carried out on a column Zorbax Eclipe Plus C18 (1.8 µm, 2.1 x 50mm) (Agilent) in series with a guard column Zorbax SB-C18, 1.8 µm (Agilent). The solvent used was: (A) acetic acid 0, 02% in water and (B) acetic acid 0, 02% in acetonitrile in a gradient of time /%B: 0/5; 11/60; 13/95; 17/95; 19/5; 20/5. The solvent flow rate was 0,3mL/min in a column temperature of 30°C. The ionization method used in the mass spectrometry was an ESI (Electrospray Ionization) following these conditions: gas temperature of 300 °C, nitrogen flow rate of 10 L/min, nebulizer pressure of 35 psi and capillary voltage of 4000 V.

The equipment was operated on mode MRM (multiple reaction monitoring). The mass of the precursor ion/fragment established was monitored by fragmentation testes of each molecule: putrescine (Put) (89/72), (B) spermidine (Spd) (203/83), (C) spermine

(Spm) (146/72), cytokinin (CK) by zeatin (Zea) (220/136), 1-aminocyclopropane-1-carboxylic acid (ACC) (102/56), abscisic acid (ABA) (263/153), salycilic acid (SA) (137/93), and jasmonate (JA) (209/59). Put, Spd, Spm, Zea, and ACC were scanned as positive mode whereas ABA, SA, and JA were scanned in the negative mode. Phytohormones were quantified via calibration curves using authentic standards (1 to 200 µg and 0.1 to 500 ng, respectively; all of Sigma-Aldrich, St. Louis, Missouri, USA). The generated data were analyzed in the software "*MassHunter Workstation*" to obtain the peak areas for each hormone in the sample and the results were expressed in ng/g of fresh tissue.

Determination of the activity of antioxidant enzymes

The activity of the enzymes superoxide dismutase (SOD - EC 1.15.1.1), catalase (CAT - EC 1.11.1.6), peroxidases (POD - EC 1.11.1) and ascorbate peroxidase (APX - 1.11.1.11) was determined. For this, fresh frozen samples of the third leaf fully expanded from the apex were previously sprayed on liquid nitrogen. Approximately 100 mg of triturated plant material were suspended in 1 mL of extraction medium (potassium phosphate buffer 0.1 M and pH 6.8; phenylmethylsulfonyl fluoride (PMSF) 1 mM; polyvinylpyrrolidone (PVPP) 1% (w/v); ethylenediaminetetraacetic acid (EDTA) 0.1 mM). The homogenized was centrifuged at 10,000 x g for 15 min, and the supernatant was used as crude enzyme extract.

The activity of SOD was determined by the addition of 10 µL of crude plant extract in 190 µL of reaction medium with potassium phosphate buffer (50 mM and pH 7.8), EDTA (0.1 mM), p-nitroblue tetrazolium (NBT, 75 mM), methionine (13 mM), and riboflavin (2 µM) (Del Longo et al., 1993).

The reaction was carried out in a chamber with fluorescent light of 15W at 25ºC for 15 minutes and the quantification of the photochemical production of formazane blue (product of the reaction) was determined at 560 nm. The blank was obtained under the same conditions but in the dark. A SOD unit was defined as the enzyme amount needed to inhibit 50 % of the NBT photoreduction (Beauchamp & Fridovich, 1971). The result expressed in U min^{-1} mg^{-1} protein.

The activity of CAT was determined by the addition of 5 µL of crude plant extract in 195 µL of reaction medium with potassium phosphate buffer (50 mM and pH 7.0) and H_2O_2 (12,5mM) (Havir & McHale, 1987). The decrease in the absorbance at 240

nm was monitored and the enzymatic activity was calculated using a molar extinction coefficient equal to 36 M^{-1} cm^{-1}. The result expressed in U min^{-1} mg^{-1} protein.

The activity of POD was determined by the addition of 10 µL of crude plant extract in 190 µL of reaction medium with potassium phosphate buffer (25mM and pH 6.8) pyrogallol (20mM) and H_2O_2 (20mM) (Kar & Mishra, 1976). The absorbance increase in 420 nm was monitored and the enzymatic activity was calculated using a molar extinction coefficient equal to 2.47 mM^{-1} cm^{-1} (Chance & Maehley, 1955). The result expressed in µmol of purpurogalin min^{-1} mg^{-1} protein.

APX activity was evaluated according to Nakano and Asada, (1981). The reaction medium consisted of the addition of the 10 µl enzyme extract in 190 µl potassium phosphate buffer (50mM and pH 6.0) ascorbic acid (0.8mM) and H_2O_2 (1mM). The oxidation of ascorbate was accompanied by the change in absorbance at 290nm for one minute. The enzymatic activity was calculated using the extinction coefficient molar ratio of 2.8 mM^{-1} cm^{-1} and expressed in µmol of ascorbic acid (AA) min^{-1} mg^{-1} protein.

Quantification of protein and proline

The determination of the protein concentration in the extracts used in the evaluation of the enzymatic activity was performed by the methodology proposed by Bradford (1976), 5 µL of crude extract was added in 195 µL of the Bradford reagent. The reaction was performed in the absence of light for 5 min and absorbance was measured at the wavelength of 595nm. The results were compared to a standard bovine serum albumin protein curve in the range of 0 to 2 g L^{-1}.

Determination of the proline concentration was performed according to Bates et al. (1973), with modifications. Samples of 100 mg of leaf tissue were homogenized in 1 mL of 3% sulfosalicylic acid (w/v), vortexed (twice for 20 s) and centrifuged at 6,300 x *g* for 10 min. Later, 200 µL of the extract was collected and added to 400 µL of ninhydrin acid solution (1.25 g of ninhydrin, 30 mL of glacial acetic acid, 20 mL of 6M phosphoric acid). The samples were incubated for 1 h at 100 °C and then the reaction was stopped in an ice bath. Samples were read at 520 nm wavelength and a calibration curve was obtained by preparing proline standard solutions (0 to 220 µg mL^{-1}; Sigma-Aldrich, St. Louis, Missouri, USA) and expressed in mmol mg^{-1} fresh weight (FW).

Determination of 20E levels

The content of 20E was determined in leaf, stem and root of plants grown in greenhouse and *in vitro* by high-performance liquid chromatography (HPLC) using methanolic extract, as described by Kamada et al, (2009). 100 mg dried plant sample was mixed with 10 mL of methanol and stored in the dark at room temperature (25 ± 2 ºC) during seven days, with daily shaking of the extract. Subsequently, the extracts were centrifuged (15 min/5000 rpm), the supernatant collected and centrifuged again (15 min/5000 rpm). Then, the supernatant was used for liquid chromatography analysis. The sample were automatically injected (10 µL) in the system HPLC Shimadzu model LC-10AI, equipped with SPD-10AI detector, CBM-10A; Bomdesil C 18 column (5.0 µm x 4.6 mm x 250 mm). The mobile phase was composed of 1:1 (v/v) methanol-water, with a flow of 1 mL min^{-1}, reading at λ = 246 nm and sample run time of 15 min. The data was integrated through the Shimadzu LC10 software. The results were compared to a standard curve in the range of 0 to 120 mg L^{-1}

RNA extraction, cDNA synthesis and RT-qPCR analysis

For the total RNA extraction was used approximately 100 mg of fresh mass with the addition of TRI Reagent® (Sigma-Aldrich, St. Louis, MI, United States), and the genomic DNA was removed using 0.5 µL DNAse I (Ambion™, Thermo Scientific NanoDrop Technologies, Wilmington, DE, United States), both following the suppliers protocol. First-strand cDNA was synthesized from 500 ng of the total RNA using the 200 units of MMLV Reverse Transcriptase (Ludwig Biotec®, Alvorada, Brazil). The genes related to the biosynthesis pathway of 20-hidroxyecysone *Phantom* and *Spook* and the internal reference *glycerol-3-phosphate dehydrogenase* (*PgGAPDH*) primers were obtained from the *P. glomerata* transcriptome (Batista et al., 2018). qRT-PCR reactions were performed on a CFX96 Touch ™ (BIO-RAD) with three biological and two technical replicates, in a reaction volume of 10 µL: 4 µL of SYBR-Green (Ludwig Biotec®, Alvorada, RS, Brasil); 1 µL (4 µM) of each primer (forward ans reverse); 2 µL of water treated with diethylpyrocarbonate; and 1 µL (40 ng) of cDNA. The amplification gradient were as follow: 2 min at 50 ºC and 10 min at 95 ºC, followed by 40 cycles of 16 s at 95ºC and 1 min at 60 ºC, and 15 s at 95 ºC, 1 min at 60 ºC, 30 s at 95 ºC, and 15 s at 60 ºC. To calculate the differences of gene expression was applied the comparative threshold method ($2^{-\Delta\Delta Ct}$) (Livak & Schmittgen, 2001).

Statistical analyzes

The experiment was designed in a completely randomized design. The data were statistically analyzed by one-way analysis of variance (ANOVA). Gene expression was tested for significant differences using Dunnett's test ($P<0.05$), while all other variables by Tukey's test ($P<0.05$). All of the statistical analyses were performed using the software Genes (Cruz, 2016).

Results

Plant growth and biomass under water deficit

Compared to the control, in greenhouse under severe water deficit plants of Ac 22 and Ac 43 showed similar reductions in leaf (38%), stem (40%), root (16%) and total dry weight (34%) (Figure 3 A-D). The total height was reduced in Ac 22 (48 %) and Ac 43 (33 %) plants (Figure 3 G). The control of Ac 22 showed the highest leaf area, including in relation to Ac 43 (Figure 3 H). Under moderate conditions, plants exhibit intermediate results for all variables. In the *in vitro* experiment, Ac 22 control exhibited taller plants than Ac 43 control (Figure 4 A-C). Compared to the controls, the water deficit induced by 0.3% PEG 6000 results in more intense decreases in the growth parameters, with leaf area decreasing 66% and plant and dry weight 60% in both accessions.

Anatomical study

For the anatomical traits of the leaves in greenhouse (Figure 5 A-L) and *in vitro* (Figure 6 A-H), a significant effect was observed for most of the studied characteristics in relation to accessions and treatment, as well as the interaction between them. In general, water deficit plants of Ac 22 and 43 resulted in changes in the thickness of the leaf blade, reduction in the leaf intercellular spaces and the constituent tissues were reductions in mesophyll thickness, abaxial and adaxial epidermis and palisade and spongy parenchyma (Figure 5 M-Q and 6 I-M). In the greenhouse, independent of the accession, the stomatal density increased according to the stress intensity (Figure 5 R-S), while for *in vitro*, the controls showed an average of 76.95 stomata mm^{-2} on the abaxial surface, with the water deficit induced by 0.3% PEG 6000 increasing the stomatal density by 3.9 times in Ac 22 (300.1 stomata mm^{-2}) and 2.8 in Ac 43 (215.46 stomata mm^{-2}). In adaxial surface, the control of Ac 22 exhibit an average of 26.9 stomata mm^{-2} and Ac 43 whit 6 stomata mm^{-2}. However, the AC 43 showed an increase at 6.8 times in 0.2 and 0.3% PEG 6000 (40 and 41 stomata mm^{-2}) and of 2.8 times for Ac 22in 0.3% PEG 6000 (75.32 stomata mm^{-2}).

Leaf pigments content

The chlorophylls and carotenoids content in leaves in both accessions were significantly affected by drought stress in greenhouse and induced by PEG 6000 (Figure

7 and 8). In the greenhouse, the Ac43 showed highest values in content of pigments of all stressed levels in relation to Ac 22 including the recovery of hydration. In general, the lower contents of pigments were found in the controls and were the stress increased, even after the irrigation recovery the chlorophylls contents still high (Figure 7 A-E), except for the carotenoids in the Ac43, which exhibited a sub reduction after rehydration (Figure 7 E).

The contents of Chl *a*, *b* and total were elevated with treatments with stress inducted by PEG 6000 with the higher values in Ac 22. After rehydration, the highest Chl *a* and total contents (Figure 8A and D) were found in plants grown *in vitro* under 0.3% of PEG 6000 from both accessions. However, the content of Chl *b* in the Ac 43 was reduced to the same level of the control and Ac 22 had a slight reduction in relation to the control (Figure 8 B). Carotenoids gradually increased with stress intensity in both accessions, with highest level in 0.3% PEG 6000. After rehydration, plants grown *in vitro* that passed through 0.1 and 0.2% PEG decreased the content of carotenoids to the level of their respective controls, with the treatment of 0.3% PEG 6000 showing intermediary values (Figure 8 E).

Photosynthetic performance

In greenhouse, independent of the accession, plants under stress showed a significant increase by approximately 41% in *A*, relative to the control, even after rehydration (Fig. 9 A), which was accompanied by decreases in *C*i, 6.2 and 15.3 % in moderate and severe deficit when compared to the control (Fig. 9 E) and after rehydration, the plants that maintained low *C*i in relation to the moderate condition of stress. In addition, g_s and *E* decreases in plants under moderate and severe water deficit, respectively (Fig. 9 C-D). After rehydration, these plants maintained low g_s and medium and intermediary *E* means in relation to the control. Plants in severe deficit increase 74% in R_d and after recover the irrigation exhibit values similar to the control (Figure 9 B). The F_v/F_m and NPQ did not vary, with averages of 0.78 and 1.66, respectively. Compared with the controls, there were significant increase of 23 and 24% in ETR and *q*P relative, even after rehydration (Figure 9 I-K). Plants of Ac 22 under severe deficit exhibit high WUE, 1.66 times higher than Ac 43 and after recover the irrigation, maintained values similar to moderate stress.

The plants grown *in vitro* had a drastic decreasing in photosynthetic performance under 0.3% PEG 6000 in relation to the control and after rehydration only the of Ac 22 cultivated under 0.1 and 0.2% PEG 6000 recovered the photosynthetic activity at the control level (Figure 4 D).

Leaf phytohormone content

In greenhouse, the content of ABA increased in both accessions under severe water deficit but was higher in Ac 22 (18.5 times) and Ac 43 increase of 12.9 times, reduced after hydration (Figure 10 A). The content of Spm, under severe stress increase in Ac 22 and in Ac 43, after rehydration, Ac 22 kept similar values to the stressed condition and the Ac 43 was reduced at the control level (Figure 10 C). Ac 43 increases in SA content under severe stress, after rehydration both accessions exhibit similar levels to moderate stress condition (Figure 10 E). Zea showed reductions in Ac 22 and Ac 43 under stress, after rehydration are maintained the same levels displayed in conditions stressed (Figure 10 G). Compared with controls exibited a significant increase in Spd, Put and JA (Figure 10 B, D and F). ACC was unresponsive to the treatments (Figure 10 H).

Plants cultured *in vitro* under stress showed a significant difference only for treatments in the content of ABA, Spn, Spd, JA, SA and Zea. The content of ABA increases according to the stress level (Figure 11 A). Spm and Spd presented the same pattern of stress response, with the lowest mean in controls and an equal increase for all PEG 6000 treatments, maintaining the same means after rehydration (Figure 11 B-C). The JA content in 0.1% PEG 6000 did not differ from controls (Figure 11 D). In PEG 6000 concentrations 0.1, 0.2 and 0.3%, the content of SA increased approximately in 72% in relation of control; after rehydration there was a recovery to a control level (Figure 11 F). ACC and Put was unresponsive to the treatments (Figure 11 G-H).

Activity of antioxidant enzymes

The results show significant changes in antioxidant enzyme activity for SOD, POX and APX only in the stress levels and for CAT in the interaction between accession and treatment in greenhouse. Plants under severe stress had greater SOD and POX activity. After the re-establishment of irrigation POX showed similar activity to control and SOD a subtle reduction but maintained intermediate activity between severe and control (Figure 12 B and C). APX maintained high activity in relation to control in all

treatments even after rehydration. In relation to Ac 22, Ac 43 shows higher CAT activity for all treatments, however, both had greater activity undersevere stress. After, rehydration reduced the level in the control to the Ac 22, and Ac43 intermediate results between plants in moderate stress condition and control (Figure 12 A).

In vitro, the CAT e POX exhibit significant changes for interaction and SOD and APX for treatments only. Between the controls, the Ac 43 shows higher CAT activity than Ac 22, but gradually increased with the different concentrations of PEG 6000, with higher activity at 0.3% for both accessions. After rehydration, CAT on Ac 43 shows similar results in control and Ac 22 liked 0.1% of the PEG stress condition. The POX activity in Ac 43 is high in 0.2 and 0.3 % PEG 6000, in Ac 22 only 0.3%, after rehydration even with reduction in activity, all treatments had means higher than the controls (Figure 13 C). SOD and APX showed high average in stress, and after the rehydration the SOD activity in all treatments was decreased to the control level and in APX only the plants grown under 0.1% PEG 6000 had a reduction at the control level, for the concentrations of 0.2 and 0.3 % the same levels of the stressed condition was maintained (Figure 13 B and D).

Proline and protein content

Proline content was affected by drought, accessions and their interactions. In greenhouse, drought stress increased the proline content in moderate and severe, proline accumulation was superior in Ac 43 (Figure 12 E). Drought stress by PEG 6000 increased the proline content in all concentrations, being higher in the control and 0.1% in Ac43, 0.2% and in 0.3% in Ac 22 (Figure 13 E).

The leaf total soluble protein content was augmented by drought stress. In greenhouse grown plants, increased in all treatments in relation of control, even after rehydration (Figure 12 F) and in the *in vitro*, the protein content increased according to the intensity of the stress, the Ac 22 exhibit values higher than Ac 43 in control and in under conditions stressed by PEG 6000. After rehydration, only the plants stressed by 0.1% PEG 6000 had similar means to the controls, at 0.3% PEG the Ac 22 subtly reduces while in Ac 43 maintained a high level of protein content (Figure 13 F).

20E content and gene expression of the 20E biosynthesis pathway

Total 20E content were affected by drought stress in greenhouse. There was an increase in the total content of 20E in the leaves in both accessions, in the roots only for the Ac 22 with the increase of the intensity of the deficit and in the stems, there was no significant difference (Figure 14 A, C and E). For the total production of 20E the interaction between the accessions and the intensity of water deficit was significant for leaves, stems and whole-plant. In the roots, there was only significant difference only between the accessions (Figure 14 B, D, F and G). Plants of Ac 22 and 43 presented a significant increase in the content of 20E in the leaves, with the highest concentrations found in severe treatment after rehydration (Figure 14A). In roots, only in the Ac 22 has increase of 32.8% in the content of 20E in the condition of severe stress and after rehydration present averages similar to control. Both accessions presented a reduction in the production of 20E with the intensity of the deficit. In the leaves, in relation to the control, the Ac 43 was the one that had reduction 36% while the Ac 22 decreased 18% in the conditions of severe stress. In the stems, Ac 22 had a 33% and 28% reduction in Ac 43 (Figure 14F). In the roots, the water deficit did not influence the total production of 20E but the Ac 43 had averages above the Ac 22 in all treatments (Figure 14 D). The production of 20E in the whole plant was higher in the control for both accessions, with the Ac 43 higher than the Ac 22 and according to the intensity of the deficit there was a reduction in the total production of 20E of 20.5 and 21.7% in the Ac 22 and 43 in the severe condition (Figure 14G). The expression of genes related to 20E biosynthesis (*Phantom* and *Spook*) in *P. glomerata* was not influenced by water deficit in greenhouse (Figure 16).

The drought stress caused by PEG 6000 *in vitro* affected the total content of 20E and the total of 20E and the interaction between accessions and stress condition was significant. The Ac 22 plants grown under 0.3% PEG had the content of 20E increased 4.2 times compared to the control while the Ac 43 increased 2.4 times. After rehydration, the Ac 22 and 43 presented a decreased in the content of 20E. Plants of Ac 43 that passed through 0.1 % of PEG had similar mean to the control, the others (0.2 and 0.3% PEG) were similar to 0.1% PEG in stressed conditions. In the Ac 22 had a reduction for all treatments, showing intermediate average between the control and the plants grown at 0.1% of PEG, however with averages lower than in plants of Ac 43

(Figure 15 A). The total production of 20E was lower in 0.3% PEG in Ac 43. The plants stressed by PEG in Ac 22 presented higher total 20E production in relation to the control (Figure 15 B).

Discussion

The present findings showed a negative relationship between drought stress and vegetative growth parameters in *P. glomerata* plants under greenhouse and *in vitro* conditions. Reduced in leaf area this probably occurs as a protection mechanism and survival strategy of the challenged plant, reducing its area exposed to light, as well as its transpiration surface, when these are exposed to adverse conditions. However, despite reduced leaf area and plant height are advantageous to face restricted water use, overall it may also result in low productivity of plants biomass.

To attain that, plants have developed several morphological adaptations effort to ensure its survival under low water availability in greenhouse and *in vitro*, since there were changes in the leaf cell structures, such as compaction of mesophyll, reduction in the thickness adaxial and abaxial epidermis, palisade parenchyma, spongy parenchyma and high stomatal density, similar to the reported in *Passiflora alata* under water deficit (Souza et al., 2018). The reduction of intercellular spaces is an alternative to reduce the loss of water evaporation, and ensure its efficient use, this is important adaptation of drought avoidance. Regulation of the number of stomata is a long-term response. Stomatal density is adjusted in developing leaves through the sensing of environmental conditions by mature leaves (Miyazawa et al., 2006). It is noted that stomatal density increased with water deficit, Xu and Zhou (2008) demonstrated that stomatal density increases under moderate water deficit. There is much information on how reduction of transpiration can be rapidly achieved through a physiological control of stomatal opening, stomatal movement is a rapid response controlled by ABA, CO_2 concentration, Blue light and humidity. (Chater et al., 2014; Sussmilch et al., 2017).

Drought stress has been reported to reduce both chlorophyll content and biosynthesis, a reason for chlorophyll content reduction is that drought stress enhances the production of reactive oxygen species (ROS) such as $O_2^{\bullet-}$ and H_2O_2 that can lead to lipidperoxidation and, consequently, chlorophyll degradation (Farooq et al., 2009). Chlorophyll decrease may contribute to the reducing the amount of photons absorbed by leaves, which leads to an enhanced photoprotective and antioxidant capacity of leaves per amount of photons absorbed (Khoyerdi et al., 2016). However, our results showed that drought stress in greenhouse and by supplementation of PEG *in vitro*, significantly increased the photosynthesis pigments, in all accessions. The increase of chlorophyll may contribute to the survival of severely stressed plant, since efficiency of the

photosynthetic process depends on the chloroplast pigments. Consequently, the content of carotenoids was elevated, act as auxiliary pigments and an effective antioxidant which protect and stabilize the photochemical processes under drought condition (Abbasi et al., 2014). In addition to carotenoids, other pathways of energy dissipation may also act on plants under stress and increase the protection of the photosynthetic apparatus against photodamage, such as photorespiration, cyclic electron transport, water-water cyclic (Yamori et al., 2016).

The water deficit induced by the addition of PEG to the culture medium *in vitro* shows a remarkable effect reducing the photosynthetic rate of plants *in vitro*. Since after rehydration, at milder levels of stress the access 22 recovered its capacity of carbon fixation. However, in greenhouse we observed proportionally increases in *R* than in *A* and ETR, concomitantly with decreases in *Ci* in g_s and *E*. The vegetal mitochondrial metabolism is highly active during drought stress responses (Pires et al., 2016). The plant respiration involves the reactions of glycolysis, the tricarboxylic acid cycle and the mitochondrial electron transport chain, but is also directly connected with many other metabolic pathways such as protein and lipid biosynthesis and photosynthesis via photorespiration (Van-Dongen et al., 2011), involves the carbon balance in the whole plant, with 20-80% of the carbon fixed in photosynthesis being released (Xu et al., 2015).

It is believed that these the increase of *A* in plants under conditions of moderate and severe stress, changes are of adaptive significance of mechanisms of tolerance to stress, an increase in photosynthetic capacity reduces susceptibility to photodamage and optimize light utilization (Walters, 2015) play an important role in acclimation. Several authors have reported limitation of gas exchange and inhibition of photosynthesis with effects of controlled water deficit in plant physiology (Sharma et al., 2015; Rivas et al., 2016; Saha et al., 2016), but the water deficit is made through the suspension of irrigation, totally depriving water availability. In the present study the plants were not deprived of water, only maintained at different water potencies in the vegetative period.

Under the conditions of the experiment in greenhouse, the water deficit shows a remarkable reduction of the stomatal conductance, possibly induced by fine adjustment of the stomatal movement to reduce. High instantaneous efficiency in water use, given by the *A*/*E* ratio is an important evaluation of the water deficit tolerance, since it denotes water saving by the plant. WUE instantaneous measurements, only at leaf level, may

not be efficient to determine the real value of this parameter, and more long term analyzes are recommended, such as the isotopic composition of carbon that depends on Rubisco CO_2 fixation capacity and stomatal conductance (Saldanha et al., 2014; Medrano et al., 2015). In addition, the relative changes to total leaf protein has by linked Rubisco content since they tend to be dominated by changes in Rubisco content, which constitutes a major proportion of total leaf protein (Ishimaru et al., 2001). Under drought stress conditions plants reduces the opening their stomata resulting in a decline in carbon isotope discrimination, thus the plant organic material is less ^{13}C-depleted (Mihoub et al., 2018).

In the water deficit conditions imposed, F_v/F_m values were kept close to 0.78 and indicate that the physical stability of the photosynthetic apparatus of the plants was not affected by stress (Murchie & Lawson, 2013). In response to PSII stability and increase in chlorophyll *a* and *b* content in plants with stress reflect the increase in the fraction of absorbed light that is dissipated photochemically (q_P) were also noted, suggesting that the stressed plants were likely efficient to fully capture and exploit the absorbed energy. Were accompanied by increase in ETR than in *A*. Reducing electron transport is a defense strategy against photodamage damage in plants whose CO2 fixation is compromised, but at the same time limits the photochemical step of photosynthesis, but is not case. In the present work, NPQ was not the main protection mechanism to prevent ROS production (Pintó-Marijuan & Munné-Bosch, 2014). This suggests that other mechanisms take place to protect *P. glomerata* plants to stress damages.

In response to the water deficit, ABA has been most extensively studied in relation to plant stress tolerance because stomatal behavior is closely related to changes in leaf levels in response to abiotic stress (Kowitcharoen et al., 2015), stress avoidance mechanism that prevents excessive loss of water via leaf transpiration, maintaining tissue hydration and contributing to greater resistance to drought (Kalladan et al., 2017). The reduction in ABA concentration in response to rehydration occurs, mainly through enzymatic degradation, through the signaling of stress relief by the recovery of the adequate water status of the plant (Roychoudhury et al., 2013). For instance, drought altered the hormonal balance in *P. glomerata* leaves in greenhouse and environment *in vitro*, which included increased ABA content and small decline zeatin content. Prolonged drought or was reported to be associated with downregulation of active CK contents (Nishiyama et al., 2011). Furthermore, a drop in endogenous cytokinins

contents amplified the response of shoots to increasing ABA content under drought (Vishwakarma et al., 2017). The cytokinins have as one of their effects delaying plant senescence during abiotic stress events (Cortleven et al., 2018).

In both environments the water deficit also had an effect on the accumulations of JA and SA are other plant hormones that can act during the water deficit, have also been found to potentially increase abiotic stress tolerance in plants, particularly tolerance to drought (Tiwari et al., 2017). Under drought, JA regulates a subset of biosynthesis responses and ABA accumulation by either signaling dependent or ABA-independent signaling pathways. Salicylic acid (SA) is also a secondary metabolite accumulated in plants under drought stress which is involved in inducing drought tolerance in plants by regulating several physiological processes through signaling (Sharma et al., 2018). SA exogenous strongly stimulated the biosynthesis of amino acids and carbohydrates involved in osmotic adjustment and energy production (Li et al., 2017) and *H. vulgare* seeds of resulted in the accumulation of proline and increase of the photosynthetic pigments (El-Tayeb, 2005).

Ethylene and another phytohormone that can act during water deficit (Cui et al., 2015) capable of promoting senescence of plant organs in plants exposed to drought (Zang et al., 2015). Nevertheless, SAM is also substrate for ethylene and PAs biosynthesis in higher plants (Montilla-Bascón et al., 2017). Hence, PAs and ethylene could act in an antagonistic manner competing for the common substrate SAM (Bitrián et al., 2012). Confirming our results, the water deficit both in greenhouse and *in vitro*, the plants of *P. glomerata* presented increases in the content of Spermine, spermidine and putrescine have been shown to inhibit the induction of ACC synthase. Whereas ethylene would contribute to senescence, PAs would favor growth and inhibit senescence, thus providing support to the view that PA-ethylene cross-regulation occurs and has important implications for tolerance to drought, associated with antioxidant defense and dehydrin genes via involvement in calcium messenger system and hydrogen peroxide signaling (Li et al., 2015).

Plants develop various strategies to behavior against these stress factors, the reduction of the water potential of the vegetal cell can cause the accumulation of solutes in the interior (Mwadzingeni et al., 2016; Jungklang et al., 2017), which contributes to the maintenance of the cellular turgor, support of the stomatal conductance and the photosynthetic and growth processes. The proline is the most important organic solute

that plays a key role on depot of energy to regulate redox potential, scavenger of ROS, cytosolic osmotic and also can be an important component of cell-wall proteins (Shinde et al., 2016; Rana et al 2017). Therefore, the accession with high proline content could be expressed more resistant to water deficit condition (Khoyerdi et al., 2016). Proline can also contribute to the recovery of the plant after the water deficit, when it is metabolized in the mitochondria, providing ATP for damage and growth recovery (Araújo et al., 2013). This may be an explanation for the reduction in proline content (*in vitro* and greenhouse) and dark-respiration (greenhouse) in the accessions after rehydration. In particular, *P. glomerata* adopted a series of acclimatization strategies for tolerance salt stress, among them osmotic adjustment by accumulation of proline, protein, and soluble sugars, and increased activities of antioxidant enzymes (Felipe, 2019).

The water deficiency causes severe changes in the operation of the energy metabolism and cellular processes in plants undergo imbalance in the production and elimination of ROS. Therefore, it is of extreme importance the activation of mechanisms of antioxidative protection, such as the enzymatic system formed mainly by SOD, CAT, POX and APX. The greatest increase in the activity of these enzymes was observed at different levels of stress induction both in greenhouse and *in vitro*, this denotes the ability of plants to avoid oxidative damage. *P. glomerata* in exposed to lead, mercury increased enzymatic and non-enzymatic antioxidants mechanisms (Calgaroto et al., 2010; Gupta et al., 2011) and is recommended supply of zinc to reverse the oxidative stress caused by mercury (Calgaroto et al., 2011).

In both studied accessions of *P. glomerata*, the water deficit in greenhouse caused an increase both in the content of 20E in the leaves and in roots only for the Ac 22. The mechanisms that allow the plant to acclimatize to drought, generally opposite a high productivity, since the allocation of resources must be destined both for acclimatization to stress and for its biomass gain (Griffiths & Paul, 2017). However, the relative expression of the *Phantom* and *Spook*, involved in the synthesis of 20E (Batista *et al*., 2018), was not directly correlated with the 20E content under water deficit, revealing that the biosynthesis of this secondary metabolite can be regulated by other factors.

In the *in vitro* environment, the stress caused by the addition of PEG 6000 in the culture medium increased up to 4 times the content of 20E in Ac 22. This directly

influenced the total production of 20E, where even stressed plants with lower biomass accumulation had higher productivity. While the Ac 43 showed similar performance to the greenhouse, even with an increase in the concentration of 20E, the reduction in biomass accumulation impacted on a loss of productive potential. The results still suggest that the water deficit cause a fall in the productivity in plants that show higher production under normal conditions, in the case of the Ac 43 that in both environments in conditions without water restriction (controls) exhibit greater content and field performance of 20E. In studies of Corrêa *et al*. (2015), *P. glomerata* were also demonstrated variations in different responses on the growth and development on genotype-dependent manner, evidencing the phenotypic plasticity of this species.

In conclusion, our findings suggest that *P. glomerata* adopts a series of acclimatization strategies that provide tolerance to the water deficit such as osmotic adjustment and increase the activities of antioxidant enzymes, implicate a reprogramming in the hormonal levels and morphoanatomic alterations in leaves, consequently the drought affects negatively the 20E production. In addition, the use of tissue culture techniques *in vitro* has the capacity to optimize propagation and assist in the selection of genotypes with greater productive potential by crop breeding programs, since the pattern of morpho-physiological responses observed *in vitro* matched with those found for greenhouse-raised plants.

Conflict of Interest

The authors declare no conflict of interest.

Acknowledgements

The authors are grateful to the Universidade Federal de Viçosa, the Instituto de Biotecnologia Aplicada à Agropecuária – BIOAGRO and especially Laboratory of Plant Anatomy/DBV for supporting anatomical analysis.

Funding

This work was supported by the Conselho Nacional de Desenvolvimento Científico e Tecnológico (CNPq) (Brasília, DF, Brazil), Fundação de Amparo à Pesquisa do Estado de Minas Gerais (FAPEMIG) (Belo Horizonte, MG, Brazil) and Fundação Arthur Bernardes (Funarbe - UFV). KC was recipient of a scholarship from Coordenação de Aperfeiçoamento de Pessoal de Nível Superior (CAPES) (Brasília, DF, Brazil).

Author Contributions

KC and WCO designed the experiment. KC, TDS, SHSF, DBS, CEV and LMF performed analyses. KC, CEV, SHSF and WCO contributed to the data interpretation and to the writing of the paper with contributions of all the authors. DSB, JM, CWS, and FMDM also collaborated effectively in drafting the final version of the paper. All authors read and approved the final paper.

References

Abbasi AR, Sarvestani R, Mohammadi B, Baghery A. (2014). Drought stress-induced changes at physiological and biochemical levels in some common vetch (*Vicia sativa* L.) Genotypes. **Journal of Agriculture, Science and Technology**. 16: 505-516.

Araújo WL, Trofimova L, Mkrtchyan G, Steinhauser D, Krall L, Graf A, Fernie AR, Burnik VI. (2013). On the role of the mitochondrial 2-oxoglutarate dehydrogenase complex in amino acid metabolism. **Amino Acids**. 44: 683-700. doi.org/10.1007/s00726-012-1392-x.

Bae H, Kim S-H, Kim MS, Sicher RC, Lary D, Strem MD, Natarajan S, Bailey BA. (2008). The drought response of *Theobroma cacao* (cacao) and the regulation of genes involved in polyamine biosynthesis by drought and other stresses. **Plant Physiology and Biochemistry**. 46:174-188. doi.org/10.1016/j.plaphy.2007.10.014.

Bates LS, Waklren RP, Teare ID. (1973). Rapid determination of free proline water stress studies. **Plant and Soil**. 39: 205-207; 1973. doi.org/10.1007/BF00018060

Batista DS, Koehler AD, Romanel E, de Souza VC, Silva TD, Almeida MC, Maciel TEF, Ferreira PRB, Felipe SHS, Saldanha CW, Maldaner J, Dias LLC, Festucci-Buselli RA, Otoni WC. (2018). De novo assembly and transcriptome of *Pfaffia glomerata* uncovers the role of photoautotrophy and the P450 family genes in 20-hydroxyecdysone production. **Protoplasma**. 1-14. doi.org/10.1007/s00709-018-1322-1.

Beauchamp C, Fridovich I. (1971). Superoxide dismutase: improved assays and an assay applicable to acrylamide gels. **Analitycal Biochemistry**, 44: 276-287. doi.org/10.1016/0003-2697(71)90370-8

Bilger W, Schreiber U, Bock M (1995) Determination of the quantum efficiency of photosystem II and non-photochemical quenching of chlorophyll fluorescence in the field. **Oecologia**, 102: 425-432. doi.org/10.1007/BF00341354

Bitrián M, Zarza X, Altabella T, Tiburcio AF, Alcázar R. (2012). Polyamines under Abiotic Stress: Metabolic Crossroads and Hormonal Crosstalks in Plants. **Metabolites**. 2: 516-528. doi.org/10.3390/metabo2030516.

Blum A. (2017). Osmotic adjustment is a prime drought stress adaptive engine in support of plant production. **Plant, cell & environment**. 40: 4-10. doi.org/10.1111/pce.12800

Bradford M. (1976) A rapid and sensitive method for the quantitation of microgram quantities of protein utilizing the principle of protein-dye binding. **Analytical Biochemistry**. 72: 248-254. doi.org/10.1016/0003-2697(76)90527-3

Calgaroto NS, Cargnelutti D, Rossato LV, Farias JG, Nunes ST, Tabaldi LA, Antes FG, Flores EMM, Schetinger MRC, Nicoloso FT. (2011). Zinc alleviates mercury-induced oxidative stress in *Pfaffia glomerata* (Spreng.) Pedersen. **Biometals**. 24, 959-971. doi.org/10.1007/s10534-011-9457-y

Calgaroto NS, Castro GY, Cargnelutti D, Pereira LB, Gonçalves JF, Rossato LV, Antes FG, Dressler VL, Flores EMM, Schetinger MRC, Nicoloso FT. (2010). Antioxidant system activation by mercury in *Pfaffia glomerata* plantlets. **Biometals**, 23: 295-305. doi.org/10.1007/s10534-009-9287-3

Cattivelli L, Rizza F, Badeck FW, Mazzucotelli E, Mastrangelo AM, Francia E, Marè C, Tondelli A, Stanca AM. (2008). Drought tolerance improvement in crop plants: An integrated view from breeding to genomics. **Field Crops Research**. 105: 1-14. doi.org/10.1016/j.fcr.2007.07.004

Caverzan A, Casassola A, & Brammer S. P. Reactive oxygen species and antioxidant enzymes involved in plant tolerance to stress. In *abiotic and biotic stress in plants-recent advances and future perspectives*; Shanker, A., Ed.; InTechOpen: London, UK, 2016; pp. 463-480. doi.org/ 10.5772/61368.

Chance B, Maehley AC. (1955) Assay of catalases and peroxidases. **Methods Enzymology**. 2: 764-775; 1955. doi.org/10.1016/S0076-6879(55)02300-8

Chater CCC, Oliver J, Casson S, Gray JE. (2014). Putting the brakes on: abscisic acid as a central environmental regulator of stomatal development. **New Phytologist.** 202: 376-391. doi.org/10.1111/nph.12713.

Choudhury FK, Rivero RM, Blumwald E, Mittler R. (2017). Reactive oxygen species, abiotic stress and stress combination. **The Plant Journal**. 90(5): 856-867. doi.org/10.1111/tpj.13299.

Claeys H, Landeghem SV, Dubois M, Maleux K, Inzé D. (2014). What Is Stress? Dose-response effects in commonly used *in vitro* stress assays. **Plant Physiology**. 165: 519-527. doi.org/10.1104/pp.113.234641

Corrêa JPO, Vital CE, Pinheiro MVM, Batista DS, Azevedo JFL, Saldanha CW, Cruz ACF, Damatta FM, Otoni WC. (2015). *In vitro* photoautotrophic potential and ex vitro photosynthetic competence of *Pfaffia glomerata* (Spreng.) Pedersen accessions. **Plant Cell, Tissue and Organ Culture**, 121: 289–300. doi.org/10.1007/s11240-014-0700-4

Cruz CD. (2016). Genes Software - extended and integrated with the R, Matlab and Selegen. **Acta Scientiarum. Agronomy**, 38: 547-552. doi.org/10.4025/actasciagron.v38i4.32629

Daszkowska-Golec A, Szarejko I. (2013). Open or close the gate-stomata action under the control of phytohormones in drought stress conditions. **Frontiers in Plant Science**. 4: 138. doi.org/10.3389/fpls.2013.00138.

Del Longo OT, González CA, Pastori GM, Trippi VS. (1993). Antioxidant defences under hyperoxygenic and hyperosmotic conditions in leaves of two lines of maize with differential sensitivity to drought. **Plant Cell Physiol**, 34: 1023-1028. doi.org/10.1093/oxfordjournals.pcp.a078515

Dietz KJ. (2016). Thiol-based peroxidases and ascorbate peroxidases: Why plants rely on multiple peroxidase systems in the photosynthesizing chloroplast? **Molecules and Cells**. 39: 20-25. doi.org/10.14348/molcells.2016.2324.

Ebad FA, Hussein EA, Neda'a AH. (2017). Impact of biotic and abiotic elicitation on morphology, growth, active constituents and antibacterial activity of *Solanum nigrum* (L.) calli induced *in vitro*. **Egyptian Journal Desert Research**. 67(1): 47-63. doi: 10.21608/EJDR.2017.5844

Egea G, Verhoef A, Vidale PL. (2011). Towards an improved and more flexible representation of water stress in coupled photosynthesis - stomatal conductance models. **Agricultural and Forest Meteorology**, 151: 1370-1384. doi.org/10.1016/j.agrformet.2011.05.019.

El-Tayeb MA. (2005). Response of barley grains to the interactive e.ect of salinity and salicylic acid. **Plant Growth Regulation**. 45: 215-224. doi.org/10.1007/s10725-005-4928-1.

Fang Y, Xiong L. (2015). General Mechanisms of drought response and their application in drought resistance improvement in plants. **Cellular and Molecular Life Sciences**. 72: 673-689. doi.org/10.1007/s00018-014-1767-0.

Farooq M, Wahid A, Kobayashi N, Fujita D, Basra SMA. (2009). Plant Drought Stress: Effects, Mechanisms and Management. In *Sustainable Agriculture*. Lichtfouse E., Navarrete M., Debaeke P., Véronique S., Alberola C. (eds). Springer, Dordrecht, pp 153-188. doi.org/10.1007/978-90-481-2666-8_12.

Felipe, S. H. S. **Salt stress and UV-B radiation modulate growth, physiology and 20-hydroxyecdysone contents in Brazilian-ginseng [*Pfaffia glomerata* (Spreng.) Pedersen]**. 2019. 78 f. Tese (Doutorado em Botânica) - Departamento de Biologia Vegetal, Universidade Federal de Viçosa, Minas Gerais. 2019.

Festucci-Buselli RA, Contim LAS, Barbosa LCA, Stuart JJ, Vieira RF, Otoni WC. (2008). Level and distribution of 20-hydroxyecdysone during *Pfaffia glomerata* development. **Brazilian Journal of Plant Physiology**. 20: 305-311. doi.org/10.1590/S1677-04202008000400006.

Foyer CH. (2018). Reactive oxygen species, oxidative signaling and the regulation of photosynthesis. **Environmental and Experimental Botany**. 154: 134-142. doi.org/10.1016/j.envexpbot.2018.05.003.

Guan X-K, Song L, Wang T-C, Turner NC, Li F-M. (2015). Effect of drought on the gas exchange, chlorophyll fluorescence and yield of six different-era spring wheat cultivars. **Journal of Agronomy and Crop Science**. 201: 253-266. doi.org/10.1111/jac.12103.

Gupta DK, Nicoloso FT, Schetinger MR, Rossato LV, Huang HG, Srivastava S, Yang XE. (2011). Lead induced responses of *Pfaffia glomerata*, an economically important Brazilian medicinal plant, under *in vitro* culture conditions. **Bulletin of Environmental Contamination and Toxicology**, 86: 272-277. doi.org/10.1007/s00128-011-0226-y

Gupta P, Sharma S, Saxena S. (2016). Effect of abiotic stress on growth parameters and steviol glycoside content in *Stevia rebaudiana* (Bertoni) raised *in vitro*. **Journal of Applied Research on Medicinal and Aromatic Plants**. 3: 160-167. doi.org/10.1016/j.jarmap.2016.03.004.

Gururani MA, Venkatesh J, Tran LSP. (2015). Regulation of photosynthesis during abiotic stress-induced photoinhibition. **Molecular Plant**. 8: 1304-1320. dx.doi.org/10.1016/j.molp.2015.05.005.

Havir EA, McHale NA. (1987). Biochemical and developmental characterization of multiple forms of catalase in tobacco leaves. **Plant Physiol,** 84:450-455. doi.org/10.1104/pp.84.2.450

Ishimaru K, Kobayashi N, Ono K, Yano M, Ohsugi R. (2001). Are contents of Rubisco, soluble protein and nitrogen in flag leaves of rice controlled by the same genetics? **Journal of Experimental Botany**. 52: 1827-1833. doi.org/10.1093/jexbot/52.362.1827.

John R, Shajitha PP, Devassy A, Mathew L. (2018). Effect of elicitation and precursor feeding on accumulation of 20-hydroxyecdysone in *Achyranthes aspera* Linn. cell suspension cultures. **Physiology and Molecular Biology of Plants**. 24: 275-284. doi.org/10.1007/s12298-018-0506-7

Jungklang J, Saengnil K, Uthaibutra J. (2017). Effects of water-deficit stress and paclobutrazol on growth, relative water content, electrolyte leakage, proline content and some antioxidant changes in *Curcuma alismatifolia* Gagnep. cv. Chiang Mai Pink. **Saudi Journal of Biological Sciences**. 24:1505-1512. doi.org/10.1016/j.sjbs.2015.09.017.

Kalladan R, Lasky JR, Chang TZ, Sharma S, Juenger TE, Verslues PE. (2017). Natural variation identifies genes affecting drought-induced abscisic acid accumulation in *Arabidopsis thaliana*. **Proceedings of the National Academy of Sciences**. 114: 11536-11541. doi.org/10.1073/pnas.1705884114.

Kamada T, Picoli EAT, Vieira RF, Barbosa LCA, Cruz CD, Otoni WC (2009) Variação de caracteres morfológicos e fisiológicos de populações naturais de *Pfaffia glomerata* (Spreng.) Pedersen e correlação com a produção de β-ecdisona. **Revista Brasileira Plantas Medicinais**, 11:247–256.

Kanojia A, Dijkwel PP. (2018). Abiotic Stress Responses are Governed by Reactive Oxygen Species and Age. **Annual Plant Reviews Online**. 1-32. doi.org/10.1002/9781119312994.apr0611

Karnovsky MJ. (1965). A formaldehyde-glutaraldehyde fixative of high osmolarity for use in electron microscopy. **Journal of Cell Biology**, 27:37–138.

Khoyerdi FF, Shamshiri MH, Estaji A. (2016). Changes in some physiological and osmotic parameters of several pistachio genotypes under drought stress. **Scientia horticulturae**. 198: 44-51. doi.org/10.1016/j.scienta.2015.11.028

Kowitcharoen L, Wongs-Aree C, Setha S, Komkhuntod R, Srilaong V, Kondo S. (2015). Changes in abscisic acid and antioxidant activity in sugar apples under drought conditions. **Scientia horticulturae**. 193: 1-6. doi.org/10.1016/j.scienta.2015.06.043.

Li L, Gu W, Li J, Li C, Xie T, Qu D, Meng Y, Li C, Wei S. (2018). Exogenously applied spermidine alleviates photosynthetic inhibition under drought stress in maize (*Zea mays* L.) seedlings associated with changes in endogenous polyamines and phytohormones. **Plant Physiology and Biochemistry**. 129: 35-55. doi.org/10.1016/j.plaphy.2018.05.017.

Li Z, Yu J, Peng Y, Huang B. (2017). Metabolic pathways regulated by abscisic acid, salicylic acid and γ-aminobutyric acid in association with improved drought tolerance in creeping bentgrass (*Agrostis stolonifera*). **Physiologia Plantarum**. 159: 42-58. doi.org/10.1111/ppl.12483.

Li Z, Zhang Y, Peng D, Wang X, Peng Y, He X, Zhang X, Ma X, Huang L, Yan Y. (2015). Polyamine regulates tolerance to water stress in leaves of white clover associated with antioxidant defense and dehydrin genes via involvement in calcium messenger system and hydrogen peroxide signaling. **Frontiers in Physiology**. 6: 280. doi.org/10.3389/fphys.2015.00280.

Lim CW, Baek W, Jung J, Kim J-H, Lee SC. (2015). Function of ABA in stomatal defense against biotic and drought stresses. **International Journal of Molecular Sciences**. 16: 15251-15270. doi.org/10.3390/ijms160715251.

Livak KJ, Schmittgen TD. (2001). Analysis of relative gene expression data using real-time quantitative PCR and the $2^{-\Delta\Delta Ct}$ method. **Methods**. 25: 402-408. doi.org/10.1006/meth.2001.1262.

Maldaner J, Nicoloso FT, Tabaldi LA, Cargnelutti D, Skrebsky EC, Rauber R, Gonçalves FB, Rossato LV. (2015). Aluminum accumulation in two *Pfaffia glomerata* genotypes and its growth effects. **Ciência Rural**, 45, 1013-1020. doi.org/10.1590/0103-8478cr20140439

Medrano H, Tomás M, Martorell S, Flexas J, Hernández E, Rosselló J, Pou A, Escalona J-M, Bota J. (2015) From leaf to whole-plant water use efficiency (WUE) in complex canopies: limitations of leaf WUE as a selection target. **The Crop Journal**. 3: 220-228. doi.org/10.1016/j.cj.2015.04.002.

Mihoub I, Badeck F-W, Aïd F, Lamothe-Sibold M, Ghashghaie J. (2018). Relationship between taproot morphological traits, carbon isotope composition and grain yield in safflower. **Arid Land Research and Management**. 32: 471-486 doi.org/10.1080/15324982.2018.1463574.

Miller G, Suzuki N, Ciftci-Yilmaz S, Mittler R. (2010). Reactive oxygen species homeostasis and signalling during drought and salinity stresses. **Plant, Cell &. Environment**. 33(4): 453-467. doi.org/10.1111/j.1365-3040.2009.02041.x.

Mishra P, Bhoomika K, Dubey RS. (2013). Differential responses of antioxidative defense system to prolonged salinity stress in salt-tolerant and salt-sensitive Indica rice (*Oryza sativa* L.) seedlings. **Protoplasma**. 250: 3-19. https://doi.org/10.1007/s00709-011-0365-3.

Miyazawa S-I, Livingston NJ, Turpin DH. (2006). Stomatal development in new leaves is related to the stomatal conductance of mature leaves in poplar (Populus trichocarpa×P. deltoides). **Journal of Experimental Botany**. 57: 373-380. doi.org/10.1093/jxb/eri278.

Montilla-Bascón G, Rubiales D, Hebelstrup KH, Mandon J, Harren FJM, Cristescu SM, Mur LAJ, Prats E. (2017). Reduced nitric oxide levels during drought stress promote drought tolerance in barley and is associated with elevated polyamine biosynthesis. **Scientific Reports**. 7: 13311. doi.org/10.1038/s41598-017-13458-1.

Munné-Bosch S, Simancas B, Müller M. (2018). Ethylene signaling cross-talk with other hormones in *Arabidopsis thaliana* exposed to contrasting phosphate availability: Differential effects in roots, leaves and fruits. **Journal of Plant Physiology**.226: 114-122. doi.org/10.1016/j.jplph.2018.04.017.

Murchie EH, Lawson T. (2013). Chlorophyll fluorescence analysis: a guide to good practice and understanding some new applications. **Journal of Experimental Botany**. 64: 3983-3998. doi.org/10.1093/jxb/ert208.

Mwadzingeni L, Shimelis H, Tesfay S, Tsilo TJ. (2016). Screening of bread wheat genotypes for drought tolerance using phenotypic and proline analyses. **Frontiers in Plant Science**. 7: 1276. doi.org/10.3389/fpls.2016.01276.

Naik PM, Al-Khayri JM. (2016). Impact of Abiotic Elicitors on *in vitro* production of plant secondary metabolites: a review. **Journal of Advanced Research in Biotechnology.** 1 (2): 7. doi.org/10.15226/2475-4714/1/2/00102.

Nakano Y, Asada K (1981) Hydrogen peroxide is scavenged by ascorbate-specific peroxidase in spinach chloroplasts. **Plant Cell Physiol**, 22: 867-880. doi.org/10.1093/oxfordjournals.pcp.a076232

Napoleão TA, Soares G, Vital CE, Bastos C, Castro R, Loureiro ME, Giordano A. (2017). Methyl jasmonate and salicylic acid are able to modify cell wall but only salicylic acid alters biomass digestibility in the model grass *Brachypodium distachyon*. **Plant Science** 263, 46–54. doi.org/10.1016/j.plantsci.2017.06.014

Niinemets Ü. (2016). Uncovering the hidden facets of drought stress: secondary metabolites make the difference. **Tree Physiology**. 36: 129-132. doi.org/10.1093/treephys/tpv128.

Nishiyama R, Watanabe Y, Fujita Y, Le DT, Kojima M, Werner T, Vankova R, Yamaguchi-Shinozaki K, Shinozaki K, Kakimoto T, Sakakibara H, Schmülling T, Tran L-SP. (2011) Analysis of cytokinin mutants and regulation of cytokinin metabolic genes reveals important regulatory roles of cytokinins in drought, salt and abscisic acid responses, and abscisic acid biosynthesis. **The Plant Cell**. 23: 2169-2183. doi.org/10.1105/tpc.111.087395.

Nishiyama Y, Murata N. (2014) Revised scheme for the mechanism of photoinhibition and its application to enhance the abiotic stress tolerance of the photosynthetic machinery. **Applied Microbiology and Biotechnology**. 98: 8777-8796. doi.org/10.1007/s00253-014-6020-0.

O'Brien TP, McCully ME. (1981). The study of plant structure: principles and selected methods. Melbourne: Termarcarphy Pty

Pandey P, Srivastava RK, Rajpoot R, Rani A, Pandey AK, Dubey RS. (2016). Water deficit and aluminum interactive effects on generation of reactive oxygen species and responses of antioxidative enzymes in the seedlings of two rice cultivars differing in stress tolerance. **Environmental Science and Pollution Research**. 23: 1516-1528. doi.org/10.1007/s11356-015-5392-8.

Park IS, Kim HJ, Jeong Y-S, Kim W-K, Kim J-S. (2017). Differential abilities of Korean soybean varieties to biosynthesize glyceollins by biotic and abiotic elicitors. **Food Science and Biotechnology**. 26: 255-261. doi.org/10.1007/s10068-017-0034-1.

Peleg Z, Blumwald E. (2011). Hormone balance and abiotic stress tolerance in crop plants. **Current Opinion in Plant Biology**. 14: 290-295. doi.org/10.1016/j.pbi.2011.02.001.

Pintó-Marijuan M, Munné-Bosch S. (2014). Photo-oxidative stress markers as a measure of abiotic stress-induced leaf senescence: advantages and limitations. **Journal of Experimental Botany**. 65: 3845-3857. doi.org/10.1093/jxb/eru086.

Pires MV, Pereira Júnior AA, Medeiros DB, Daloso DM, Pham PA, Barros KA, Engqvist MKM, Florian A, Krahnert I, Maurino VG, Araújo WL, Fernie AR. (2016). The influence of alternative pathways of respiration that utilize branched-chain amino acids following water shortage in *Arabidopsis*. **Plant, Cell & Environment**. 39: 1304-1319. doi.org/10.1016/j.sajb.2015.08.008.

Ramakrishna A, Ravishankar GA. (2011). Influence of abiotic stress signals on secondary metabolites in plants. **Plant Signaling & Behavior**. 6: 1720-1731. doi.org/10.4161/psb.6.11.17613.

Rana V, Ram S, Nehra K. (2017). Review Proline Biosynthesis and its Role in Abiotic Stress. **International Journal of Agriculture Innovations and Research.** 6: 2319-1473.

Ren J, Sun LN, Zhang QY, Song XS. (2016). Drought tolerance is correlated with the activity of antioxidant enzymes in *Cerasus humilis* seedlings. **BioMed Research International**. 9: id 9851095. doi.org/10.1155/2016/9851095

Rivas R, Falcão HM, Ribeiro RV, Machado EC, Pimentel C, Santos MG. (2016). Drought tolerance in cowpea species is driven by less sensitivity of leaf gas exchange to water deficit and rapid recovery of photosynthesis after rehydration. **South African Journal of Botany**. 103: 101-107. doi:10.1016/j.sajb.2015.08.008.

Rosa HS, De Camargo VB, Camargo G, Garcia CV, Fuentefria AM, Mendez ASL. (2015). Ecdysteroids in *Sida tuberculata* R.E. Fries (Malvaceae): chemical composition by LC-ESI-MS and selective anti-Candida krusei activity. **Food Chemistry**. 182: 193-199. doi.org/10.1016/j.foodchem.2015.02.144.

Rosa HS, Salgueiro ACF, Colpo AZC, Paula FR, Mendez ASL, Folmer V. (2016). *Sida tuberculata* (Malvaceae): a study based on development of extractive system and in silico and in vitro properties. **Brazilian Journal of Medical and Biological Research**. 49: e5282. dx.doi.org/10.1590/1414-431X20165282

Roychoudhury A, Paul S, Basu S. (2013). Cross-talk between abscisic acid-dependent and abscisic acid-independent pathways during abiotic stress. **Plant Cell Reports**. 32: 985-1006. doi.org/10.1007/s00299-013-1414-5.

Saha P, Sade N, Arzani A, Wilhelmi MDMR, Coe KM, Li B, Blumwald E. (2016). Effects of abiotic stress on physiological plasticity and water use of *Setaria viridis* (L.). **Plant Science**. 251: 128-138. doi.org/10.1016/j.plantsci.2016.06.011.

Saldanha CW, Otoni CG, de Azevedo JLF, Dias LLC, do Rêgo MM, Otoni WC. (2012). A low-cost alternative membrane system that promotes growth in nodal cultures of Brazilian ginseng [*Pfaffia glomerata* (Spreng.) Pedersen]. **Plant Cell, Tissue and Organ Culture**. 110: 413-422. doi.org/10.1007/s11240-012-0162-5.

Saldanha CW, Otoni CG, Rocha DI, Cavatte PC, Detmann KDSC, Tanaka FAO, Dias LLC, DaMatta FM, Otoni WC. (2014). CO2-enriched atmosphere and supporting material impact the growth, morphophysiology and ultrastructure of in vitro Brazilian-ginseng [*Pfaffia glomerata* (Spreng.) Pedersen] plantlets**. Plant Cell, Tissue and Organ Culture (PCTOC)**. 118: 87-99. doi.org/10.1007/s11240-014-0464-x.

Sanders GJ, Arndt SK. (2012). Osmotic adjustment under drought conditions. In *Plant responser to drought stress*. Aroca R. (eds). Springer, Berlin, Heidelberg, pp199-229. doi.org/10.1007/978-3-642-32653-0_8.

Schneider CA, Rasband WS, Eliceiri KW (2012) "NIH Image to ImageJ: 25 years of image analysis". **Nature Methods**, 9: 671-675. doi.org/10.1038/nmeth.2089

Sharma G, Giri J, Tyagi AK. (2015). Rice OsiSAP7 negatively regulates ABA stress signalling and imparts sensitivity to water-deficit stress in Arabidopsis. **Plant Science**. 237: 80-92. doi.org/10.1016/j.plantsci.2015.05.011.

Sharma M, Gupta SK, Majumder B, Maurya VK, Deeba F, Alam A, Pandey V. (2018). Proteomics unravel the regulating role of salicylic acid in soybean under yield limiting drought stress. **Plant Physiology and Biochemistry**. 130: 529-541. doi.org/10.1016/j.plaphy.2018.08.001.

Shinde S, Villamor JG, Lin W, Sharma S, Verslues PE. (2016). Proline coordination with fatty acid synthesis and redox metabolism of chloroplast and mitochondria. **Plant Physiology**. 172: 1074-1088. doi.org/10.1104/pp.16.01097.

Silva EN, Ribeiro RV, Ferreira-Silva SL, Vieira SA, Ponte LFA, Silveira JAG. (2012). Coordinate changes in photosynthesis; sugar accumulation and antioxidative

enzymes improve the performance of *Jatropha curcas* plants under drought stress. **Biomass and Bioenergy**. 45: 270-279. doi.org/10.1016/j.biombioe.2012.06.009.

Skrebsky EC, Tabaldi LA, Pereira LB, Rauber R, Maldaner J, Cargnelutti D, Gonçalves JF, Castro GY, Shetinger MRC, Nicoloso FT. (2008). Effect of cadmium on growth, micronutrient concentration, and δ-aminolevulinic acid dehydratase and acid phosphatase activities in plants of *Pfaffia glomerata*. **Brazilian Journal of Plant Physiology**, 20: 285-294. doi.10.1590/S1677-04202008000400004.

Souza PU, Lima LKS, Soares TL, de Jesus ON, Coelho Filho MA, Girardi EA. (2018). Biometric, physiological and anatomical responses of *Passiflora* spp. to controlled water deficit. **Scientia Horticulturae**. 229: 77-90. doi.org/10.1016/j.scienta.2017.10.019.

Su L, Dai Z, Li S, Xin H. (2015). A novel system for evaluating drought–cold tolerance of grapevines using chlorophyll fluorescence. **BMC Plant Biology**. 15: 82. doi: 10.1186/s12870-015-0459-8.

Sussmilch FC, Brodribb TJ, McAdam SA. (2017). Up-regulation of NCED3 and ABA biosynthesis occur within minutes of a decrease in leaf turgor but AHK1 is not required. **Journal of Experimental Botany**. 68: 2913-2918. doi.org/10.1093/jxb/erx124.

Tenhaken R. (2015). Cell wall remodeling under abiotic stress. **Frontiers in Plant Science**. 5: 771. doi.org/10.3389/fpls.2014.00771.

Tiwari S, Lata C, Singh Chauhan P, Prasad V, Prasad M. (2017). A functional genomic perspective on drought signaling and its crosstalk with phytohormone-mediated signalling pathways in plants. **Currents Genomics**. 18: 469-482. doi.org/10.2174/1389202918666170605083319.

Turkan I, Uzilday B, Dietz K-J, Bräutigam A, Ozgur RO. (2018). Reactive oxygen species and redox regulation in mesophyll and bundle sheath cells of C4 plants. **Journal of Experimental Botany**. 69: 3321-3331. doi.org/10.1093/jxb/ery064.

Turner NC. (2017). Turgor maintenance by osmotic adjustment, an adaptive mechanism for coping with plant water deficits. **Plant, Cell & Environment**. 40: 1-3. doi.org/10.1111/pce.12839.

Turner NC. (2018). Turgor maintenance by osmotic adjustment: 40 years of progress. **Journal of Experimental Botany**. 69: 3223-3233. doi.org/10.1093/jxb/ery181.

Van Dongen JT, Gupta KJ, Ramírez-Aguilar SJ, Araújo WL, Nunes-Nesi A, Fernie AR. (2011). Regulation of respiration in plants: A role for alternative metabolic pathways. **Journal of Plant Physiology**. 168: 1434-1443. doi.org/10.1016/j.jplph.2010.11.004.

Verslues PE, Agarwal M, Katiyar-Agarwal S, Zhu J, Zhu JK. (2006). Methods and concepts in quantifying resistance to drought, salt and freezing, abiotic stresses that affect plant water status. **The Plant Journal**. 45: 523-539. doi.org/10.1111/j.1365-313X.2005.02593.x.

Vishwakarma K, Upadhyay N, Kumar N, Yadav G, Singh J, Mishra RK, Kumar V, Verma R, Upadhyay RG, Pandey M, Sharma S. (2017). Abscisic acid signaling and abiotic stress tolerance in plants: a review on current knowledge and future prospects. **Frontiers in Plant Science**. 8: 161. doi.org/10.3389/fpls.2017.00161.

Walters RG. (2005). Towards an understanding of photosynthetic acclimation. **Journal of Experimental Botany**. 56: 435-447. doi.org/10.1093/jxb/eri060.

Wang QJ, Zheng LP, Sima YH, Yuan HY, Wang JW. (2013). Methyl jasmonate stimulates 20-hydroxyecdysone production in cell suspension cultures of *Achyranthes bidentata*. **Plant Omics**. 6: 116-120.

Wellburn AR. (1994). The spectral determination of chlorophylls a and b, as well as total carotenoids, using various solvents with spectrophotometers of different resolution. J Plant Physiol 144:307-313

Xu Z, Jiang Y, Zhou G. (2015). Response and adaptation of photosynthesis, respiration, and antioxidant systems to elevated CO2 with environmental stress in plants. **Frontiers in Plant Science**. 6: 701. doi.org/10.3389/fpls.2015.00701.

Xu Z, Zhou G. (2008). Responses of leaf stomatal density to water status and its relationship with photosynthesis in a grass. **Journal of Experimental Botany**. 59: 3317-3325. doi.org/10.1093/jxb/ern185.

Yamori W. (2016). Photosynthetic response to fluctuating environments and photoprotective strategies under abiotic stress. **Journal of Plant Research**. 129: 379-395. doi.org/10.1007/s10265-016-0816-1.

Zhang H, Liu K, Wang Z, Liu L, Yang J. (2015). Abscisic acid, ethylene and antioxidative systems in rice grains in relation with grain filling subjected to postanthesis soil-drying. **Plant Growth Regulation**. 76: 135-146. doi.org/10.1007/s10725-014-9983-z.

Zhang X, Ervin EH, Liu Y, Hu G, Shang C, Fukao T, Alpuerto J. (2015). Differential responses of antioxidants, abscisic acid, and auxin to deficit irrigation in two perennial ryegrass cultivars contrasting in drought tolerance. **Journal of the American Society for Horticultural Science**. 140(6): 562-572. doi.org/10.21273/JASHS.140.6.562

Figure Captions

Figure 1. Potential water leaf in accessions *P. glomerata* under water deficit (moderate and severe) in greenhouse. Vertical bars represent standard errors of the means.

Figure 2. Detail of the union of two magentas inverted (A) and the bridges of plastic cup and a paper disc and explants contact with medium culture (B).

Figure 3. Growth parameters in *P. glomerata* plants after 15 days grown under water deficit in greenhouse. (A) Leaf dry weight; (B) Stem dry weight; (C) Root dry weight; (D) Total dry weight; (G) Plant height; (H) Leaf area; (E) Accession 22 (Ac 22 control, moderate and severe); and (F) Accession 43 (Ac 43 control, moderate and severe). Vertical bars represent standard errors of the means. Same letters uppercase between accessions and lowercase between stress conditions do not differ at 5% level by Tukey's test.

Figure 4. Growth parameters and photosynthetic gas exchange in *P. glomerata* plants after 20 days grown under water deficit by PEG 6000 *in vitro* and 7 days after rehydratation. (A) Leaf area; (B) Plant height; (C) Dry weight; (D) Net CO_2 assimilation rate (*A*); (E) Accession 22 (Ac 22 control, PEG 6000 0.1, 0.2 , and 0.3 %); and (F) Accession 43 (Ac 43 control, PEG 6000 0.1, 0.2 , and 0.3 %). Vertical bars represent standard errors of the means. Same letters uppercase between accessions and lowercase between stress conditions do not differ at 5% level by Tukey's test.

Figure 5. Cross sections of the edge and median portion of leaf in *P. glomerata* plants after 15 days grown under water deficit in greenhouse. (A, C, E, G, I, and K) Median portion; (B, D, F, H, J, and L) Edge of the leaf; (M) Adaxial epidermis; (N) Abaxial epidermis; (O) Mesophilic layer; (P) Palisade parenchyma; (Q) Spongy parenchyma; (R) Abaxial stomata density (STD); and (S) Adaxial stomata density (STD). Vertical bars represent standard errors of the means. Same letters uppercase between accessions and lowercase between stress conditions do not differ at 5% level by Tukey's test.

Figure 6. Cross sections of the median portion of leaf in *P. glomerata* plants after 20 days grown under water deficit by PEG 6000 *in vitro*. (A, C, E, an G) Median portion in Ac 22; (B, D, F, and H) Median portion in Ac 43; (I) Adaxial epidermis; (J) Abaxial epidermis; (K) Mesophilic layer; (L) Palisade parenchyma; (M) Spongy parenchyma; (N) Abaxial stomata density (STD); and (O) Adaxial stomata density (STD). Vertical bars represent standard errors of the means. Same letters uppercase between accessions and lowercase between stress conditions do not differ at 5% level by Tukey's test.

Figure 7. Pigment content in *P. glomerata* leaf after 15 days grown under water deficit and 7 days after rehydratation in greenhouse. (A) Chlorophyll *a*; (B) Chlorophyll *b*; (C) Chlorophyll *a*+*b*; (D) Chlorophyll *a/b*; and (E) Carotenoids. Vertical bars represent standard errors of the means. Same letters uppercase between accessions and lowercase between stress conditions do not differ at 5% level by Tukey's test.

Figure 8. Pigment content in *P. glomerata* plants after 20 days grown under water deficit by PEG 6000 and 7 days after rehydratation *in vitro*. (A) Chlorophyll *a*; (B) Chlorophyll *b*; (C) Chlorophyll *a*+*b*; (D) Chlorophyll *a/b*; and (E) Carotenoids. Vertical bars represent standard errors of the means. Same letters uppercase between accessions and lowercase between stress conditions do not differ at 5% level by Tukey's test.

Figure 9. Gas exchange and chlorophyll fluorescence parameters in *P. glomerata* leaf after 15 days grown under water deficit and 7 days after rehydratation in greenhouse. (A) Net CO_2 assimilation rate (A); (B) Dark respiration (R_d); (C) Stomatal conductance to water vapor (g_s); (D) Transpiration rate (E); (E) Internal CO_2 concentration (C_i); (F) Ratio C_i/C_a; (G) PS II maximum quantum yield (F_v/F_m); (H) Photochemical quenching (qP); and (I) Electron transport rate (ETR); (J) Water use efficiency (WUE); and (K) Non-photochemical quenching (NQP). Vertical bars represent standard errors of the means. Same letters uppercase between accessions and lowercase between stress conditions do not differ at 5% level by Tukey's test.

Figure 10. Phytohormone contents in *P. glomerata* leaf after 15 days grown under water deficit and 7 days after rehydratation in greenhouse. (A) Abscisic acid (ABA); (B) Spermidine (Spd); (C) Spermine (Spm); (D) Putrescine (Put); (E) Salicylic acid (SA), (F) Jasmonate (JA); (G) Zeatin (Zea); and (H) 1-carboxylic acid-1-aminocyclopropane (ACC). Vertical bars represent standard errors of the means. Same letters uppercase between accessions and lowercase between stress conditions do not differ at 5% level by Tukey's test.

Figure 11. Phytohormone contents in *P. glomerata* plants after 20 days grown under water deficit by PEG 6000 and 7 days after rehydratation *in vitro*. (A) Abscisic acid (ABA); (B) Spermine (Spm); (C) Spermidine (Spd); (D) Jasmonate (JA); (E) Zeatin (Zea), (F) Salicylic acid (SA); (G) 1-carboxylic acid-1-aminocyclopropane (ACC); and (H) Putrescine (Put). Vertical bars represent standard errors of the means. Same letters do not differ at 5% level by Tukey's test.

Figure 12. The activities of antioxidant enzymes and content of proline and soluble proteins in *P. glomerata* leaf after 15 days grown under water deficit and 7 days after rehydratation in greenhouse. (A) Catalase (CAT); (B) Superoxide dismutase (SOD); (C) Peroxidases (POD); (D) Ascorbate peroxidase (APX), (E) Proline; and (F) Protein. Vertical bars represent standard errors of the means. Same letters uppercase between accessions and lowercase between stress conditions do not differ at 5% level by Tukey's test.

Figure 13. The activities of antioxidant enzymes and content of proline and soluble proteins in *P. glomerata* plants after 20 days grown under water deficit by PEG 6000 and 7 days after rehydratation *in vitro*. (A) Catalase (CAT); (B) Superoxide dismutase (SOD); (C) Peroxidases (POD); (D) Ascorbate peroxidase (APX), (E) Proline; and (F) Protein. Vertical bars represent standard errors of the means. Same letters uppercase between accessions and lowercase between stress conditions do not differ at 5% level by Tukey's test.

Figure 14. 20-hydroxyecdysone (20E) content and field yield of 20E in *P. glomerata* plants after 15 days grown under water deficit in greenhouse. The content of 20E in leaf (A), stem (C), and root (D); Total field yield 20E in leaf (B), stem (D), root (E), and whole-plant (F). Vertical bars represent standard errors of the means. Same letters uppercase between accessions and lowercase between stress conditions do not differ at 5% level by Tukey's test.

Figure 15. 20-hydroxyecdysone (20E) content and field yield of 20E in *P. glomerata* plants after 20 days grown under water deficit by PEG 6000 *in vitro*. (A) 20E content whole-plant; and (B) 20E Total whole-plant. Vertical bars represent standard errors of the means. Same letters uppercase between accessions and lowercase between stress conditions do not differ at 5% level by Tukey's test.

Figure 16. Normalized relative expression of *Phantom* and *Spook* genes in *P. glomerata* leaves after 15 days grown under water deficit and 7 days after rehydratation in greenhouse. (A) *Phantom* gene and (B) *Spook* gene. Gene expression relative to the control gene *glyceraldehyde-3-phosphate dehydrogenase*. Vertical bars represent standard errors of the means. Do not differ at 5% level by Dunnett's test.

Figure 1.

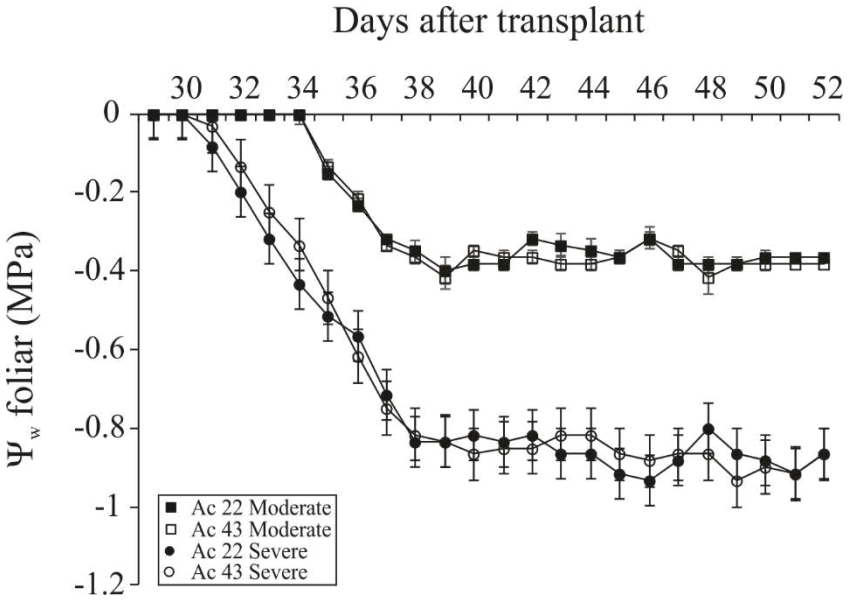

Figure 2.

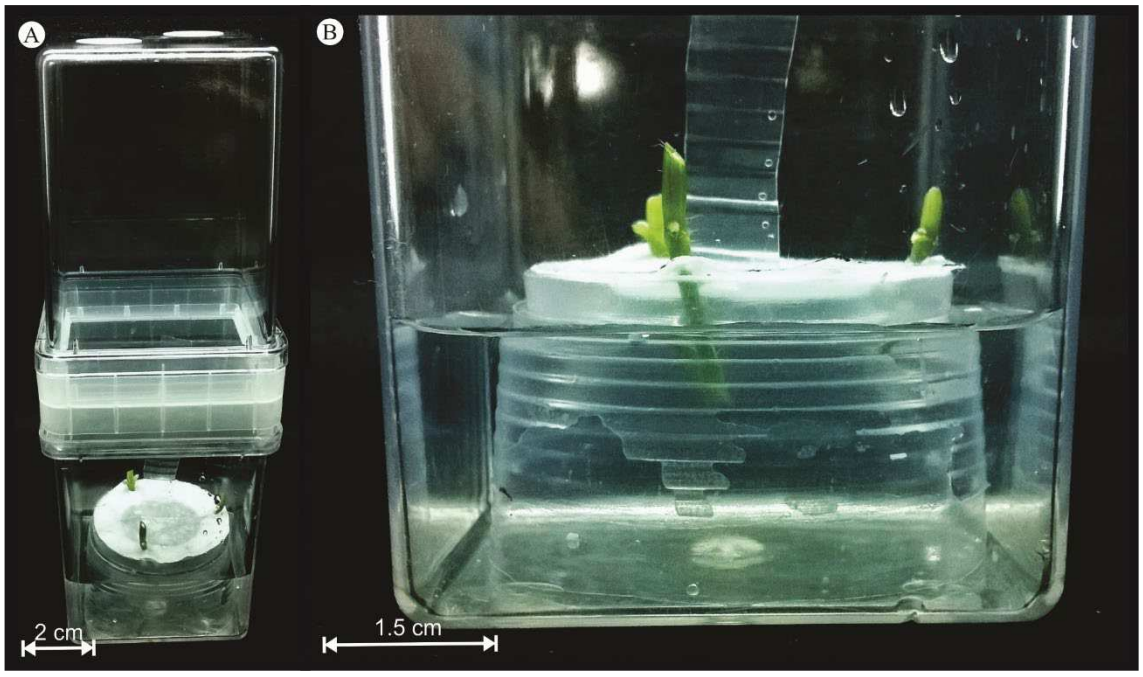

Figure 3.

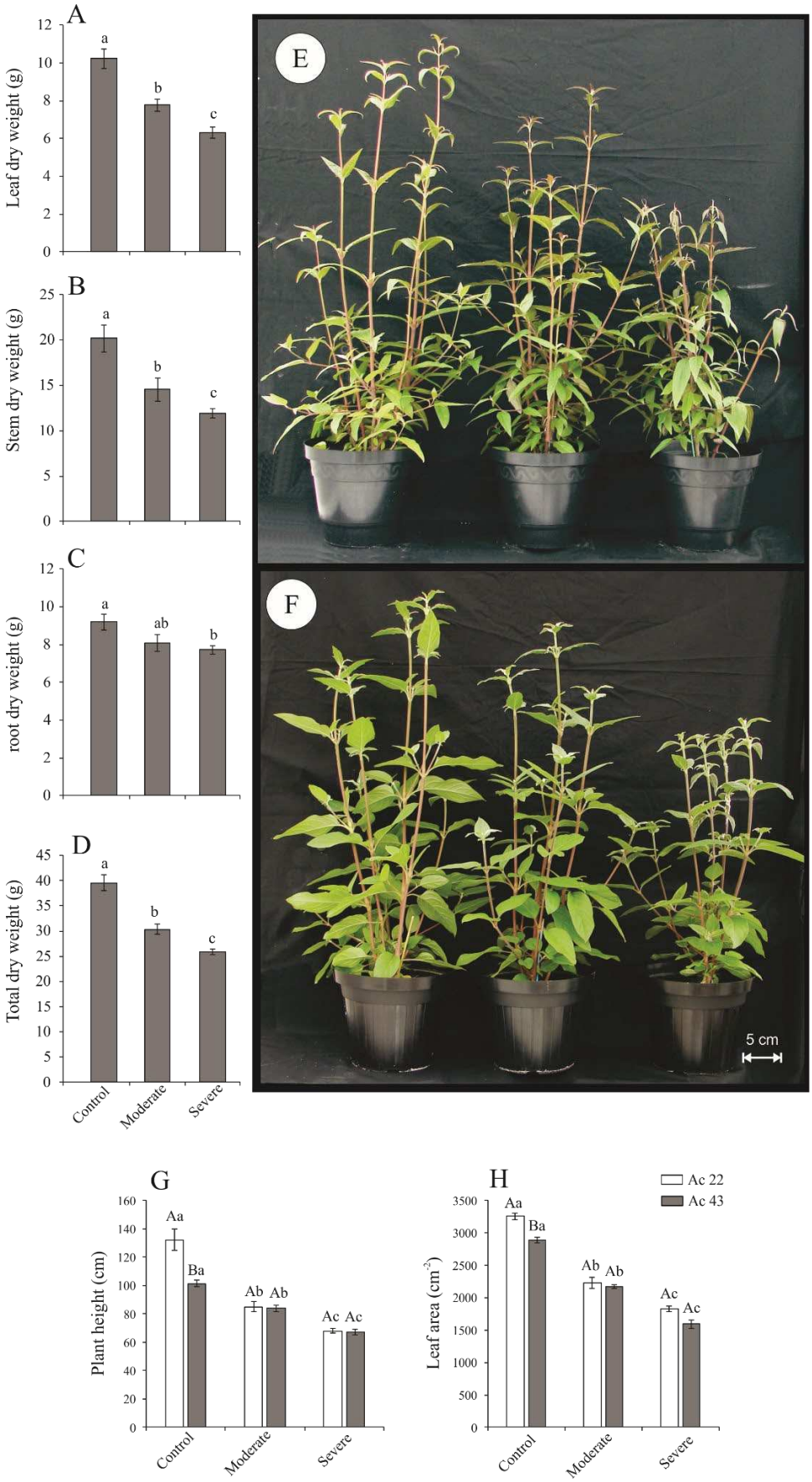
A
Leaf dry weight (g)
a
b
c
B
Stem dry weight (g)
a
b
c
C
root dry weight (g)
a
ab
b
D
Total dry weight (g)
a
b
c
Control
Moderate
Severe
E
F
5 cm
G
Plant height (cm)
Aa
Ba
Ab Ab
Ac Ac
Control
Moderate
Severe
H
Ac 22
Ac 43
Leaf area (cm-2)
Aa
Ba
Ab Ab
Ac Ac
Control
Moderate
Severe

Figure 4

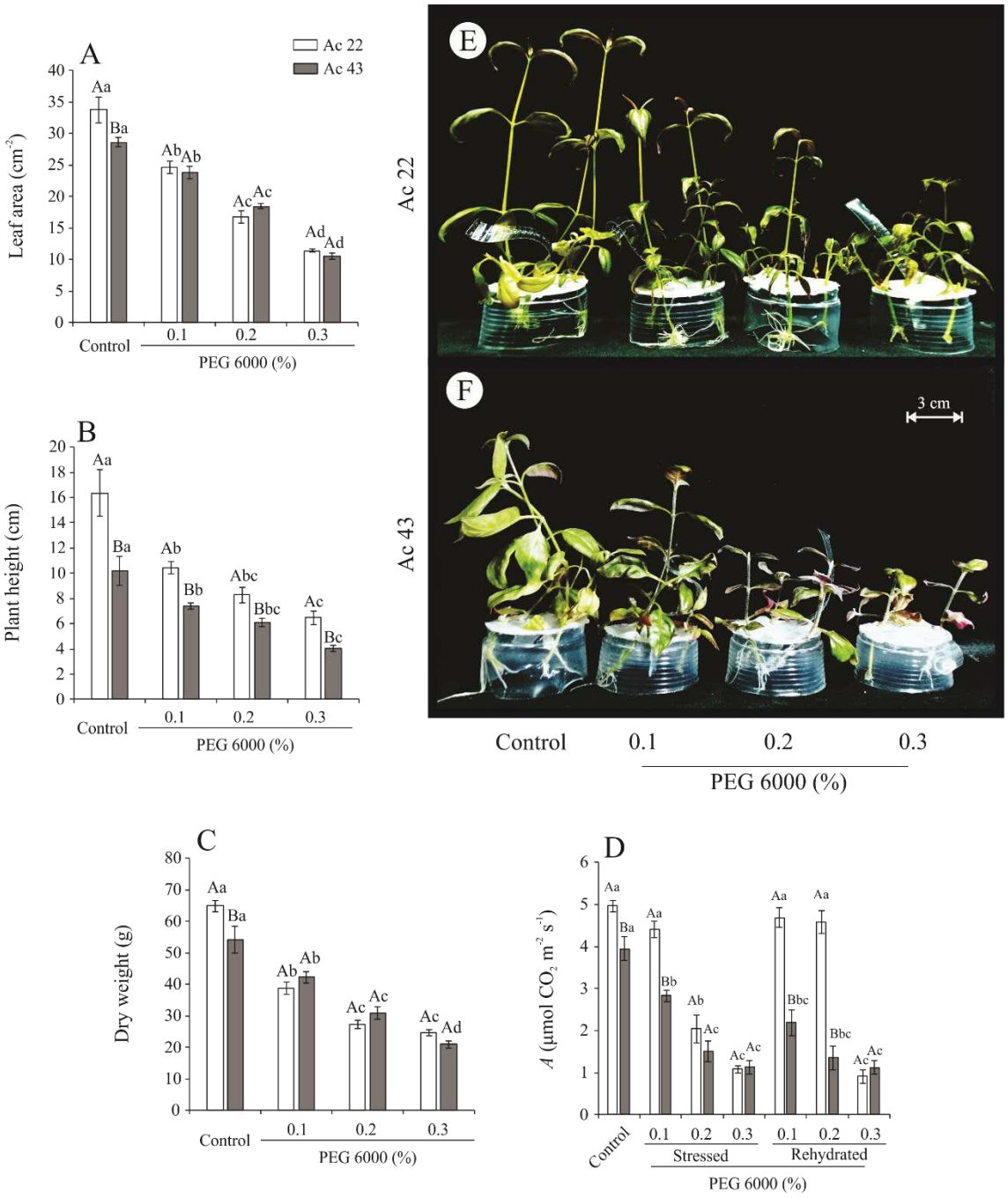
A
Ac 22
Ac 43
Leaf area (cm-2)
Aa
Ba
Ab Ab
Ac Ac
Ad Ad
Control
0.1
0.2
0.3
PEG 6000 (%)
B
Plant height (cm)
Aa
Ba
Ab
Bb
Abc
Bbc
Ac
Bc
C
Dry weight (g)
Ab Ab
Ac Ac
Ac Ad
D
A (μmol CO2 m-2 s-1)
Aa
Ba
Aa
Bb
Ab
Ac
Ac Ac
Aa
Bbc
Aa
Bbc
Ac Ac
Stressed
Rehydrated
E
F
Ac 22
Ac 43
3 cm
Control
0.1
0.2
0.3
PEG 6000 (%)

Figure 5

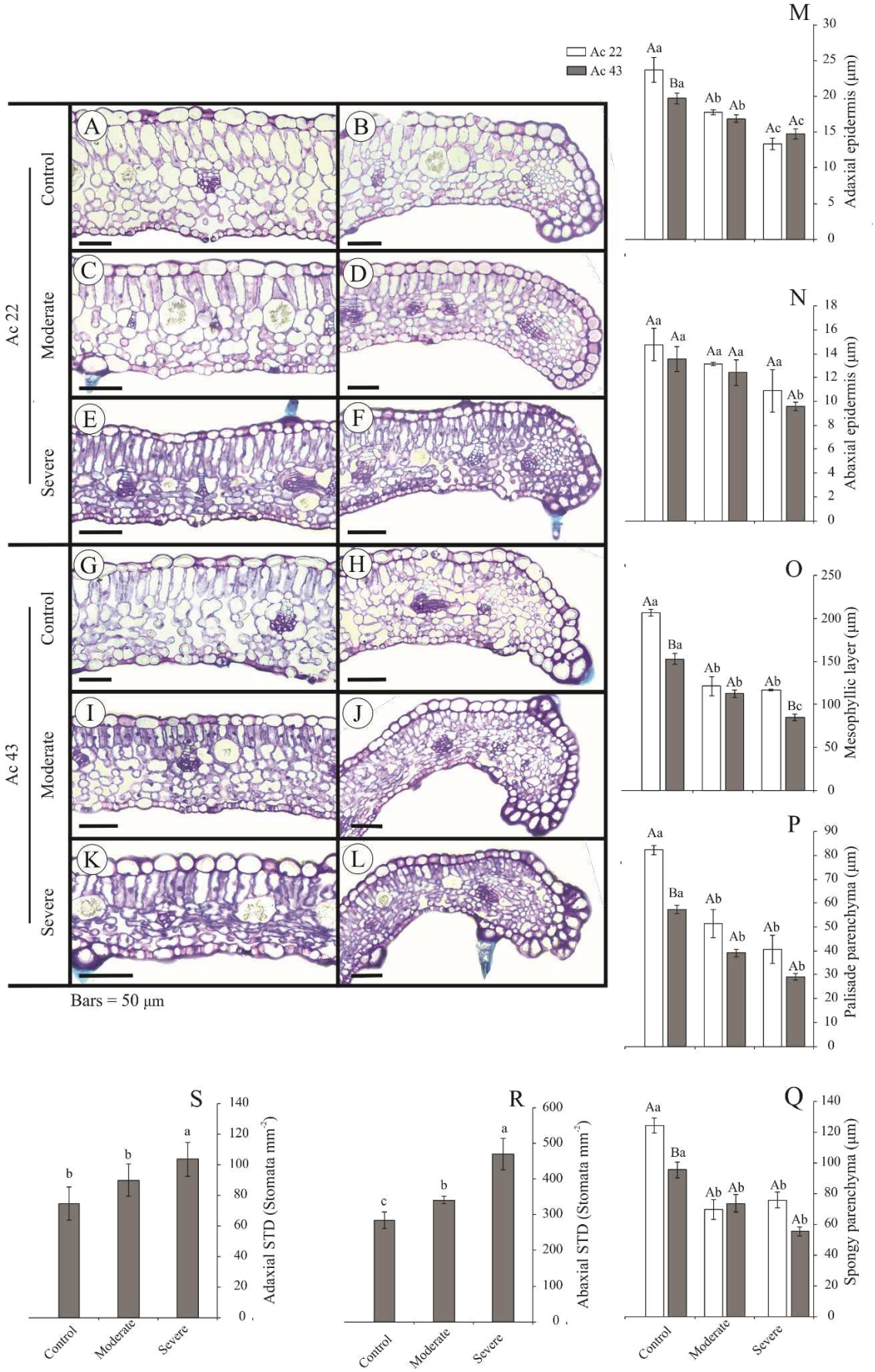
Ac 22
Ac 43
Control
Moderate
Severe
A
B
C
D
E
F
G
H
I
J
K
L
Bars = 50 µm
M
Adaxial epidermis (µm)
N
Abaxial epidermis (µm)
O
Mesophyllic layer (µm)
P
Palisade parenchyma (µm)
Q
Spongy parenchyma (µm)
S
Adaxial STD (Stomata mm-2)
R
Abaxial STD (Stomata mm-2)

Figure 6

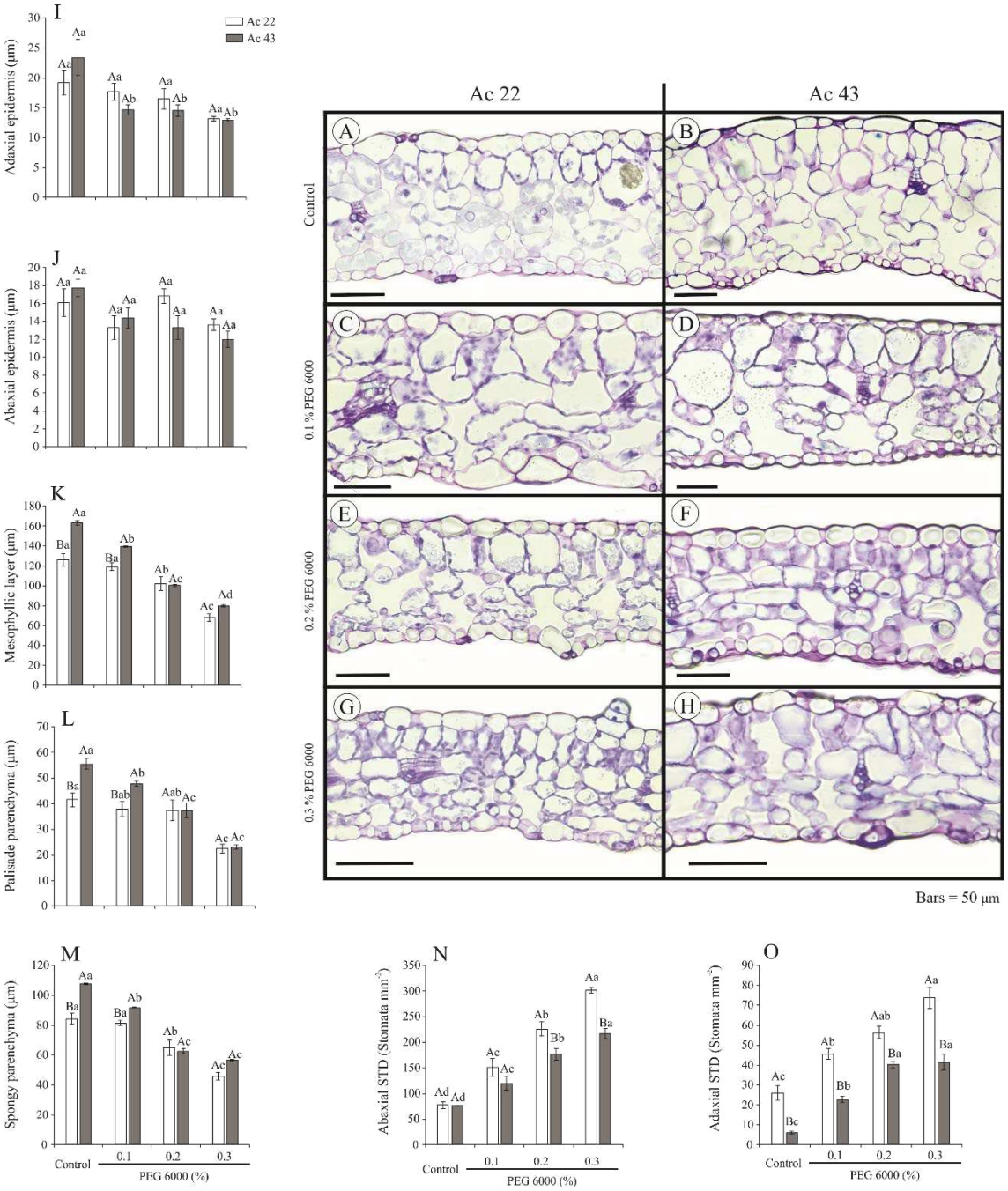
I
Ac 22
Ac 43
Adaxial epidermis (µm)
J
Abaxial epidermis (µm)
K
Mesophyllic layer (µm)
L
Palisade parenchyma (µm)
M
Spongy parenchyma (µm)
Control
PEG 6000 (%)
Ac 22
Ac 43
Control
0.1 % PEG 6000
0.2 % PEG 6000
0.3 % PEG 6000
A
B
C
D
E
F
G
H
Bars = 50 µm
N
Abaxial STD (Stomata mm-2)
O
Adaxial STD (Stomata mm-2)

Figure 7.

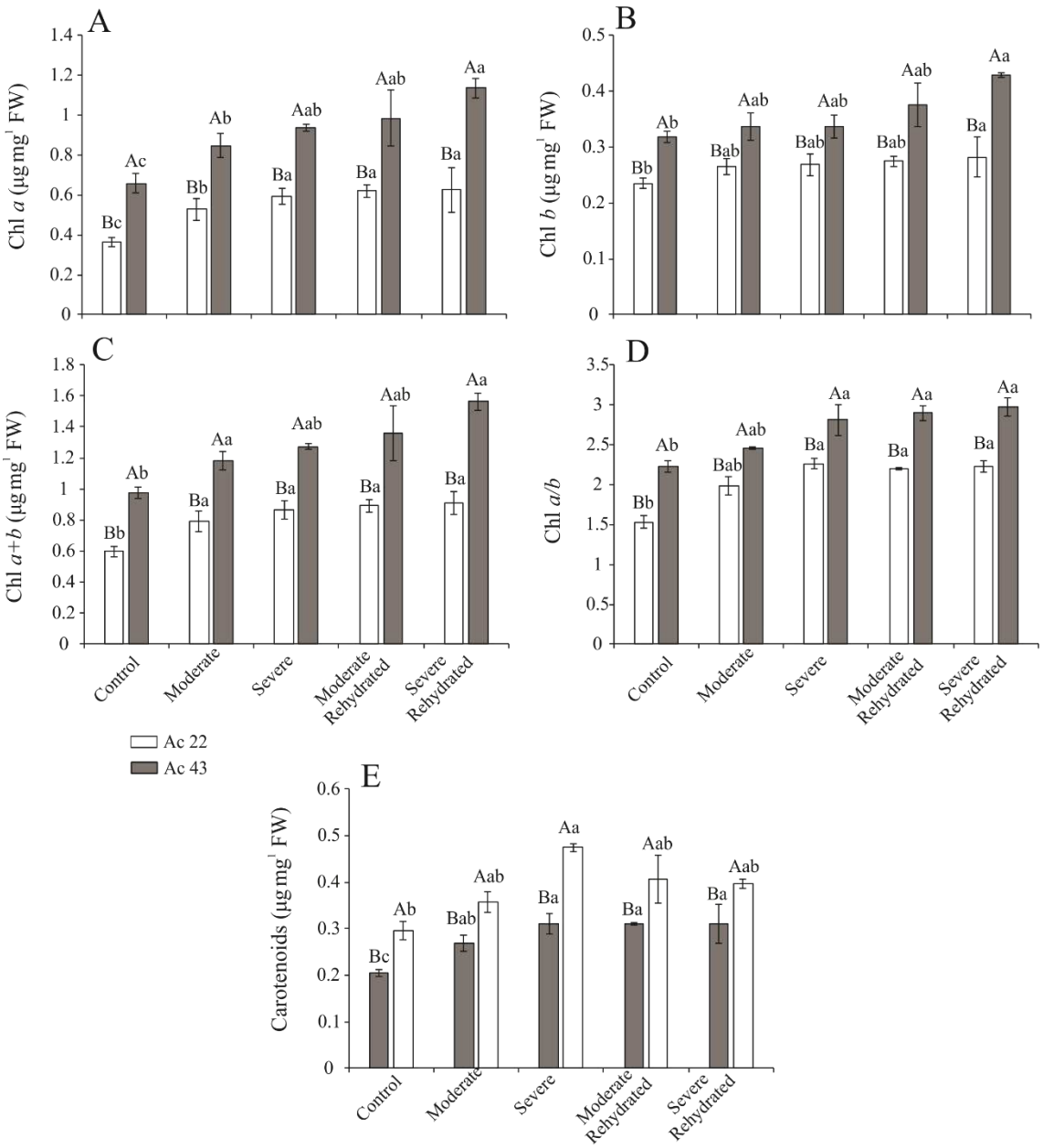
A
Chl a (µg mg-1 FW)
1.4
1.2
1
0.8
0.6
0.4
0.2
0
Bc
Ac
Bb
Ab
Ba
Aab
Ba
Aab
Ba
Aa
B
Chl b (µg mg-1 FW)
0.5
0.4
0.3
0.2
0.1
0
Bb
Ab
Bab
Aab
Bab
Aab
Bab
Aab
Ba
Aa
C
Chl a+b (µg mg-1 FW)
1.8
1.6
1.4
1.2
1
0.8
0.6
0.4
0.2
0
Bb
Ab
Ba
Aa
Ba
Aab
Ba
Aab
Ba
Aa
D
Chl a/b
3.5
3
2.5
2
1.5
1
0.5
0
Bb
Ab
Bab
Aab
Ba
Aa
Ba
Aa
Ba
Aa
Control
Moderate
Severe
Moderate Rehydrated
Severe Rehydrated
Ac 22
Ac 43
E
Carotenoids (µg mg-1 FW)
0.6
0.5
0.4
0.3
0.2
0.1
0
Bc
Ab
Bab
Aab
Ba
Aa
Ba
Aab
Ba
Aab
Control
Moderate
Severe
Moderate Rehydrated
Severe Rehydrated

Figure 8.

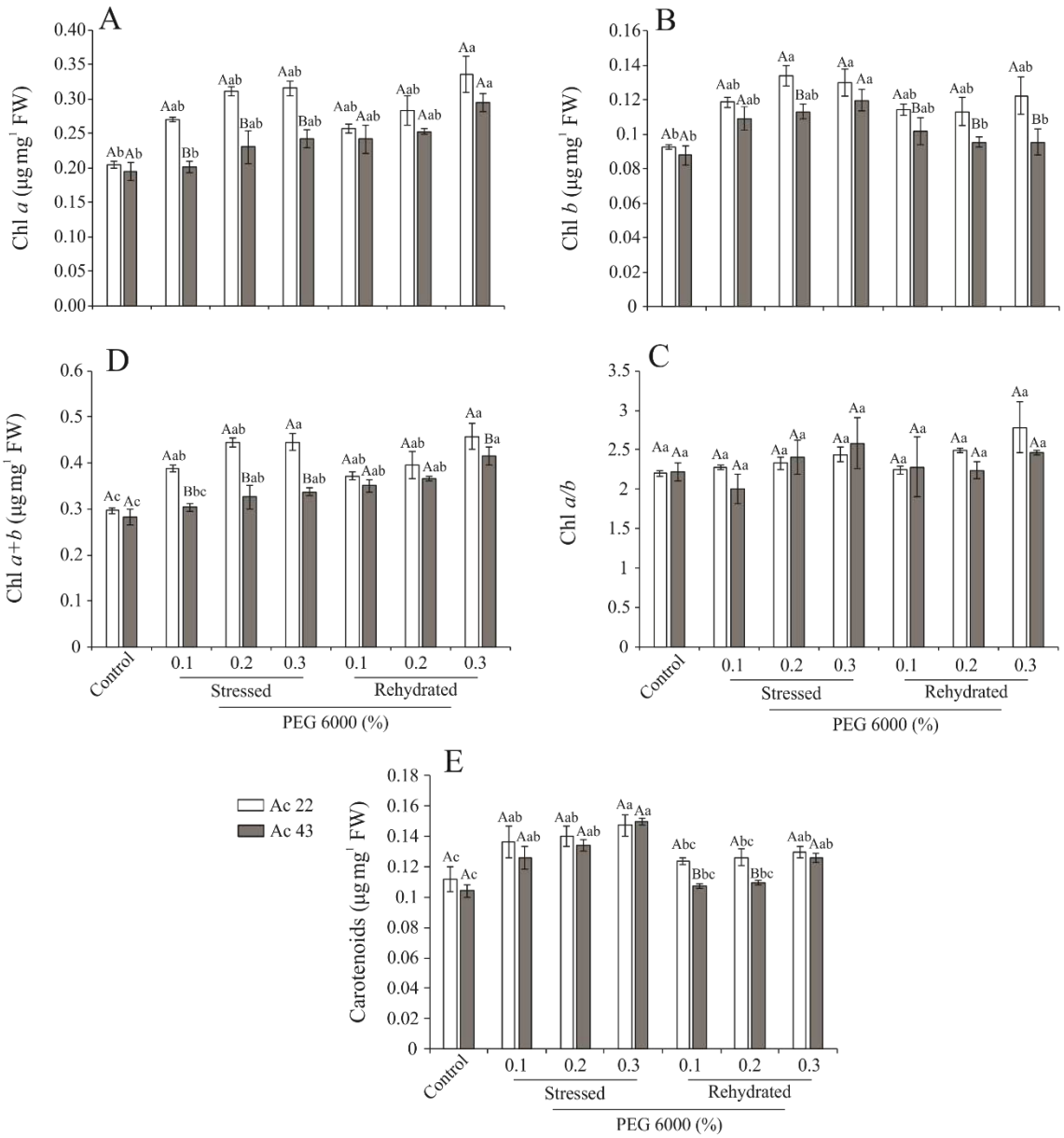
A
Chl a (μg mg-1 FW)
B
Chl b (μg mg-1 FW)
D
Chl a+b (μg mg-1 FW)
C
Chl a/b
E
Carotenoids (μg mg-1 FW)
Ac 22
Ac 43
Control
Stressed
Rehydrated
PEG 6000 (%)

Figure 9.

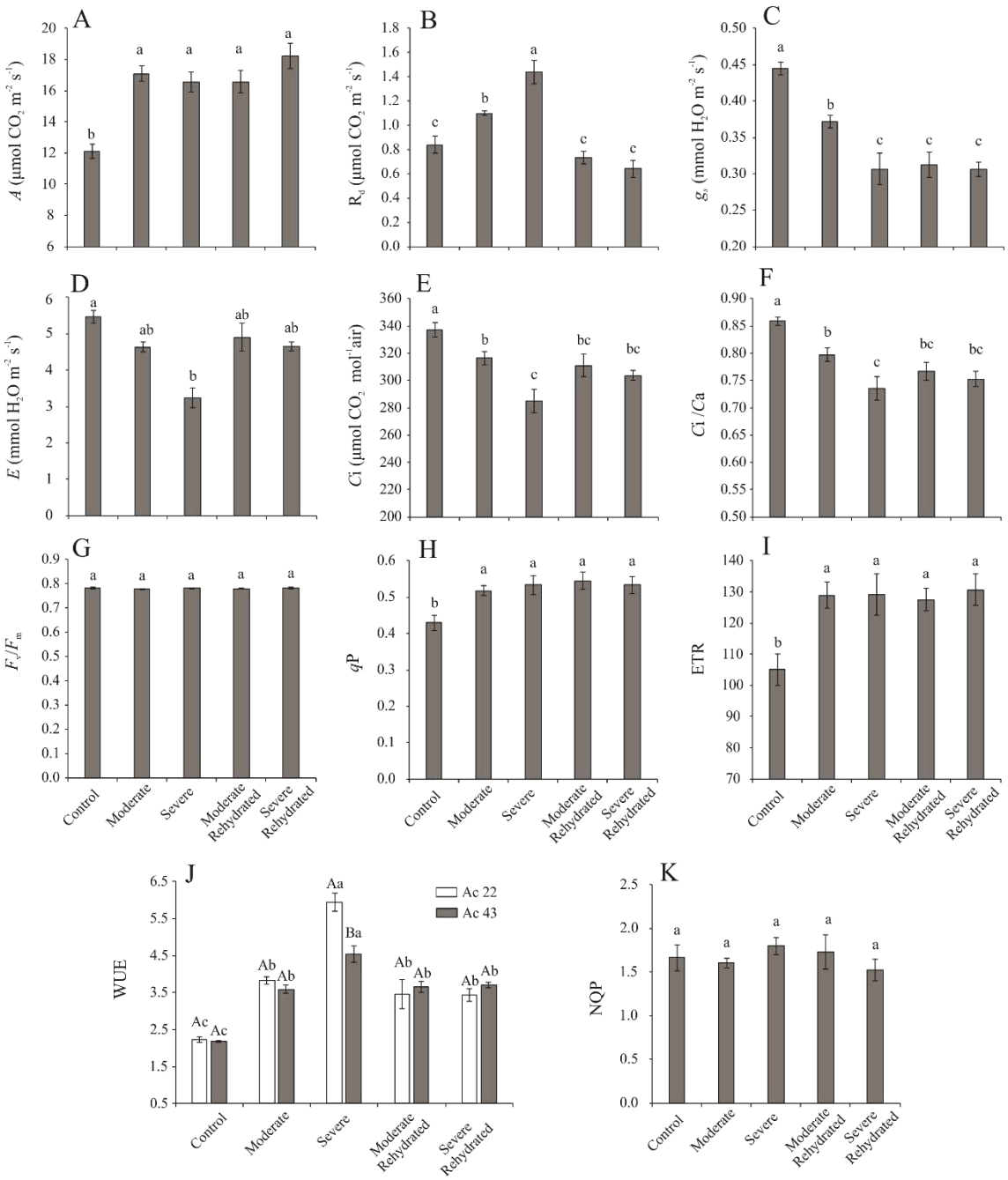
A
B
C
D
E
F
G
H
I
J
K
Control
Moderate
Severe
Moderate Rehydrated
Severe Rehydrated
Ac 22
Ac 43
WUE
NQP
ETR
qP
Ci /Ca

Figure 10.

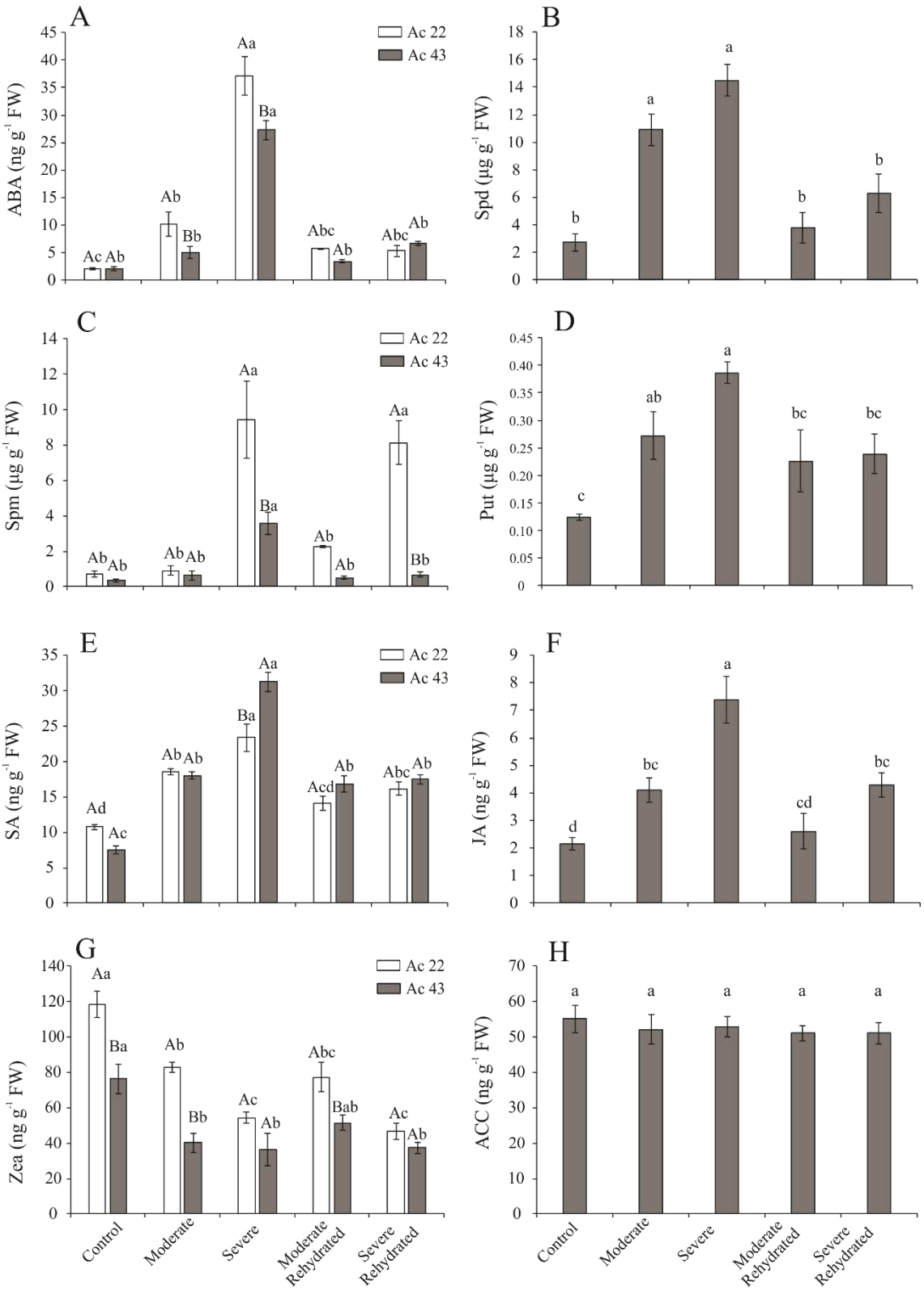
A
ABA (ng g-1 FW)
Ac 22
Ac 43
Ac Ab
Ab Bb
Aa Ba
Abc Ab
Abc Ab
B
Spd (µg g-1 FW)
b
a
a
b
b
C
Spm (µg g-1 FW)
Ab Ab
Ab Ab
Aa Ba
Ab Ab
Aa Bb
D
Put (µg g-1 FW)
c
ab
a
bc
bc
E
SA (ng g-1 FW)
Ad Ac
Ab Ab
Ba Aa
Acd Ab
Abc Ab
F
JA (ng g-1 FW)
d
bc
a
cd
bc
G
Zea (ng g-1 FW)
Aa Ba
Ab Bb
Ac Ab
Abc Bab
Ac Ab
H
ACC (ng g-1 FW)
a a a a a
Control
Moderate
Severe
Moderate Rehydrated
Severe Rehydrated

Figure 11.

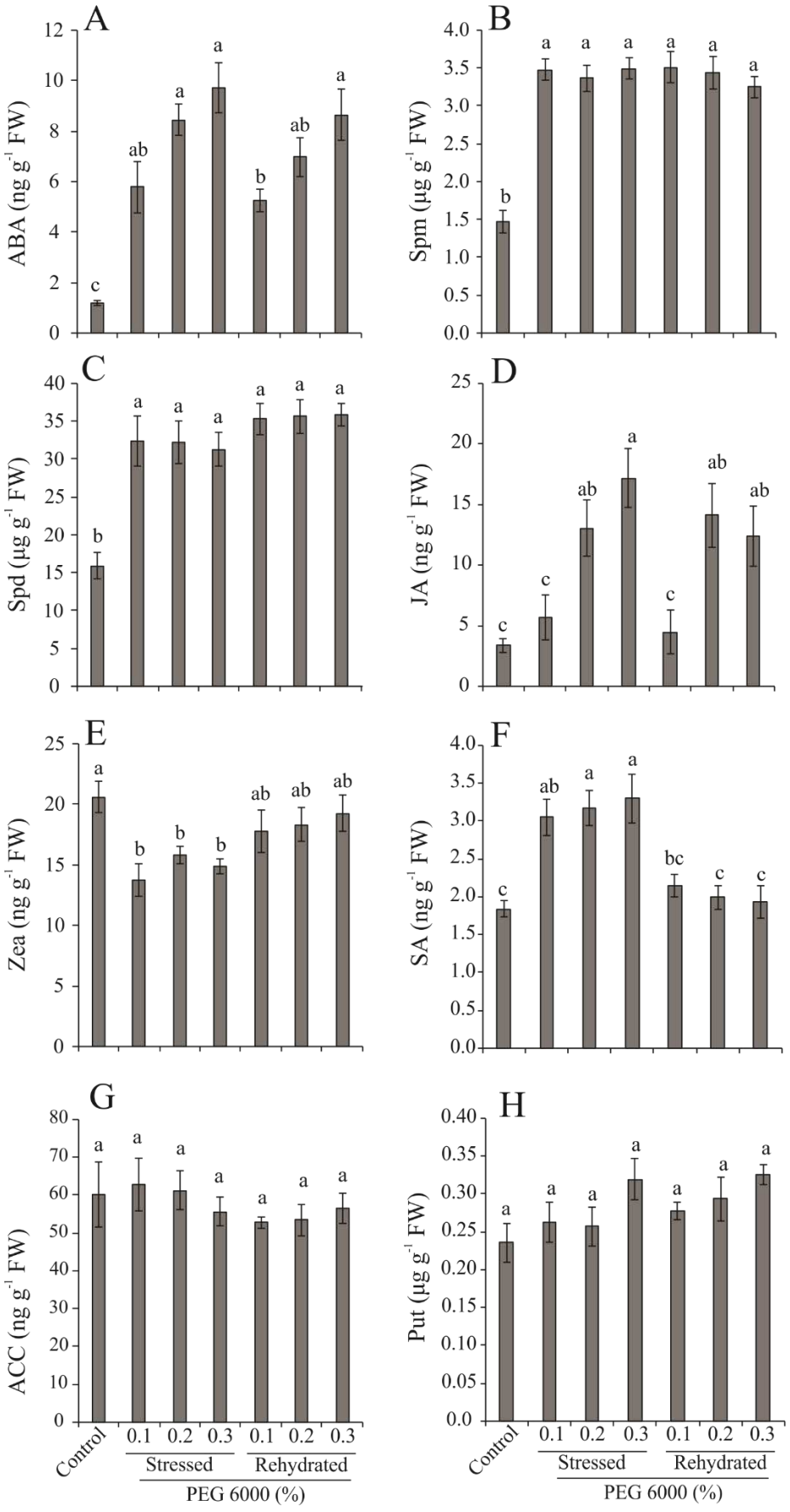
A
ABA (ng g-1 FW)
B
Spm (µg g-1 FW)
C
Spd (µg g-1 FW)
D
JA (ng g-1 FW)
E
Zea (ng g-1 FW)
F
SA (ng g-1 FW)
G
ACC (ng g-1 FW)
H
Put (µg g-1 FW)
Control
0.1
0.2
0.3
0.1
0.2
0.3
Stressed
Rehydrated
PEG 6000 (%)

Figure 12.

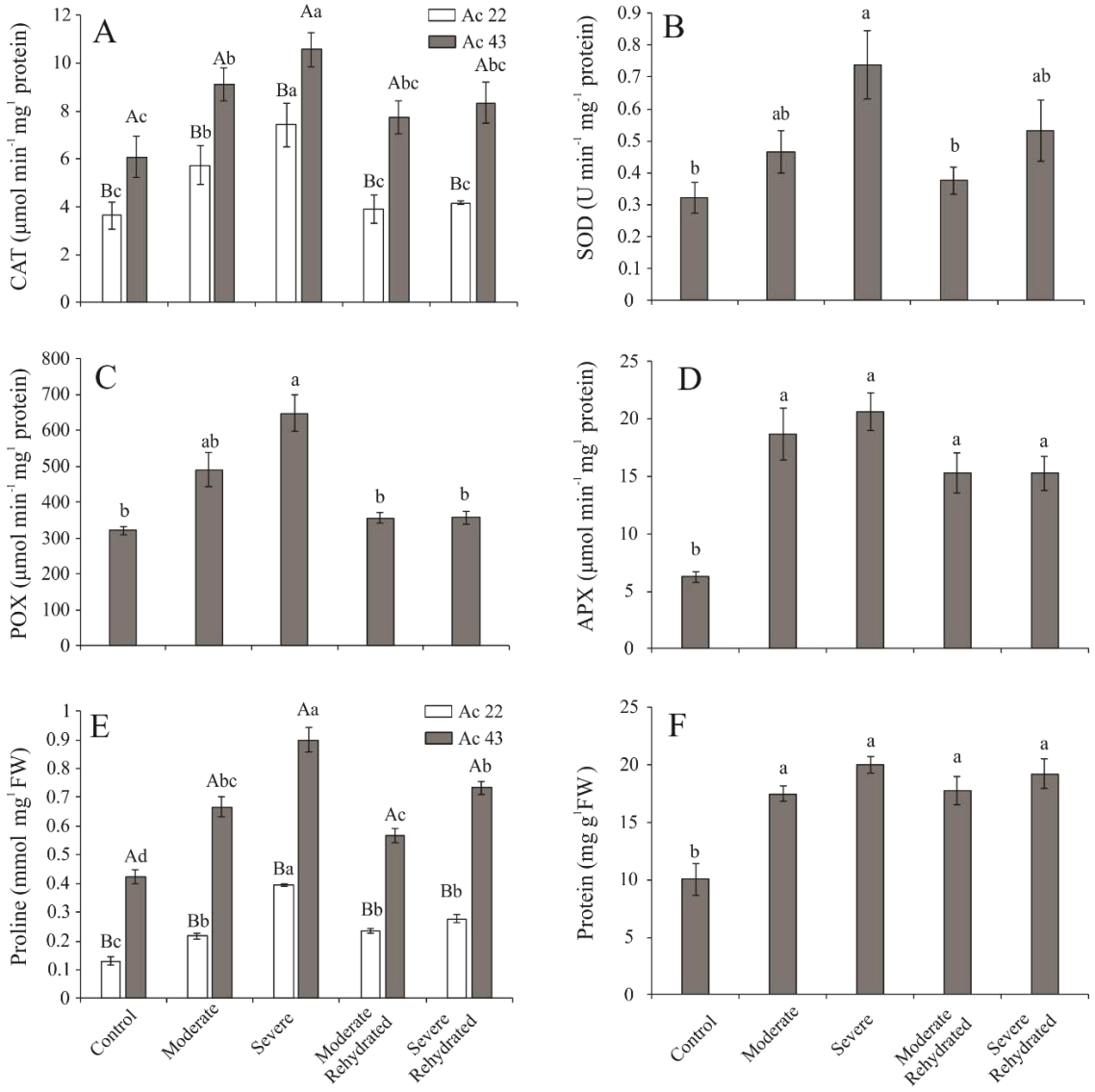
A
CAT (µmol min-1 mg-1 protein)
Ac 22
Ac 43
Bc
Ac
Bb
Ab
Ba
Aa
Bc
Abc
Bc
Abc
B
SOD (U min-1 mg-1 protein)
b
ab
a
b
ab
C
POX (µmol min-1 mg-1 protein)
b
ab
a
b
b
D
APX (µmol min-1 mg-1 protein)
b
a
a
a
a
E
Proline (mmol mg-1 FW)
Bc
Ad
Bb
Abc
Ba
Aa
Bb
Ac
Bb
Ab
F
Protein (mg g-1 FW)
b
a
a
a
a
Control
Moderate
Severe
Moderate Rehydrated
Severe Rehydrated

Figure 13.

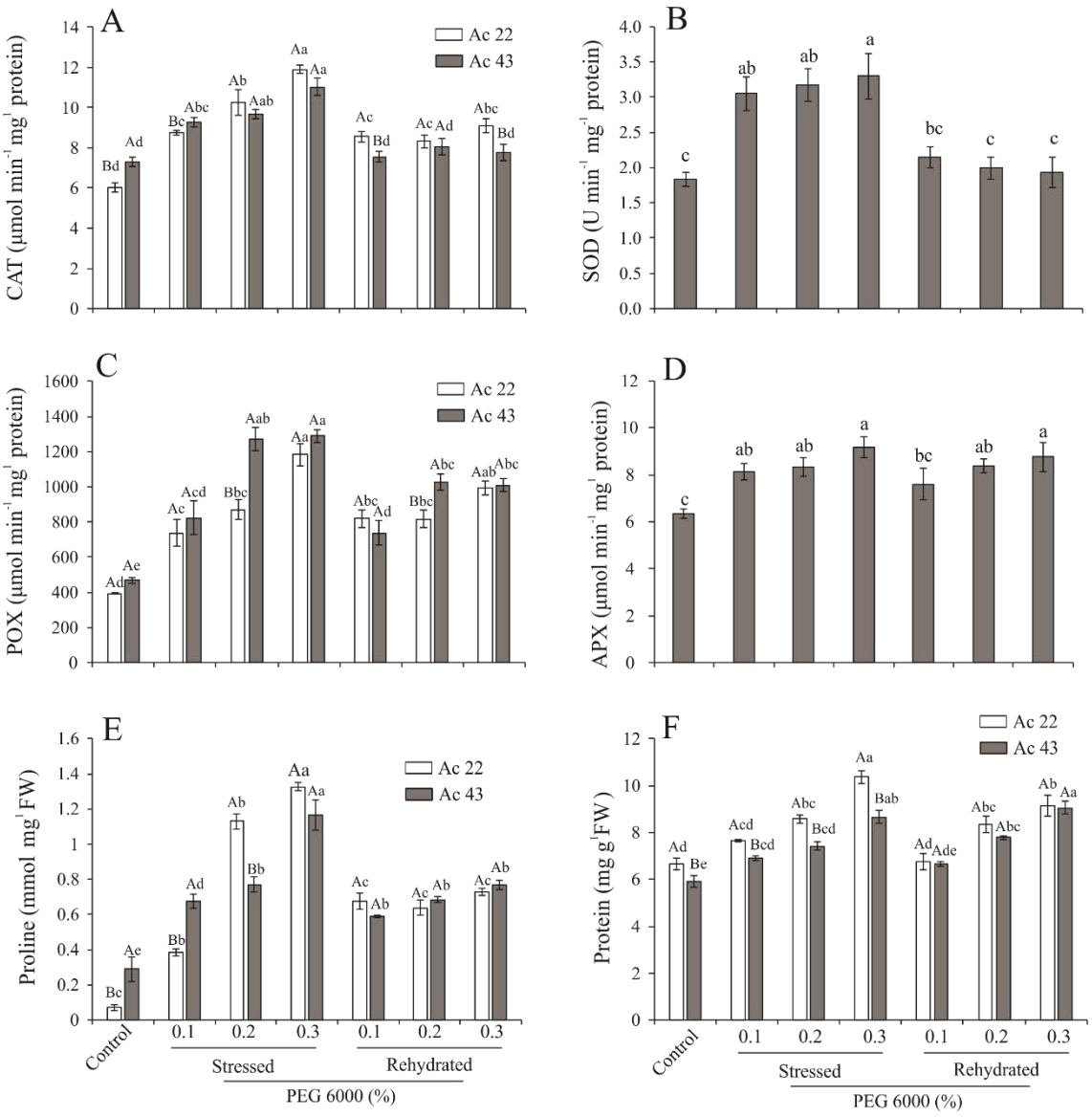
A
CAT (μmol min-1 mg-1 protein)
Ac 22
Ac 43
B
SOD (U min-1 mg-1 protein)
C
POX (μmol min-1 mg-1 protein)
D
APX (μmol min-1 mg-1 protein)
E
Proline (mmol mg-1 FW)
F
Protein (mg g-1 FW)
Control
0.1
0.2
0.3
Stressed
Rehydrated
PEG 6000 (%)

Figure 14.

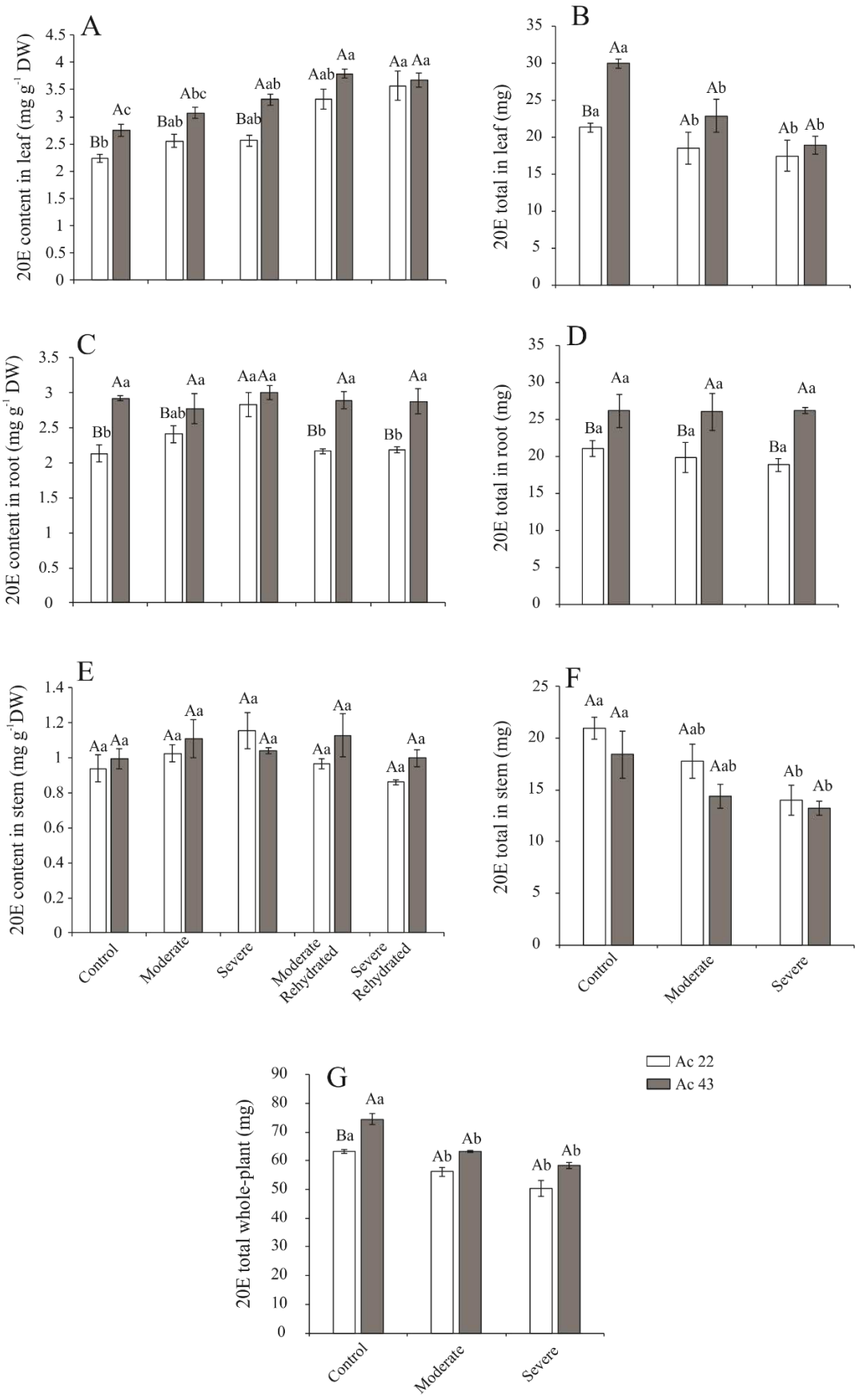
A
20E content in leaf (mg g-1 DW)
Bb Ac
Bab Abc
Bab Aab
Aab Aa
Aa Aa
B
20E total in leaf (mg)
Ba Aa
Ab Ab
Ab Ab
C
20E content in root (mg g-1 DW)
Bb Aa
Bab Aa
Aa Aa
Bb Aa
Bb Aa
D
20E total in root (mg)
Ba Aa
Ba Aa
Ba Aa
E
20E content in stem (mg g-1DW)
Aa Aa
Aa Aa
Aa Aa
Aa Aa
Aa Aa
Control
Moderate
Severe
Moderate Rehydrated
Severe Rehydrated
F
20E total in stem (mg)
Aa Aa
Aab Aab
Ab Ab
Control
Moderate
Severe
Ac 22
Ac 43
G
20E total whole-plant (mg)
Ba Aa
Ab Ab
Ab Ab
Control
Moderate
Severe

Figure 15.

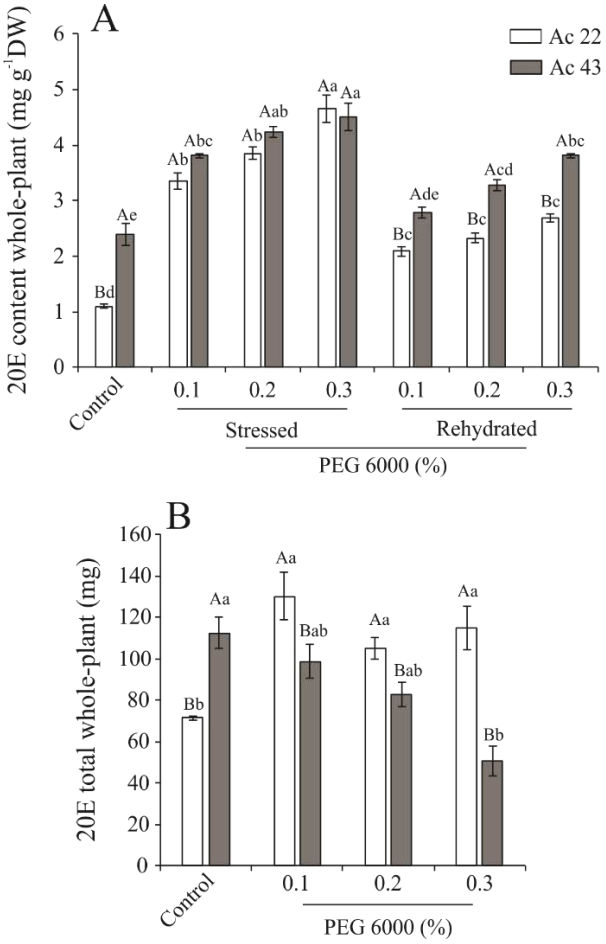

Figure 16

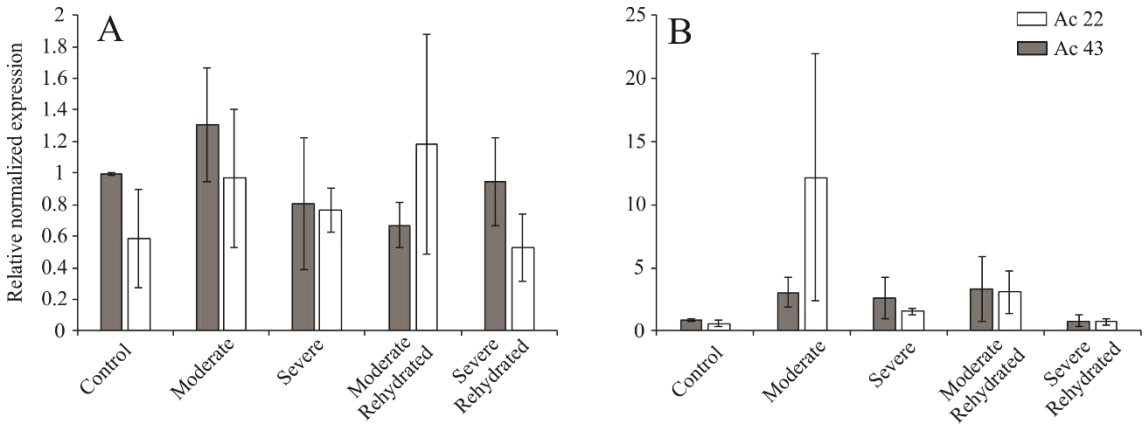

CONCLUSIONS

The following conclusions can be drawn from the present study:

- The designed light chamber of white LEDs source photosynthetic photon flux (600 μmol m^{-2} s^{-1}) showed proven reliability and versatility in measurements of plant photosynthesis *in vitro*;
- The polyploids exhibited lower number, and greater thicker and more expanded of leaves, increased stomata size and reduced stomata density compared to the diploids;
- The photosynthetic performance of *P. glomerata* under photoautotrophic culture *in vitro* was not affected by morphogenetic changes caused by induced polyploidy;
- *P. glomerata* adopts a series of acclimation strategies that provide tolerance to the water deficit;
- Drought affects negatively the 20E production;
- The different responses on the 20E content and development among the accessions is genotype-dependent, evidencing the phenotypic plasticity of this species;
- Morpho-physiological responses observed *in vitro* matched with those found for greenhouse plants, allowing the use of the technique in plant breeding programs in pre-selection